FAIRSEA (ID 10046951)

"Fisheries in the AdriatIc Region - a Shared Ecosystem Approach"

D 4.3.1-Spatio-temporal distribution of marine species

Work Package:	WP4 - Implementation of a shared and integrated platform Activity 4.3 – BSTAT Spatial distribution of marine resources
Type of Document	Description of the results of the application of BioIndex and BioStand routine to fishery independent survey data of GSA17, GSA18 and GSA19 for the time series 1994-2018
Use	Internal
Responsible PP	PP6-CoNISMa: Carlucci R., Cipriano G., Ricci P., Capezzuto F., D'Onghia G., Maiorano P., Sion L., Tursi A.
Authors	PP6-CoNISMa: Roberto Carlucci, Cipriano Giulia, Pasquale Ricci, Maddalena Laggini, Chiara Manfredi, Corrado Piccinetti. PP5-COISPA: Walter Zupa, Isabella Bitetto, Loredana Casciaro, Maria Teresa Spedicato. PP3-CNR: Francesco Masnadi, Giuseppe Scarcella. LP-OGS: Diego Panzeri, Simone Libralato
Version and date	V.01, 31/12/2019

Deliverable 4.3.1

Spatio-temporal distribution of marine species

FAIRSEA – Fisheries in the Adriatic Region – a shared Ecosystem Approach

FAIRSEA is financed by Interreg V-A IT-HR CBC Programme (Priority Axis 1 – Blue innovation)

Start date: 01 January 2019

End date: 28 February 2021

Contents

Acronyms used

GIS	Geographic Information System
CFP	Common Fisheries Policy
EAF	Ecosystem Approach to Fisheries
EAFM	Ecosystem Approach to Fisheries Management
FAIRSEA	Fisheries in the AdrIatic Region – a Shared Ecosystem Approach
GAM	Generalized Additive Models
GSA	FAO Geographical Sub Areas
GVC	Generalized Cross-Validation
IT	Italy
LP	Lead Partner
OGS	Istituto Nazionale di Oceanografia e di Geofisica Sperimentale
PP	Project Partner
WP	Work packages

About FAIRSEA Project

The FAIRSEA is a European Territory Cooperation project financed under the priority 1 “Blue innovation”, Specific Objective 1.1 “Enhance the framework conditions for innovation in the relevant sectors of the blue economy within the cooperation area” of the INTERREG V-A Italy –Croatia Programme 2014-2020. The project focuses on the fisheries sector, key driver for the blue growth of the Adriatic communities, towards a sustainable co-management of resources and marine ecosystem protection. The transboundary nature of marine resources requires a cross-border cooperation and a shared “Vision” to properly tackle and address the different socio-economic and environmental challenges related to fisheries activities management. In this context, FAIRSEA Project aims at enhancing transnational capacity and cooperation in order to promote the sharing of knowledge and good practices between regional and transnational key actors in the sector of sustainable fisheries management in the Adriatic Sea as well as to implement innovative approaches adopting an ecosystem approach to fisheries (EAF).

Coordinated by the OGS of Trieste (IT), the project involves a consortium of 12 strategic and operational partners from Italy and Croatia that will make to best use of their complementary expertise to address and support the application of the EAF ensuring a strong and interactive engagement of institutional, technical and socio-economic stakeholder in project activities.

The main result of the FAIRSEA Project will be the development of an integrated platform for a quantitative ecosystem approach to fisheries that goes across territorial boundaries and across several disciplines. The platform will integrate biological/ecological processes (i.e. considering water mass circulation, physical-chemical properties, plankton productivity, dynamics of resources including their interactions) and fisheries bio-economic dynamics (including fisheries displacement). This high technological and innovative platform will be used as a planning tool to implement demonstrative testing of applicable fisheries policies both at local (subareas) and Adriatic scales. It will provide scientific basis for formulating and evaluating the shared management advice in the local and international participatory processes, involving management authorities, experts and

stakeholders. The Project will also provide an answer to the need of reference points, best practices and guidelines for the optimisation between ecological and socio-economical sustainability of fisheries in the Adriatic Sea.

1. INTRODUCTION

The distribution of main fishery resources in a spatio-temporal dynamic, called module BSTAT (Activity 4.3), is one of the cornerstone elements of the integrated platform designed in the WP4 of the FAIRSEA project.

Fishery-independent surveys provide the basic information for estimating the population indices and the spatial distribution of species of commercial interest. These species, possibly around 20-30, are planned to be selected in the present Deliverable 4.3.1 according to their abundance at sea and/or importance for fisheries. Bottom trawl surveys (mainly MEDITS, SOLEMON, GRUND until 2008 and other occasional samplings) as well as acoustic surveys (MEDIAS and other projects) have been conducted in the Adriatic Sea and in the Western Ionian Sea by several FAIRSEA partners, on a regular or a sporadic basis, during the past 20 years.

Indeed the knowledge on the spatial and temporal distribution of demersal fisheries resources mainly relies on the time series of the scientific trawl survey MEDITS (Spedicato et al., 2019a), which is the longer available and can provide primary information to support evaluations of demersal fish population and communities through:

- standardised indices (abundance and biomass) of the whole population or life stages;
- indicators of population demography and structure;
- spatial occupation indices;
- evaluation of vulnerable species and Essential Fish Habitats
- community indicators;
- new scientific insights linked to the spatial management.

The first two outputs are also routinely used in the stock assessment process.

Indicators, both at aggregated and detailed spatial levels, can support the evaluation on the state of fishery resources and easy communicated to stakeholders. BSTAT module then focused on the estimation of such indicators.
Outputs from scientific surveys are also complementary for the implementation of the Food Web Modelling foreseen in the activity 4.7 of FAIRSEA. This is also the reason why the analysis was extended to a wide range of species.

1.1 Activity 4.3.BSTAT – Spatial distribution of marine resources

The main objective of BSTAT activity and of this deliverable D4.3.1 - *Spatio-temporal distribution of marine species* is to produce a database of standardised indices and maps of commercial species distribution based on the knowledge from the past 20 years. Where the information is available from the survey, the identification of main areas of aggregation, including areas of persistent presence of critical life stages, such as nursery and spawning area, is another objective.
Outputs from trawl surveys, using some specifically designed open source tools, as R-routine BioIndex and BioStand (see 2.4 and 2.5 sub-chapters for details), can also be used in the WP4 platform. Through GIS-based applications it is possible to visualize, for example, the spatial distribution and temporal trends of the key indicators related to the state of the main fish populations in the Adriatic and Western Ionian seas (Geographical Sub-areas 17, 18 and 19).
Regarding the transferability of project results, the objective is to develop open source tools, i.e. R routines, to be made available via the web and from the R community users, production of web viewers allowing the disseminations/consultation of results in terms of maps and demo files.

2. MATERIALS AND METHOD

2.1 Data

MEDITS data and SOLEMON data were considered the most suitable source of information for BSTAT, because these data are available both at aggregated and detailed spatial level, while MEDIAS data are not available at detailed spatial level (single hauls). MEDITS and SOLEMON data, collected within the EU DCF (Data Collection Framework), were requested and obtained from the competent Authorities, following a Data Call issued by the FAIRSEA project to the Ministry of Croatia, Italy and Slovenia. The project partners provided additional information where needed.

MEDITS is the co-ordinated international bottom trawl survey in the EU Mediterranean waters that started in 1994. The survey includes the trawlable areas over the shelves and the upper slopes from 10 to 800 m depth off the coasts of the partner countries, with monitoring done mainly in late spring-early summer. The sampling scheme is random stratified by depth and latitude. Depth limits are: 10-50, 51-100, 101-200, 201-500 and 501-800 m. Hauls have been randomly selected with allocation kept as far as possible stationary along the time. The survey adopts a standardized trawl net (GOC 73) with a very fine stretched mesh size (20-mm) in the cod-end. The net was designed to catch the wide range of species characterised within Mediterranean demersal communities in a large range of sizes. A list of thirty common target species (including fish, molluscs and crustaceans) was established at the beginning of the MEDITS project, considering the commercial relevance of these species and their accessibility by a bottom trawl. This list has been considerably enlarged in the following years. All the details on the MEDITS protocol can be found in Spedicato et al. (2019a) and in Anonymous (2017). The MEDITS time series has been recently used for investigating the fish population and community spatio-temporal dynamics at north Mediterranean scale (Spedicato et al., 2019b).

SOLEMON is a survey conducted from 2005 using a modified beam trawl called ‘Rapido’ with the aim to monitor the continental shelves of the Northern Adriatic Sea

(GSA 17) up to a depth of 100 m. The survey focuses on flatfish species like common sole (*Solea solea);* further target species include spottail mantis shrimp (*Squilla mantis*), common cuttlefish (*Sepia officinalis*).

2.2 Ranking of the species

To select a set of relevant species at sub-area level a ranking was necessary among all the species monitored in the MEDITS survey. The ranking of the species for the objectives of the BSTAT was done according to the following criteria.

Time frame: The time series used for ranking the species is the last ten years of MEDITS data (2009-2018) and SOLEMON (for the GSA17) because they are considered suitable to work with a stable time series, without including old observations.

List of species: All the MEDITS lists of species are taken into account, except the benthos, which monitoring was included in the MEDITS protocol since 2013.

Two lists of species are compiled: one including all the species (List All) and a second one including only the commercial species (List Com).

Method: the lists of species of each type (All or Com) from the different years are pooled to compile a unique list per type. Small pelagics species (anchovy and sardine) are excluded given that the survey is targeting demersal species. For the ranking of the species, the averaged biomass index among the years is weighed by the logarithm of the average abundance index. The descending cumulative distributions are used to allow the selection of a number of species covering 75% and 90% of the cumulative distribution. The following excel file contains an example.

Ranking example.xlsx

This methodology was shared among the partners and applied in the different GSAs of the Adriatic and Western Ionian Sea.

In the final list of the selected species, other factors such as the interaction of accessibility and vulnerability of the species –or species life stages-to the MEDITS gear and survey should be taken into account. In addition, the two species common sole (*Solea solea*) and the spottail mantis shrimp (*Squilla mantis*) target of SOLEMON surveys were included in the list of selected species, especially for the GSA17.

2.3 Selection of indicators

The indicators relevant for an Ecosystem Approach to Fishery Management (EAFM) taking into account population abundance, structure and spatial occupation were selected on the basis of the pertinent literature (e.g Trenkel et al., 2007; Cotter et al., 2009a; 2009b). To catch the relevant signal while avoiding redundancy the following indicators were retained:

1. **number of positive hauls to the species,** the spreading area of a stock is mainly dependent on its abundance; a decrease of the indices can be an effect of fishing impact;
2. **mean biomass and abundance indices (kg/km^2; number/km^2),** changes (decrease) in these indices can be caused by an excessive fishing pressure, but also by habitat disruption; abundance might be substantially affected by large recruitment pulses in the stock;
3. **inverse of mean abundance Coefficient of Variation (CV),** can be seen as a descriptor of the stability of the variable under investigation (higher is the metrics, more stable is the variable);
4. **mean individual weight (MIW),** synthesizes the structure of the population (Piet and Jennings, 2005) and its changes in time, decreasing is possibly linked to the fishing pressure, though also to recruitment peaks. This influence is expected to be less pronounced if older individuals in the population are well represented. Mean weight is particularly useful for those species caught in the trawl surveys for which no data on individual size is collected.
5. **sex-ratio,** Sex ratio provides information on the distribution of female and male individuals present in a population. It represents the proportion of females in a population and indicates the level of sex dominance (Adebiyi, 2013). Generally, this is a peculiar trait of the population. The sex-ratio, as the proportion of the females on the overall number of individuals, can be considered correlated with the stock productivity and renewal;
6. **index of recruits (number/km^2),** recruits are often measured as the individuals belonging to the first component of the length frequency distributions, or as the individuals of the first age class, according to the

recruitment mode, population structure and species. Thresholds to split the recruits from the whole population index can be also obtained from different areas or from literature. Excessive fishery can reduce the recruitment by negative effects on the spawners; habitat disruption may play a similar effect;

7. **index of spawners (number/km²),** excessive fishery can negatively impact the reproductive potential*;* As individuals in spawning phase are not always intercepted by surveys, spawners can be approximated using the indices of adult individuals, i.e. those larger than the size at first maturity;
8. **length at 95° percentile (L0.95),** the different percentiles of a length frequency distribution (LFD) are expected to respond differently to fishing, recruitment pulses, and loss of spawning stock. A large percentile of the population length distribution (L0.95) is an index of the numbers of adult, older fish. This indices can be negatively (decrease) affected by an excessive fishing pressure.

2.4 Estimates of key population indicators for the list of selected species

BioIndex routine developed by COISPA (available at: https://www.coispa.it) (Zupa W., L. Casciaro, I. Bitetto, M.T. Spedicato. 2020. BioIndex v.2.1.2) in R software allows to perform survey data analysis at different levels, estimating the time series of a wide set of population state-indicators for the selected number of species. Figure 2.4.A schematises the estimates of the indicators both at non –spatial and spatial level that can be obtained using BioIndex.

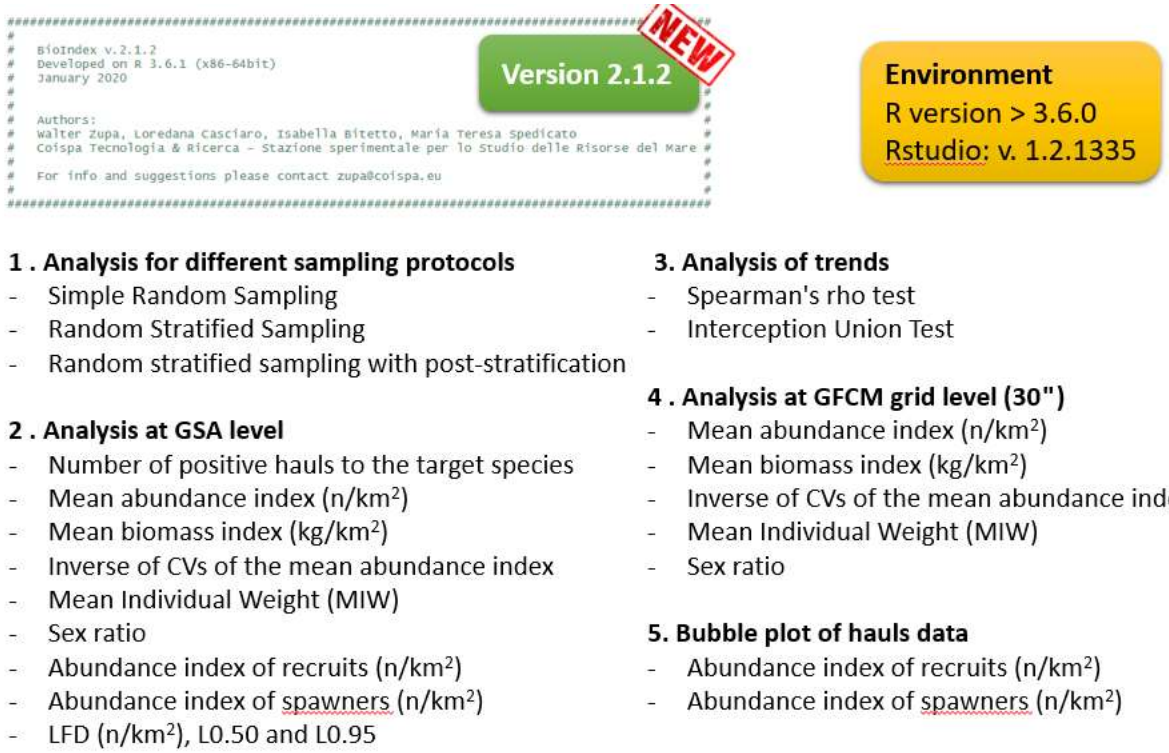

Figure 2.4.A - Summary of the indicators estimated on the time series for trend analysis and at spatial level using BioIndex R routine.

Three different sampling protocols (Cochran, 1977), simple random sampling; random stratified sampling and random stratified sampling with post-stratification, can be managed in BioIndex. The analysis is performed at GSA level, but if two or more countries are included in the same GSA, the analysis could be also performed at country level. GSAs can be also merged if deemed appropriate. Moreover, the analysis is performed considering the appropriate bathymetric range of distribution of the species selected, considering three different macro-strata 10-200, 10-800 or 200-800 m, with an extension shown in Table 2.4.a.

Table 2.4.a – Surface area (km²) of macro-strata considered in the analysis for each GSA.

Macro-strata	Surface area (km²)		
	GSA 17	GSA 18	GSA 19
10-200 m	85002	19529	6489
10-800 m	92261	29008	16347
200-800 m	7259	9479	9858

Temporal trend and spatial patterns can be estimated. In presence of a ***short trawl survey time series*** the significance of the **temporal trend** is estimated using nonparametric statistical tests as ***Spearman rho***, (also known as the Hotelling-Pabst test) (e.g. Cotter, 2009). Generalised Additive Models (GAM), as in the **Intersection Union Test** developed by Trenkel and Rochet (2009), can be applied for longer time series. This method estimates the direction of recent changes making use of first and second derivatives of smoothed indicator time series and the position of the most recent years with respect to the full time series.

BioIndex software also gives the possibility to perform a simplified spatial analysis of the above-described indices. Indeed, placing the indices in the **spatial dimension** is very useful for several objectives:

- the knowledge of the distribution and abundance of the species at local and regional spatial scale;
- the identification of areas with certain peculiarities;
- the localization of sensitive life stage of the population, etc…

The spatial analysis allows to place in the spatial dimension a selection among the 9 proposed indicators computed as average of a recent time span (for example 5 or 10 years): biomass, abundance, mean individual weight, sex ratio and inverse of abundance coefficient of variation. For the mapping of such indicators, the GFCM grid is considered the most appropriate spatial scale to be used in the different steps of the analysis, especially considering the subsequent possible overlap with maps of the fishing effort spatial distribution. In particular, the plot output of the spatial analysis

done by BioIndex was improved clipping the GFCM grid to three different macro-strata (10-200, 10-800, 200-800 m). This will avoid to show the species out of the range of its own distribution. Bubble plots of recruits and spawners, as abundance indices by year are an output for the identification of areas where critical life stages (juveniles and spawners) are more concentrated (using maps).

Several features of BioIndex routine and working details are schematised in the presentation here embedded.

Presentazione
FAIRSEA_28-01_BIOIN

BioIndex produces as output a wide database with time series of the indicators at aggregated levels, plots of such time series trends, and results of trend analysis. In addition, simple maps representing some indicators at spatial level are also the default outputs of BioIndex. Such outputs can be used for the different purposes of the FAIRSEA project.

2.5 Standardization of main indices for a set of key species

BioStand routine developed by COISPA (available at: https://www.coispa.it) (Zupa W., L. Casciaro, I. Bitetto, M.T. Spedicato. 2020. BioIndex v.2.1.2) is an R software included in the BioIndex package. It helps user in the standardization of indices in a time series.

It is also worth to highlight that within stock assessment working groups of the Mediterranean and Black Sea, it was often pointed out the need of using standardized survey indices and CPUE to overcome the possibility to produce inaccurate results. Indeed, the use of unstandardized indices as tuning index in stock assessment models could likely bias the perception of the stocks.

One of the most frequent approaches to the standardization of fishery dependent and independent data is the use of Generalized Additive Models (GAM) (Denis et al., 2002; Mateo and Hanselman, 2014; Wood, 2001). These models are a generalization of Generalized Linear Models (GLM) in which the linear relationships between the response and predictor variables are replaced by non-linear 'smooths'. The advantage of these models is that they are nonparametric additive models in which also factorial predictors could be used producing step functions (Wood, 2017). In BioStand the standardization process is divided in four steps (Figure 2.5.A):

1. Data preparation for the analysis
2. Explorative analysis of data
3. Modelling
4. Time series standardization

As BioIndex, BioStand allows to perform the analysis both at GSA and country level.

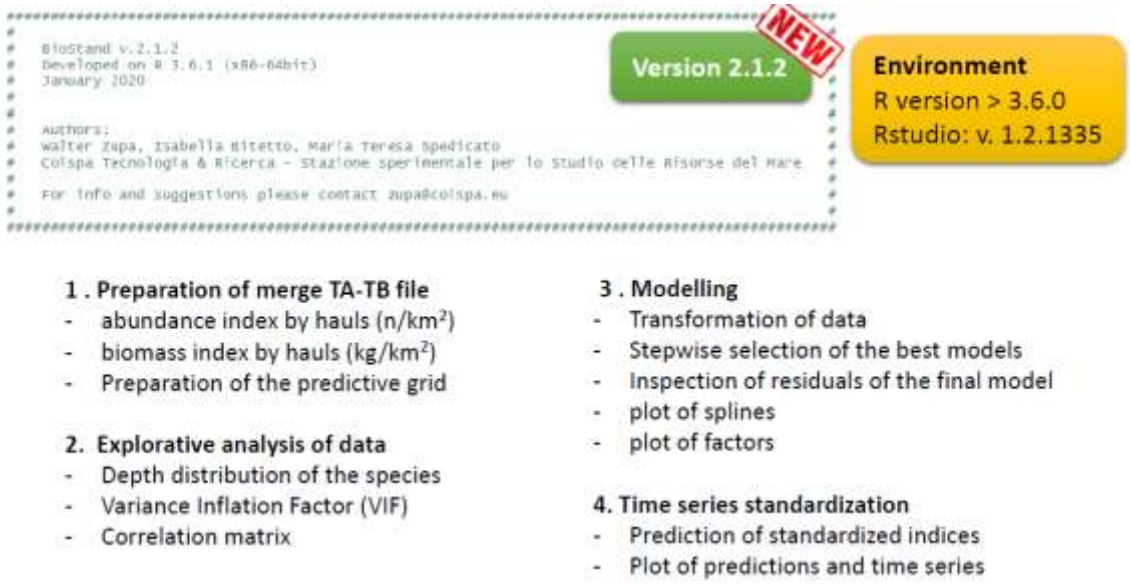

Figure 2.5.A – BioStand main features.

The steps of the modelling GAM approach adopted in BioStand is reported in the Figure 2.5.B.

Explanatory variables

- geographical position (latitude, longitude and depth)
- year
- month
- shooting time (hour)
- Hauls number per year
- stratum

Exploratory analysis

- Variance Inflation Factor (VIF)
- Pearsons' coefficient

Family distributions

- Gaussian
- Quasi-Poisson
- Tweedie

Link functions (transformations)

- identity
- Log
- Sqrt
- Inverse

Selection of best model

- Selection of the best model testing only the non-redundant variables using REML, stepwise procedures evaluating GCV, AIC, explained deviance, etc...
- inspection of residuals, splines and partial effect of factor variables
- Prediction of the standardized time series using a regular grid and the sampling points (hauls positions); plot of annual prediction maps

Figure 2.5.B – Main steps of GAM modelling.

The BioStand routine also provides the possibility to plot the annual maps of both the predictions of the final model and the bubble plots of the observed data. The raster file of each annual map is also saved in the "raster" folder. The maps could be useful to assess the quality of the prediction returned by the final model. In any case, the outputs of the raster files can be used to support several types of applications, including the visualization from the FAIRSEA WP4 platform. Also BioStand routine, as BioIndex, produces as output a wide database.

Several features of BioStand routine and working details are schematised in the presentation here embedded.

Presentazione FAIRSEA_28-01_BIOS

The standardization of trawl survey data, for the 5 species selected in each GSA, has involved the application of different data transformation and of different family distributions in order to find the best model for the standardization. Details for each GSA are provided in specific section (see 3.1.3, 3.2.3 and 3.3.3 section).

The modelling process followed a forward stepwise procedure for the selection of variables. The model characterized by the lowest Generalized Cross-Validation (GCV), by significant explanatory variables and the highest explained deviance was selected in each step of the procedure, until the final phase, where the best model for the standardization of biomass index was selected.

The predictive grid was made of reticulate of points regularly distributed in the space with a resolution of 0.0625 degrees in latitude and longitude. Depth data were derived for each point of the grid from the DTM data provided by EMODnet Bathymetry Consortium (2018).

3. RESULTS

In the following sub-chapters the results are reported for the main set of indicators estimated on the whole available time series for the species selected as reported at the sub-chapter 2.3.
Some relevant characteristic at spatial scale as regards the distribution of recruits and spawners are also highlighted.
For each geographical subarea, the results of the standardization of trawl survey data using BioStand are also reported for a selected number of key species, with a special focus to the ones subject to stock assessment.
Extended outputs have been uploaded on the project sharepoint (WP4-Integrated platform/Activity 4.3-BSTAT/D4.3.1Spatial distribution of marine species).

3.1 GSA17 – Northern Adriatic Sea

3.1.1 Ranking of the species from MEDITS survey

In the following Table 3.1.1.a, it is reported the ranking obtained for the commercial species represented in the MEDITS and SOLEMON surveys. Considering a cumulative percentage of 90%, 13 species were considered for MEDITS. To these, the common sole and the spottail mantis shrimp, which are also important in the GSA 17, have been added from SOLEMON survey, thus for a total of 15 species.

Table 3.1.1.a - Ranking of MEDITS and SOLEMON species selected for the GSA17.

GSA17 (west)		
Species	**MEDITS CODE**	**CUMULATIVE %**
Mullus barbatus	MULLBAR	30.3
Illex coindetii	ILLECOI	41.7
Merluccius merluccius	MERLMER	50.7
Micromesistius poutassou	MICMPOU	59.3
Merlangus merlangus	GADUMER	67.3
Trachurus mediterraneus	TRACMED	73.0
Trachurus trachurus	TRACTRA	78.6
Eledone moschata	ELEDMOS	82.4

Boops boops	BOOPBOO	84.2
Loligo vulgaris	LOLIVUL	86.1
Pagellus erythrinus	PAGEERY	87.5
Trisopterus capelanus	TRISCAP	88.8
Parapenaeus longirostris	PAPELON	90.1
Species	**SOLEMON CODE**	
Solea solea	SOLEVUL	
Squilla mantis	SQUIMAN	

3.1.2 Analysis of trawl survey data with BioIndex

BioIndex (version 2.1.2) was carried out to derive all the indicators provided by the software and described in the Methods section. The outputs are provided in an Excel file and a selection is summarized in terms of trend significance and ranges in Table 3.1.2.a. The extended outputs in terms of tables of indicators, plots and raster files are reported on the sharepoint (WP4-Integrated platform/Activity 4.3-BSTAT/D4.3.1Spatial distribution of marine species).

The trends of abundance, biomass and positive hauls are increasing for about 50% of the examined species (Table 3.1.2.a). In some situations, decreasing trends of population structure are highlighted. For *Merluccius merluccius* such trends are associated to a decreasing of the biomass index.

As regards the aggregation of recruits and spawners at spatial level, the Figure 3.1.2.A shows that for *M. merluccius* both recruits and spawners are mainly concentrated in the area of central Adriatic Sea, particularly along the east coast, close to Croatia country and Pomo Area.

Recruits and spawners of *P. longirostris* are concentrated in the south of GSA 17 (Figure 3.1.2.B), higher abundance for species were observed in the southern side of Croatia coasts, between 100 and 200 m depth, and also in the southern costs of Italy of the GSA 17.

Recruits of *M. barbatus* (Figure 3.1.2.C) could be observed sporadically, given the usual period of the MEDITS survey. Spawners can be observed on both sides of the

GSA, though recruits appear to be more abundant on the west side and spawners on the east one.
Finally, the recruits and spawners of *I. coindetii* (Figure 3.1.2.D) are concentrated in the central part of GSA 17, along east coast for recruits, especially central and south part of the GSA and west coast for spawners, along the entire area.

Table 3.1.2.a – Summary table of the principal indicators calculated by BioIndex for all the species analysed.

Species	Depth range	abundance n/km²	CV abundance	biomass (kg/km²)	CV biomass (kg/km²)	Positive hauls	50th perc	CV 50th perc	95th perc	CV 95th perc	Abundance trend	Biomass trend	Positive hauls	50th perc trend	95th perc trend
MULL BAR	10-200	228-9812	0.25-0.20	7.43-125.66	0.25-0.09	43.02-98.9	103.3-141	0.0006-0.0027	153.9-187.7	0.0007-0.0066	↗	↗	↗	↔	↔
ILLEC OI	10-200	18.34-1931	0.06-0.2	2.011-35.88	0.06-0.19	38.37-91.59	64.6-152.7	0.0017-0.022	114.4-199	0.0019-0.012	↗	↗	↗	↔	↘
MERL MER	10-200	324.61-1622.56	0.07-0.19	16.79-59.55	0.06-0.13	74.41-97.67	104-178.8	0.0017-0.0077	240.5-318	0.0028-0.014	↔	↔	↔	↔	↗
MICM POU	10-500	51.26-3007.29	0.17-0.71	2.21-56.16	0.16-0.63	2.32-28.33	NA	NA	NA	NA	NA	NA	NA	NA	NA
GADU MER	10-100	28.19-5411.71	0.12-0.53	2.15-63.01	0.12-0.46	15.29-55.81	NA	NA	NA	NA	↔	↔	↔	NA	NA
TRAC MED	10-100	10.51-4176.02	0.11-0.58	0.47-39.84	0.11-0.50	15.73-73.25	NA	NA	NA	NA	↗	↗	↗	NA	NA
TRAC TRA	10-100	100-5489.05	0.14-0.38	1.04-40	0.14-0.42	52.32-93.02	NA	NA	NA	NA	↔	↔	↔	NA	NA
ELED MOS	10-200	18.21-336.62	0.11-0.36	2.02-31.70	0.11-0.47	19.76-43.33	NA	NA	NA	NA	↔	↔	↔	NA	NA
BOOP BOO	10-100	370.46-321.123	0.17-0.54	5.12-35.71	0.18-0.50	31.39-67.44	NA	NA	NA	NA	↔	↔	↔	NA	NA
LOLI VUL	10-100	4.65-1037.31	0.12-0.54	0.17-20.29	0.12-0.39	12.22-73.59	NA	NA	NA	NA	↔	↔	↔	NA	NA
PAGE ERY	10-100	12.04-568.15	0.18-0.42	0.41-23.36	0.24-0.66	15.29-56.28	NA	NA	NA	NA	↗	↗	↗	NA	NA
TRISC AP	10-200	146.72-2708.99	0.07-0.61	2.63-40.41	0.09-0.75	61.11-81.39	NA	NA	NA	NA	↘	↘	↔	NA	NA
PAPE LON	10-200	0-2449.8	0.09-0.72	0-11.95	0.09-0.76	3.48-58.89	NA	NA	NA	NA	↗	↗	↗	NA	NA
SOLE VUL	10-100	212.7-920.70	0.13-0.30	24.77-91.04	0.10-0.19	76.11-95.52	NA	NA	NA	NA	↗	↗	NA	NA	NA

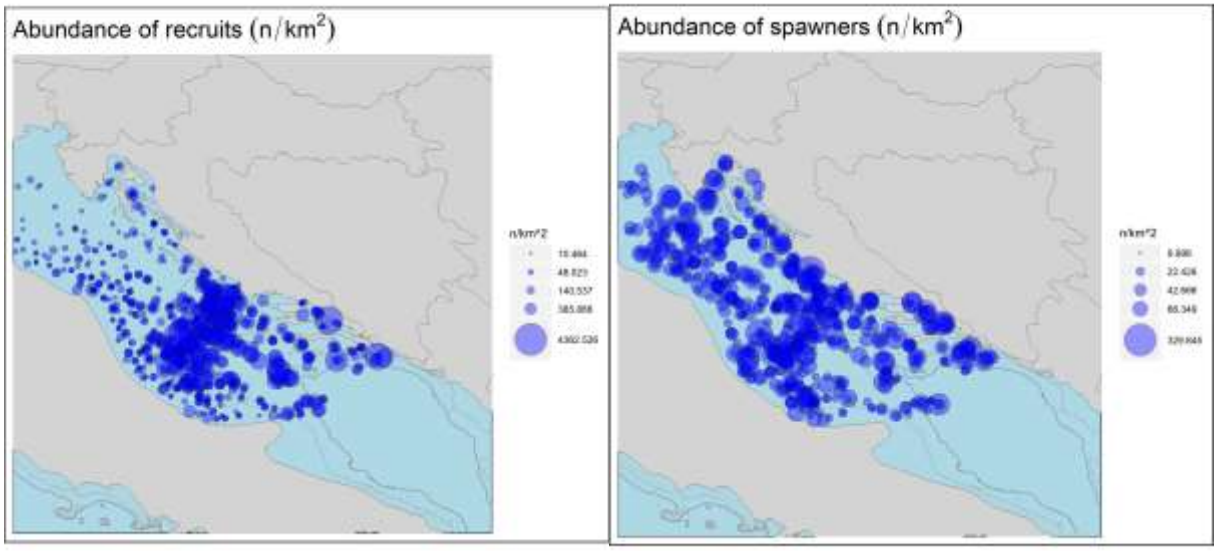

Figure 3.1.2.A – Spatial distribution of recruits and spawners of *M. merluccius* in GSA 17 during the time series 2014-2018.

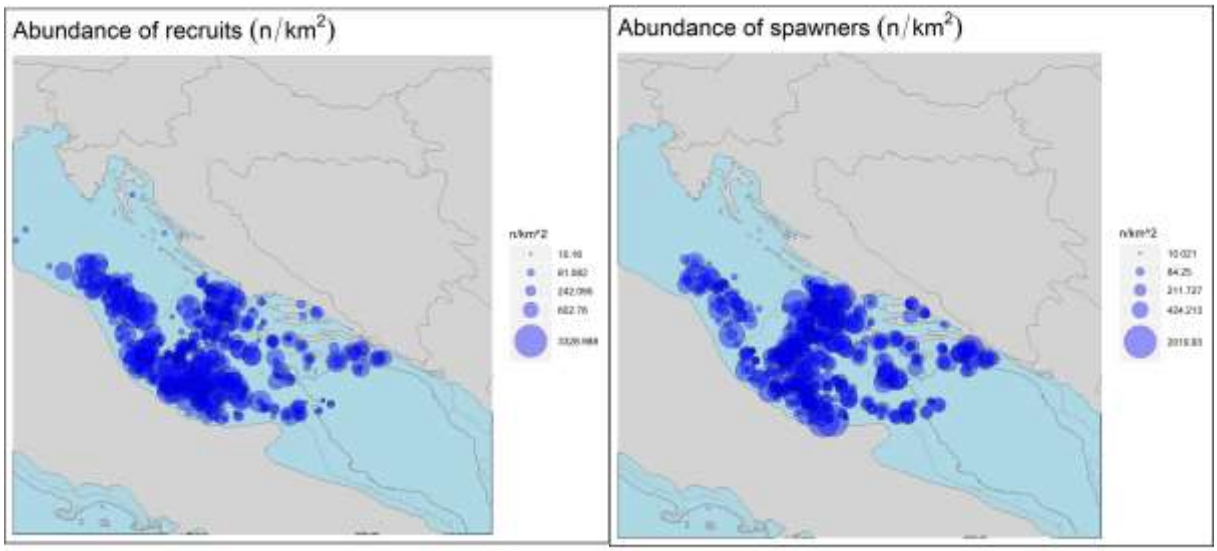

Figure 3.1.2.B – Spatial distribution of recruits and spawners of *P. longirostris* in GSA 17 during the time series 2014-2018.

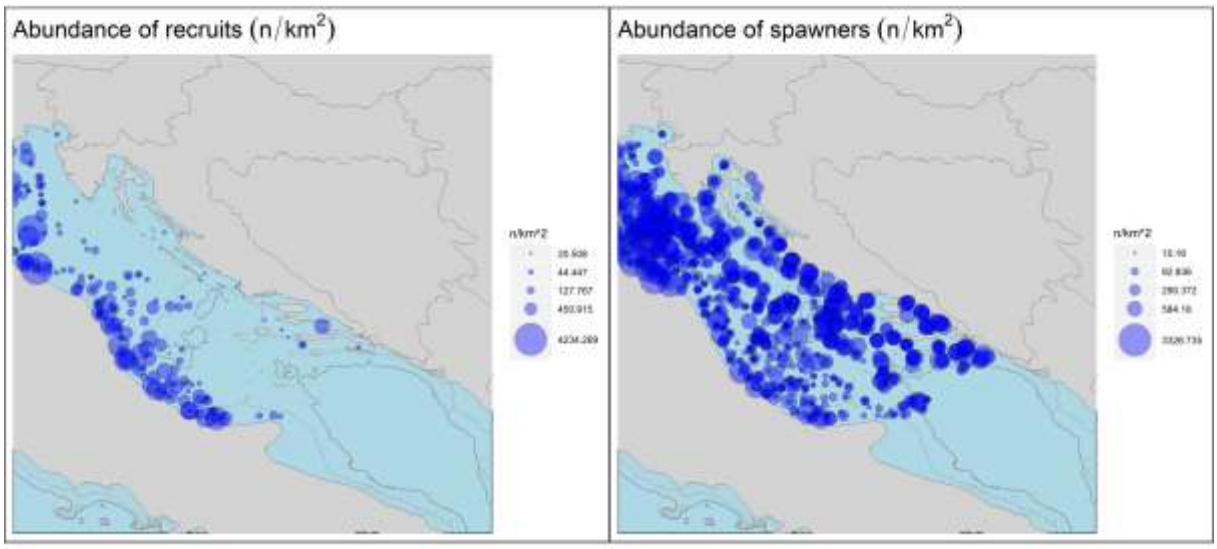

Figure 3.1.2.C – Spatial distribution of recruits and spawners of *M. barbatus* for GSA 17 during the time series 2014-2018.

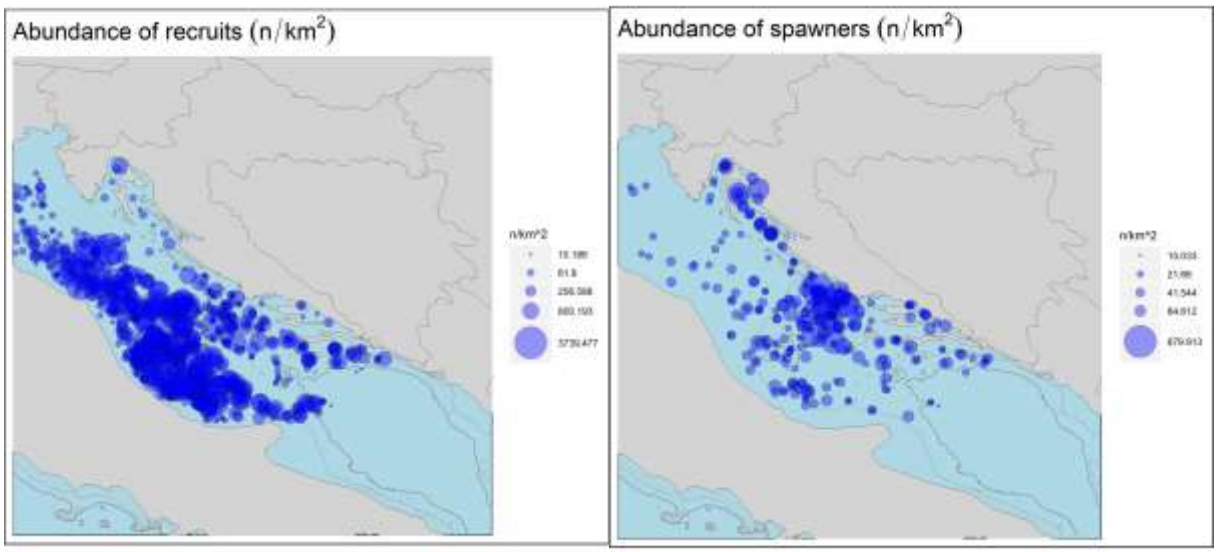

Figure 3.1.2.D – Spatial distribution of recruits and spawners of *I. coindetii* for GSA 17 during the time series 2014-2018.

3.1.3 Standardization of trawl survey data with BioStand

BioStand (version 2.1.2) was carried out to standardize the data described in Data section for the following selected species: *M. merluccius, M. barbatus, P. longirostris, I. coindetii, S. solea*. For all the species, different data transformation as identity, log normal and squared root data with different family distributions such as Gaussian, Gamma and Tweedie were explored.

3.1.3.1 *Merluccius merluccius*

The analysis was performed using data from MEDITS survey conducted in the period between the 1994 and 2018, focusing on the bathymetrical range 10-500 m.

The presence of correlations among the explanatory variables was tested using the Pearson's correlation coefficients (Table 3.1.3.1.a). The correlation matrix reported in the table 3.1.3.1.a shows a correlation coefficient of -0.73 for latitude and longitude while, for these two variables VIF values of 2.25 (longitude) and 2.67 (latitude) were estimated. Being the VIF values lower than the threshold value (3), no collinearity was detected between these variables.

Table 3.1.3.1.a - Correlation table among the quantitative explanatory variables explored for *M. merluccius* in GSA 17.

	year	**month**	**hour**	**Y**	**X**	**depth**
year		0.40	0.05	0.00	0.08	0.05
month	0.40		-0.14	-0.09	0.06	0.05
hour	0.05	-0.14		0.01	0.06	0.05
Y	0.00	-0.09	0.01		-0.73	-0.59
X	0.08	0.06	0.06	-0.73		0.67
depth	0.05	0.05	0.05	-0.59	0.67	

The explanatory variables considered are the year, month, depth, hour, latitude, longitude, sampling intensity (expressed as number of hauls, defined as a factor).
The list of the most relevant models explored is reported in Table 3.1.3.1.b; in bold the best performing model is reported.

Table 3.1.3.1.b – Selection of the models explored for *M. merluccius* in GSA 17 (biomass index kg/km^2). In bold the best performing model is reported.

	Model (Gaussian, transf: sqrt)	**% Deviance**	**GCV**
1	$s(X_{i,j}) + \varepsilon_{i,j}$	32.8%	6.69
2	$s(Y_{i,j}) + \varepsilon_{i,j}$	21.2%	7.85
3	$s(X_{i,j},Y_{i,j}) + \varepsilon_{i,j}$	39.8%	6.03
4	$s(depth_{i,j}) + \varepsilon_{i,j}$	36.3%	6.35
5	$f(year_j) + \varepsilon_{i,j}$	7.94%	9.29
6	$f(month_{i,j}) + \varepsilon_{i,j}$	1.76%	9.80
7	$s(X_{i,j},Y_{i,j,}) + s(depth_{i,j}) + f(nb\_hauls_{i,j}) + \varepsilon_{i,j}$	56%	4.53
8	$s(X_{i,j}, Y_{i,j}) + s(depth_{i,j}) + f(month_j) + \varepsilon_{i,j}$	55.8%	4.55
	Model (Gaussian, transf: log)	**% Deviance**	**GCV**
9	$s(Xi,j) + \varepsilon i,j$	39.3%	1.28

10	*s(Yi,j) + εi,j*	27.1%	1.54
11	*s(Xi,j,Yi,j) + εi,j*	46.8%	1.13
12	*s(depthi,j) + εi,j*	48%	1.10
13	*f(yearj) + εi,j*	7.06%	1.99
14	*f(monthi,j) + εi,j*	2.22%	2.07
15	*s(Xi,j,Yi,j)+s(depthi,j)+f(nb_haulsi,j) + εi,j*	64.2%	0.78
16	*s(Xi,j, Yi,j) + s(depthi,j,) + f(monthj) + εi,j*	64%	0.78

	Model (tw)	**% Deviance**	**REML**
17	***s(Xi,j, Yi,j) + s(depthi,j,) + s(yearj) + εi,j***	**49.6%**	**11460**
18	*s(Xi,j, Yi,j) + s(depthi,j,) + s(yearj) +f(nb_haul)+ εi,j*	50.7%	11443

Although the highest value of Deviance explained was associated to the model 15, the best model in terms of better fitting the observation data is the model 17 (18 is overfitted). The model summary is reported in Table 3.1.3.1.c and indicates the significance of the geographical position, depth and year. The residuals of the model and the q-q plot, reported in Figure 3.1.3.1.A show a quite normal distribution.

The estimation of the splines was found significant (Table 3.1.3.1.c and Figure 3.1.3.1.B).

Table 3.1.3.1.c – Summary of the estimates, GVC and deviance explained of the best GAM for *M. merluccius* in GSA 17.

Summary (mod 17)

****
family: tw
link : log
transformation: identity
****
-- Summary of the model --

Family: Tweedie(p=1.442)
Link function: log

Formula:
response ~ s(year) + s(X, Y) + s(depth)

Parametric coefficients:

	Estimate	Std. Error	t value	Pr(>|t|)	
(Intercept)	3.04096	0.01526	199.3	<2e-16	***

Signif. codes: 0 '***' 0.001 '**' 0.01 '*' 0.05 '.' 0.1 ' ' 1

Approximate significance of smooth terms:

	edf	Ref.df	F	p-value	
s(year)	8.558	9	78.75	<2e-16	***
s(X,Y)	26.257	29	39.60	<2e-16	***
s(depth)	8.668	9	36.27	<2e-16	***

Signif. codes: 0 '***' 0.001 '**' 0.01 '*' 0.05 '.' 0.1 ' ' 1

R-sq.(adj) = 0.369 Deviance explained = 49.6%

-REML = 11460 Scale est. = 4.0729 n = 3974

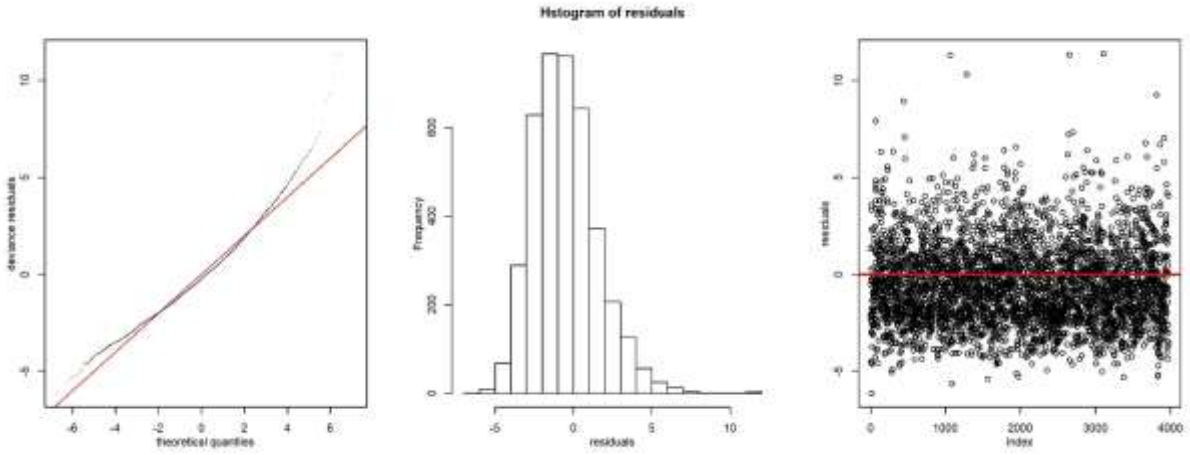

Figure 3.1.3.1.A – Diagnostic plots of residuals for *M. merluccius* in GSA 17.

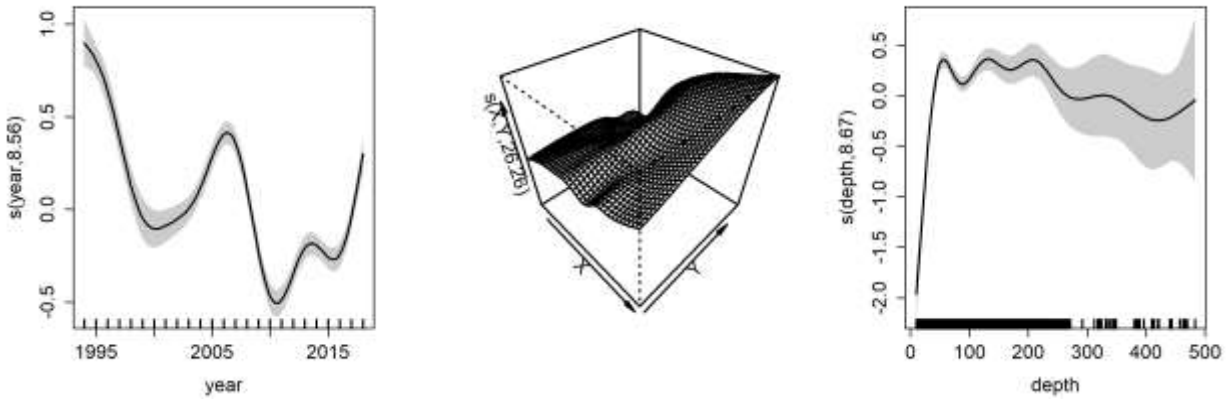

Figure 3.1.3.1.B – Splines of the best model for *M. merluccius* in GSA 17.

Only the points of the predictive grid corresponding to a depth comprised in the 10-500 m range were selected. Depth data were derived for each point of the grid from the DTM data provided by EMODnet Bathymetry Consortium (2018). The grid points were also linked to the values of the other variables included in the best GAM and useful to predict the model in the standardized conditions: year, month (for standardization was used July) and number of hauls.

In Figure 3.1.3.1.C the comparison is reported between the original indices estimated on rough data according to Souplet (1996) and the indices estimated on the predicted results, predicted over the grid with the corresponding confidence intervals (Figure 3.1.3.1.C left). The prediction was also done on the original haul positions (Figure 3.1.3.1.C right).

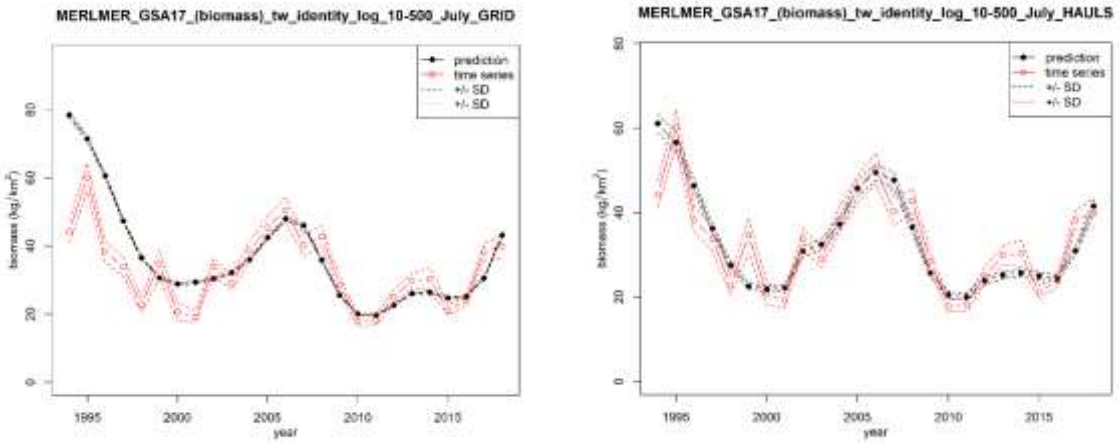

Figure 3.1.3.1.C – Comparison between the original and standardized biomass indices of *M. merluccius* in GSA 17 predicted on the grid (left) and on the haul positions (right).

3.1.3.2 *Parapenaeus longirostris*

The analysis was performed using data from MEDITS survey conducted in the period between the 1994 and 2018, focusing on the bathymetrical range 10-500 m.

The presence of correlations among the explanatory variables was tested using the Pearson's correlation coefficients (Table 3.1.3.2.a). The correlation matrix shows a correlation coefficient of -0.73 for latitude and longitude while, for these two variables VIF values of 2.25 (longitude) and 2.67 (latitude) were estimated. Being the VIF values lower than the threshold value (3), no collinearity was detected between these variables.

Table 3.1.3.2.a - Correlation table among the quantitative explanatory variables explored for *P. longirostris* in GSA 17.

	year	**month**	**hour**	**Y**	**X**	**depth**
year		0.40	0.05	0.00	0.08	0.05
month	0.40		-0.14	-0.09	0.06	0.05
hour	0.05	-0.14		0.01	0.06	0.05
Y	0.00	-0.09	0.01		-0.73	-0.59
X	0.08	0.06	0.06	-0.73		0.67
depth	0.05	0.05	0.05	-0.59	0.67	

The explanatory variables considered are the year, month, depth, hour, latitude, longitude, sampling intensity (expressed as number of hauls, defined as a factor). The list of the most relevant models explored is reported in Table 3.1.3.2.b; in bold the best performing model is reported.

Table 3.1.3.2.b – Selection of the models explored for *P. longirostris* in GSA 17 (biomass index kg/km^2). In bold the best performing model is reported.

	Model (Gaussian, transf: sqrt)	**% Deviance**	**GCV**
1	$s(X_{i,j}) + \varepsilon_{i,j}$	27.2%	1.59
2	$s(Y_{i,j}) + \varepsilon i,j$	18.3%	1.79
3	$s(X_{i,j},Y_{i,j}) + \varepsilon_{i,j}$	30.5%	1.53
4	$s(depth_{i,j}) + \varepsilon_{i,j}$	29.2%	1.55
5	$f(year_j) + \varepsilon_{i,j}$	13.9%	1.90
6	$f(monthi,j) + \varepsilon_{i,j}$	6.03%	2.05
7	$s(X_{i,j},Y_{i,j}) + s(depth_{i,j}) + f(nb\_hauls_{i,j}) + \varepsilon_{i,j}$	55.4%	1.00
8	$s(X_{i,j},Y_{i,j}) + s(depth_{i,j}) + f(month_{j,j}) + \varepsilon_{i,j}$	55.1%	1.01
Model (Gaussian, transf: log)		**% Deviance**	**GCV**
9	$s(X_{i,j}) + \varepsilon_{i,j}$	29.5%	0.65
10	$s(Y_{i,j}) + \varepsilon_{i,j}$	20.4%	0.74
11	$s(X_{i,j},Y_{i,j}) + \varepsilon_{i,j}$	33.3%	0.62
12	$s(depth_{i,j}) + \varepsilon_{i,j}$	31.9%	0.63
13	$f(year_j) + \varepsilon_{i,j}$	14%	0.80
14	$f(month_{i,j}) + \varepsilon_{i,j}$	6.94%	0.86
15	$s(X_{i,j},Y_{i,j,})+s(depth_{i,j})+f(nb\_hauls_{i,j}) + \varepsilon_{i,j}$	58.7%	0.39
16	$s(X_{i,j}, Y_{i,j}) + s(depth_{i,j}) + f(month_{i,j}) + \varepsilon_{i,j}$	57.2%	0.36
	Model (tw)	**% Deviance**	**REML**
17	$\boldsymbol{s(X_{i,j}, Y_{i,j}) + s(depth_{i,j}) + s(year_j) + \varepsilon_{i,j}}$	**74.2%**	**3302**
18	$s(Xi,j, Yi,j) + s(depthi,j,) + s(year_j)+f(nb\_haul_{i,j}) + \varepsilon i,j$	75.2%	3343.8

The best model result in model number 17 (18 is overfitted), data identity, family Tweedie, link log, depth range 10-500 m, factor month.

The model summary is reported in Table 3.1.3.2.c and indicates the significance of the geographical position, depth and year. The residuals of the model and the q-q plot, reported in Figure 3.1.3.2.A show a left skewed distribution. The estimation of the splines was found significant (Table 3.1.3.2.c and Figure 3.1.3.2.B).

Table 3.1.3.2.c – Summary of the estimates, GVC and deviance explained of the best GAM for *P. longirostris* in GSA 17.

****

family: tw
link : log

transformation: identity
****

-- Summary of the model --

Family: Tweedie (p=1.562)
Link function: log

Formula:
response ~ s(year) + s(X, Y) + s(depth)

Parametric coefficients:
            Estimate Std. Error t value Pr(>|t|)
(Intercept) -4.1321   0.2044 -20.21   <2e-16 ***

Signif. codes: 0 ‘***’ 0.001 ‘**’ 0.01 ‘*’ 0.05 ‘.’ 0.1 ‘ ’ 1

Approximate significance of smooth terms:
           edf Ref.df   F p-value
s(year)   7.704   9 171.25 <2e-16 ***
s(X,Y)   27.416   29 48.55 <2e-16 ***
s(depth) 5.609   9 13.21 <2e-16 ***

Signif. codes: 0 ‘***’ 0.001 ‘**’ 0.01 ‘*’ 0.05 ‘.’ 0.1 ‘ ’ 1

R-sq.(adj) = -0.0944   Deviance explained = 74.2%
-REML = 3379.3 Scale est. = 3.1717   n = 3974

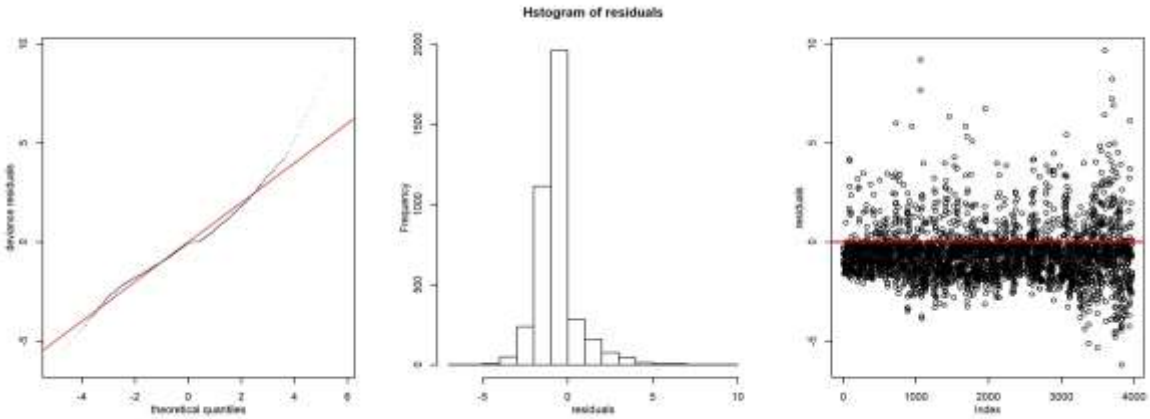

Figure 3.1.3.2.A – Diagnostic plots of residuals for *P. longirostris* in GSA 17.

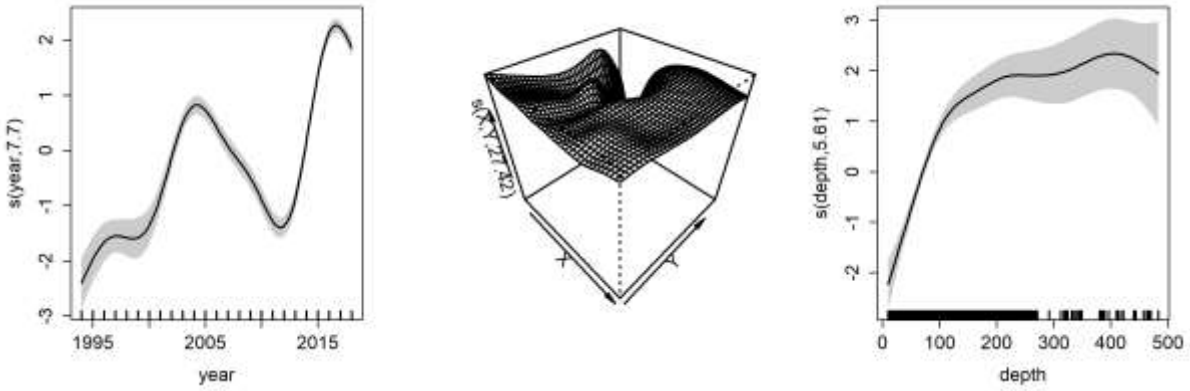

Figure 3.1.3.1.B – Splines of the best model for *P. longirostris* in GSA 17.

Only the points of the predictive grid corresponding to a depth comprised in the 10-500 m range were selected. The grid points were also linked to the values of the other variables included in the best GAM and useful to predict the model in the standardized conditions: year, month and number of hauls.

In Figure 3.1.3.2.C the comparison is reported between the original indices estimated on rough data according to Souplet (1996) and the indices estimated on the predicted results, predicted over the grid with the corresponding confidence intervals (Figure 3.1.3.2.C left). The prediction was done also on the original haul positions (Figure 3.1.3.2.C right).

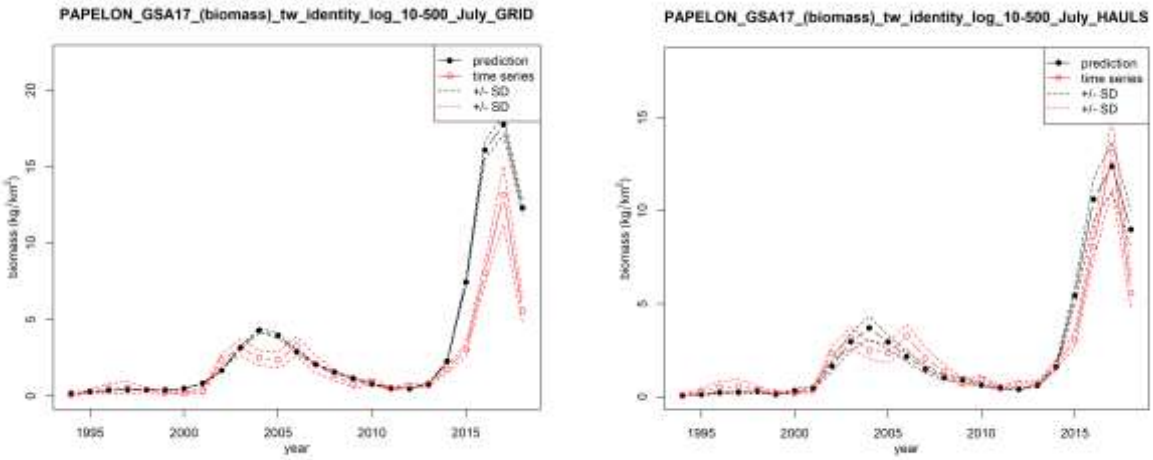

Figure 3.1.3.2.C – Comparison between the original and standardized biomass indices of *P. longirostris* in GSA 17 predicted on the grid (left) and on the haul positions (right).

3.1.3.3 *Mullus barbatus*

The analysis was performed using data from MEDITS survey conducted in the period between the 1994 and 2018, focusing on the bathymetrical range 10-200 m.
The presence of correlations among the explanatory variables was tested using the Pearson's correlation coefficients (Table 3.1.3.3.a). The correlation matrix reported in the table 3.1.3.3.1 shows a correlation coefficient of -0.66 for latitude and longitude while, for these two variables VIF values of 1.79 (longitude) and 2.33 (latitude) were estimated. Being the VIF values lower than the threshold value (3), no collinearity was detected between these variables.

Table 3.1.3.3.a - Correlation table among the quantitative explanatory variables explored for *M. barbatus* in GSA 17.

	year	**month**	**hour**	**Y**	**X**	**depth**
year		0.42	0.06	0.02	0.07	0.04
month	0.42		-0.14	-0.05	0.05	-0.01
hour	0.06	-0.14		0.03	0.04	0.08
Y	0.02	-0.05	0.03		-0.66	-0.36
X	0.07	0.05	0.04	-0.66		0.58
depth	0.04	-0.01	0.08	-0.36	0.58	

The explanatory variables considered are the year, month, depth, hour, latitude, longitude, sampling intensity (expressed as number of hauls, defined as a factor). The list of the most relevant models explored is reported in Table 3.1.3.3.b; in bold the best performing model is reported.

Table 3.1.3.3.b – Selection of the models explored for *M. barbatus* in GSA 17 (biomass index kg/km^2). In bold the best performing model is reported.

	Model (*Gaussian, transf: sqrt*)	% Deviance	GCV
1	$s(X_{i,j}) + \varepsilon_{i,j}$	8.36%	24.51
2	$s(Y_{i,j}) + \varepsilon_{i,j}$	8.63%	24.47
3	$s(X_{i,j},Y_{i,j}) + \varepsilon_{i,j}$	19.4%	21.65
4	$s(depth_{i,j}) + \varepsilon_{i,j}$	6.46%	25.07
5	$f(year_j) + \varepsilon_{i,j}$	17.6%	22.34
6	$f(month_{i,j}) + \varepsilon_{i,j}$	7.43%	24.8
7	$s(X_{i,j},Y_{i,j,})+s(depth_{i,j})+f(nb\_hauls_{i,j}) + \varepsilon_{i,j}$	51.9%	13.3
8	$s(X_{i,j}, Y_{i,j}) + s(depth_{i,j,}) + f(month_j) + \varepsilon_{i,j}$	51%	13.57
	Model (*Gaussian, transf: log*)	**% Deviance**	**GCV**
9	$s(X_{i,j}) + \varepsilon_{i,j}$	13.3%	3.17
10	$s(Y_{i,j}) + \varepsilon_{i,j}$	11.8%	3.22
11	$s(X_{i,j},Y_{i,j}) + \varepsilon_{i,j}$	28%	2.64
12	$s(depth_{i,j}) + \varepsilon_{i,j}$	8.04%	3.36
13	$f(year_j) + \varepsilon_{i,j}$	18.8%	3.00
14	$f(month_{i,j}) + \varepsilon_{i,j}$	8.27%	3.35
15	$s(X_{i,j},Y_{i,j,},)+s(depth_{i,j})+f(nb\_hauls_{i,j}) + \varepsilon_{i,j}$	61.9%	1.44
16	$\mathbf{s(X_{i,j}, Y_{i,j}) + s(depth_{i,j}) + s(year_j)+ \varepsilon_{i,j}}$	**59.4.%**	**1.52**
	Model (tw)	**% Deviance**	**REML**
17	$s(X_{i,j},Y_{i,j,},)+s(depth_{i,j})+f(month_{i,j}) + \varepsilon_{i,j}$	52%	10056
18	$s(X_{i,j},Y_{i,j,},)+s(depth_{i,j})+f(nb\_haul_{i,j}) + \varepsilon_{i,j}$	50.0%	10078

The best model result in model number 16 (17 is overfitted), data log transformed, family Gaussian, link Identity, depth range 10-200 m, factors month.

The model summary is reported in Table 3.1.3.3.c and indicates the significance of the geographical position, depth and year. The residuals of the model and the q-q plot, reported in Figure 3.1.3.3.A show a quite normal distribution. The estimation of the splines was found significant (Table 3.1.3.3.c and Figure 3.1.3.3.B).

Table 3.1.3.3.c – Summary of the estimates, GVC and deviance explained of the best GAM for *M. barbatus* in GSA 17.

****
family: gaussian
link : identity
transformation: log
****
-- Summary of the model --
Family: gaussian

Link function: identity

Formula:
response ~ s(year) + s(X, Y) + s(depth)

Parametric coefficients:
Estimate Std. Error t value Pr(>|t|)
(Intercept) 2.19345 0.02006 109.3 <2e-16 ***

Signif. codes: 0 '***' 0.001 '**' 0.01 '*' 0.05 '.' 0.1 ' ' 1

Approximate significance of smooth terms:
edf Ref.df F p-value
s(year) 7.607 9 145.64 <2e-16 ***
s(X,Y) 27.904 29 111.56 <2e-16 ***
s(depth) 8.286 9 80.07 <2e-16 ***

Signif. codes: 0 '***' 0.001 '**' 0.01 '*' 0.05 '.' 0.1 ' ' 1

R-sq.(adj) = 0.589 Deviance explained = 59.4%
GCV = 1.5275 Scale est. = 1.4944 n = 3713

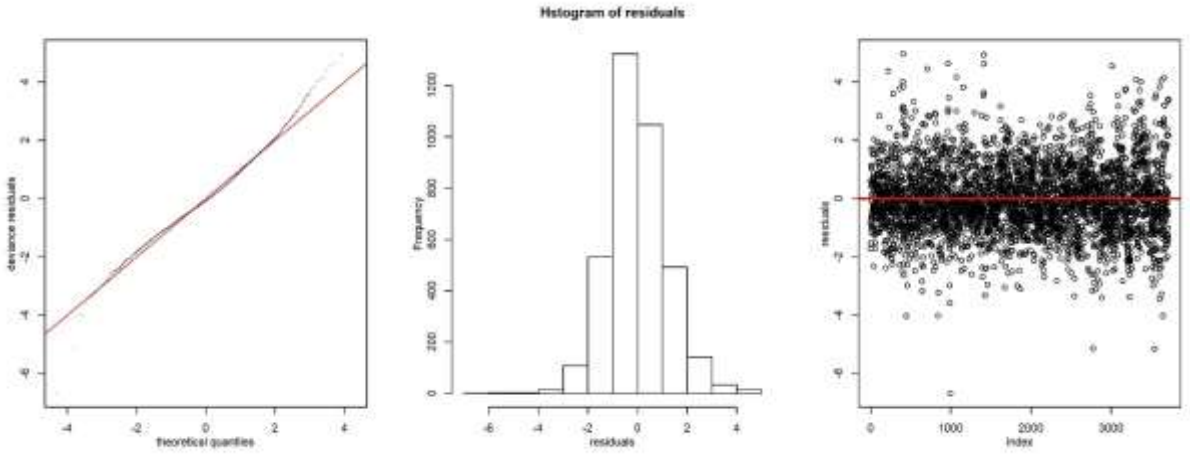

Figure 3.1.3.3.A – Diagnostic plots of residuals for *M. barbatus* in GSA 17.

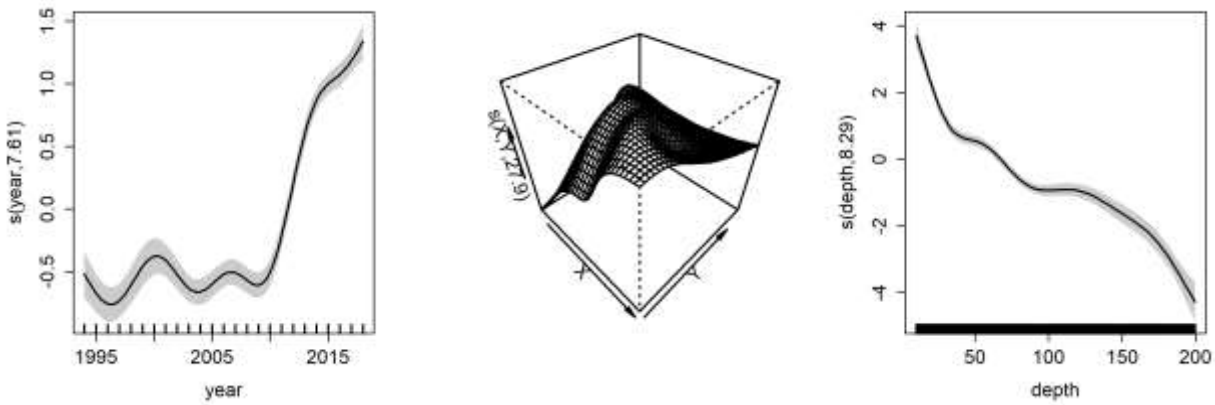

Figure 3.1.3.3.B – Splines of the best model for *M. barbatus* in GSA 17.

Only the points of the predictive grid corresponding to a depth comprised in the 10 - 200 m range were selected. The grid points were also linked to the values of the other variables included in the best GAM and useful to predict the model in the standardized conditions: year and number of hauls.

In Figure 3.1.3.3.C the comparison is reported between the original indices estimated on rough data according to Souplet (1996) and the indices estimated on the predicted results, predicted over the grid with the corresponding confidence intervals (Figure 3.1.3.3.C left). The prediction was also done on the original haul positions (Figure 3.1

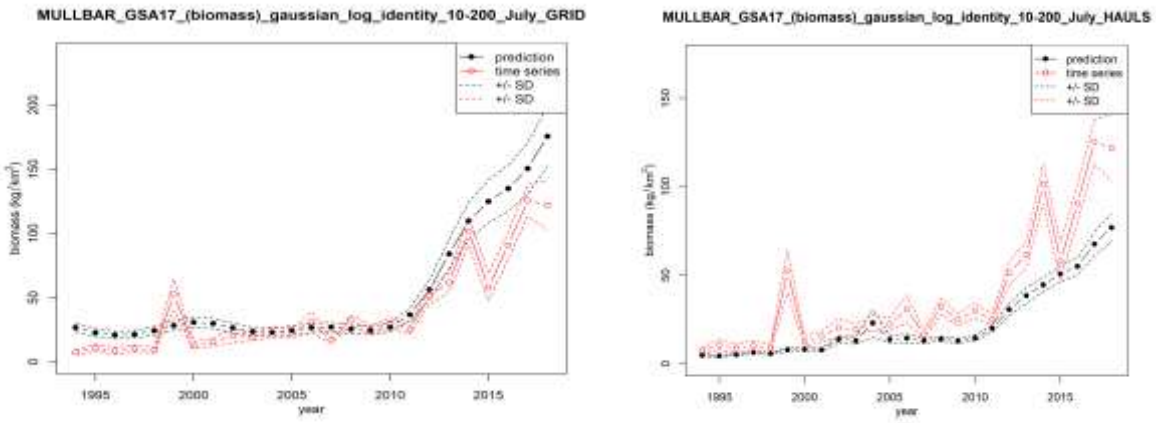

Figure 3.1.3.3.C – Comparison between the original and standardized biomass indices of *M. barbatus* in GSA 17 predicted on the grid (left) and on the haul positions (right).

3.1.3.4 *Illex coindetii*

The analysis was performed using data from MEDITS survey conducted in the period between the 1994 and 2018, focusing on the bathymetrical range 10-500 m.
The presence of correlations among the explanatory variables was tested using the Pearson's correlation coefficients (Table 3.1.3.4.a). The correlation matrix shows a correlation coefficient of -0.73 for latitude and longitude while, for these two variables VIF values of 2.25 (longitude) and 2.67 (latitude) were estimated. Being the VIF values lower than the threshold value (3), no collinearity was detected between these variables.

Table 3.1.3.4.a - Correlation table among the quantitative explanatory variables explored for *I. coindetii* in GSA 17.

	year	**month**	**hour**	**Y**	**X**	**depth**
year		0.40	0.05	0.00	0.08	0.05
month	0.40		-0.14	-0.09	0.06	0.05
hour	0.05	-0.14		0.01	0.06	0.5
Y	0.00	-0.09	0.01		-0.73	-0.59
X	0.08	0.06	0.06	-0.73		0.67
depth	0.05	0.05	0.05	-0.59	0.67	

The explanatory variables considered are the year, month, depth, hour, latitude, longitude, sampling intensity (expressed as number of hauls, defined as a factor). The list of the most relevant models explored is reported in Table 3.1.3.4.b; in bold the best performing model is reported.

Table 3.1.3.4.b - Selection of the models explored for *I. coindetii* in GSA 17 (biomass index kg/km^2). In bold the best performing model is reported.

	Model (*Gaussian, transf: sqrt*)	% Deviance	GCV
1	$s(X_{i,j}) + \varepsilon_{i,j}$	23.8%	6.85
2	$s(Y_{i,j}) + \varepsilon_{i,j}$	23.7%	6.86
3	$s(X_{i,j},Y_{i,j}) + \varepsilon_{i,j}$	28.6%	6.45
4	$s(depth_{i,j}) + \varepsilon_{i,j}$	39.4%	5.44
5	$f(year_j) + \varepsilon_{i,j}$	13.6%	7.85
6	$f(month_{i,j}) + \varepsilon_{i,j}$	5.13%	8.53
7	$s(X_{i,j},Y_{i,j,})+s(depth_{i,j})+f(nb\_hauls_{i,j}) + \varepsilon_{i,j}$	57%	3.99
8	$s(X_{i,j}, Y_{i,j}) + s(depth_{i,j}) + f(month_j) + \varepsilon_{i,j}$	56.8%	4.00
	Model (*Gaussian, transf: log*)	**% Deviance**	**GCV**
9	$s(X_{i,j}) + \varepsilon_{i,j}$	29.6%	1.64
10	$s(Y_{i,j}) + \varepsilon_{i,j}$	29.7%	1.64
11	$s(X_{i,j},Y_{i,j}) + \varepsilon_{i,j}$	35.4%	1.52
12	$s(depth_{i,j}) + \varepsilon_{i,j}$	49.3%	1.18
13	$f(year_j) + \varepsilon_{i,j}$	12.8%	2.06
14	$f(month_{i,j}) + \varepsilon_{i,j}$	4.28%	2.24
15	$s(X_{i,j},Y_{i,j,})+s(depth_{i,j})+f(nb\_hauls_{i,j}) + \varepsilon_{i,j}$	66.6%	0.81
16	$s(X_{i,j}, Y_{i,j}) + s(depth_{i,j}) + f(month_j) + \varepsilon_{i,j}$	66%	0.82
	Model (*tw*)	**% Deviance**	**REML**
17	$s(X_{i,j},Y_{i,j,})+s(depth_{i,j})+f(nb\_hauls_{i,j}) + \varepsilon_{i,j}$	57.5%	9207.5
18	$s(X_{i,j},Y_{i,j,})+s(depth_{i,j})+f(month_{i,j}) + \varepsilon_{i,j}$	57.6%	9190.4
19	$\boldsymbol{s(X_{i,j},Y_{i,j,})+s(depth_{i,j})+s(year_{i,j}) + \varepsilon_{i,}}$	**53%**	**9325**

The best model apparently result in model number 15, or 18, but the final plot are overfitted. We selected the model number 19, data identity, family Tweedie, link log, depth range 10-500 m.
The model summary is reported in Table 3.1.3.4.c and indicates the significance of the geographical position, depth and year. The residuals of the model and the q-q plot, reported in Figure 3.1.3.4.A show a left skewed distribution. The estimation of the splines was found significant (Table 3.1.3.4.c and Figure 3.1.3.4.B).

Table 3.1.3.4.3 – Summary of the estimates, GVC and deviance explained of the best GAM for *I. coindetii* in GSA 17.

****
family: tw
link : log
transformation: identity
****
-- Summary of the model --
Family: Tweedie(p=1.494)
Link function: log
Formula:
response ~ s(year) + s(X, Y) + s(depth)

Parametric coefficients:
            Estimate Std. Error t value Pr(>|t|)
(Intercept) 2.08151   0.02286   91.04   <2e-16 ***

Signif. codes: 0 ‘***’ 0.001 ‘**’ 0.01 ‘*’ 0.05 ‘.’ 0.1 ‘ ’ 1
Approximate significance of smooth terms:
            edf Ref.df   F p-value
s(year)   8.458   9 70.86 <2e-16 ***
s(X,Y)   26.943   29 23.28 <2e-16 ***
s(depth) 7.882   9 60.47 <2e-16 ***

Signif. codes: 0 ‘***’ 0.001 ‘**’ 0.01 ‘*’ 0.05 ‘.’ 0.1 ‘ ’ 1
R-sq.(adj) = 0.291   Deviance explained =   53%-REML =   9325 Scale est. = 4.2276   n = 3974

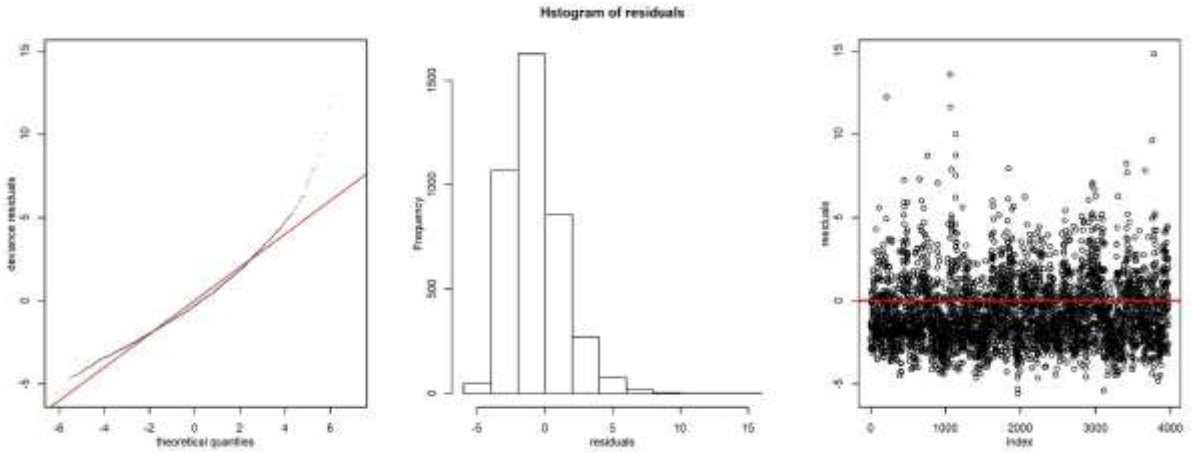

Figure 3.1.3.4.A – Diagnostic plots of residuals for *I. coindetii* in GSA 17.

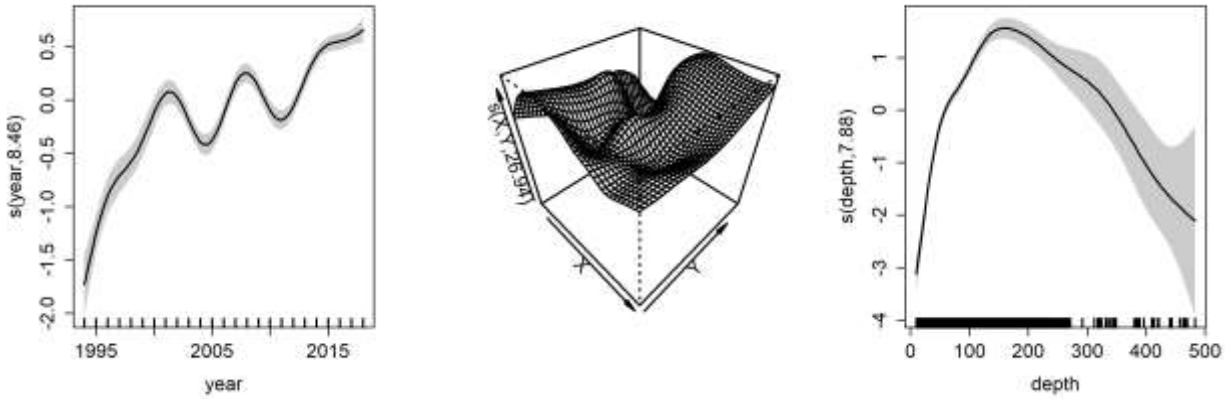

Figure 3.1.3.4.B – Splines of the best model for *I. coindetii* in GSA 17.

Only the points of the predictive grid corresponding to a depth comprised in the 10 - 200 m range were selected. The grid points were also linked to the values of the other variables included in the best GAM and useful to predict the model in the standardized conditions: year and number of hauls.

In Figure 3.1.3.4.C the comparison is reported between the original indices estimated on rough data according to Souplet (1996) and the indices estimated on the predicted results, predicted over the grid with the corresponding confidence intervals (Figure 3.1.3.4.C left). The prediction was also done on the original haul positions (Figure 3.1.3.4.C right).

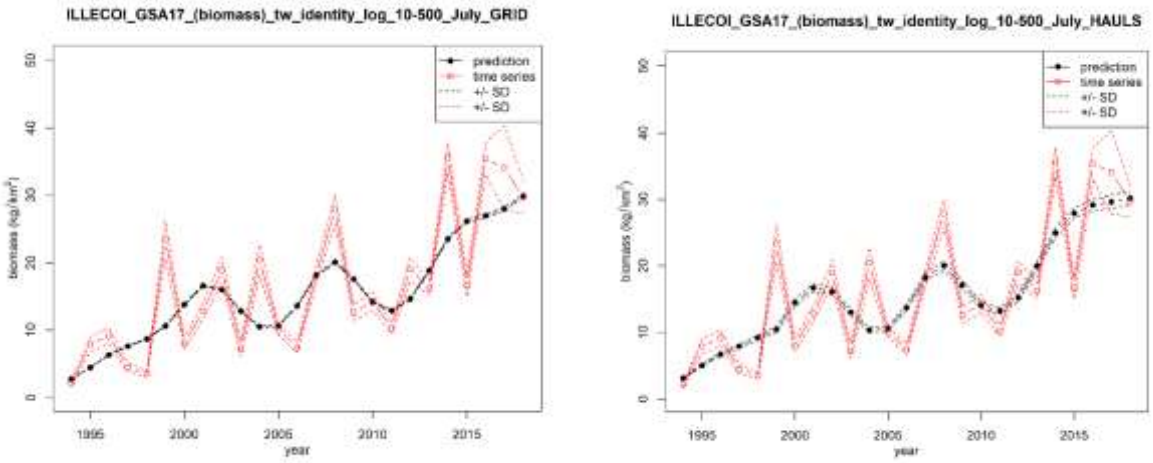

Figure 3.1.3.4.C – Comparison between the original and standardized biomass indices of *I. coindetii* in GSA 17 predicted on the grid (left) and on the haul positions (right).

3.1.3.5 *Solea solea*

The analysis was performed using data from SOLEMON survey conducted in the period between the 2005 and 2018, focusing on the bathymetrical range 10-100 m.
The presence of correlations among the explanatory variables was tested using the Pearson's correlation coefficients (Table 3.1.3.5.a). The correlation matrix shows a correlation coefficient of -0.61 for latitude and longitude while, for these two variables VIF values of 1.78 (longitude) and 1.62 (latitude) were estimated. Being the VIF values lower than the threshold value (3), no collinearity was detected between these variables.

Table 3.1.3.4.a - Correlation table among the quantitative explanatory variables explored for *S. solea* in GSA 17.

	year	**month**	**hour**	**Y**	**X**	**depth**
year		0.31	-0.02	0.01	-0.08	-0.03
month	0.31		0.04	0.08	0.01	0.06
hour	-0.02	0.04		0.03	-0.02	0.03
Y	0.01	0.08	0.03		-0.61	-0.19
X	-0.08	0.01	-0.02	-0.61		0.35
depth	-0.03	0.06	0.03	-0.19	0.35	

The explanatory variables considered are the year, month, depth, hour, latitude, longitude, sampling intensity (expressed as number of hauls, defined as a factor). The list of the most relevant models explored is reported in Table 3.1.3.5.b; in bold the best performing model is reported.

Table 3.1.3.5.b – Selection of the models explored for *S. solea* in GSA 17 (biomass index kg/km^2). In bold the best performing model is reported.

	Model (*Gaussian, transf:* sqrt)	% Deviance	GCV
1	$s(X_{i,j}) + \varepsilon_{i,j}$	10.6%	71.48
2	$s(Y_{i,j}) + \varepsilon_{i,j}$	4.57%	75.11
3	$s(X_{i,j},Y_{i,j}) + \varepsilon_{i,j}$	8.37%	72.73
4	$s(depth_{i,j}) + \varepsilon_{i,j}$	69.8%	24.74
5	$f(year_j) + \varepsilon_{i,j}$	66.8%	26.37
6	$f(month_{i,j}) + \varepsilon_{i,j}$	0.0000%	78.29
7	$s(X_{i,j},Y_{i,j,})+s(depth_{i,j})+f(nb\_hauls_{i,j}) + \varepsilon_{i,j}$	67.8%	10.21
8	$s(X_{i,j}, Y_{i,j}) + s(depth_{i,j}) + f(month_j) + \varepsilon_{i,j}$	67.9%	10.11
	Model (*Gaussian, transf:* log)	**% Deviance**	**GCV**
9	$s(X_{i,j}) + \varepsilon_{i,j}$	4.62%	13.86
10	$s(Y_{i,j}) + \varepsilon_{i,j}$	2.53%	14.14
11	$s(X_{i,j},Y_{i,j}) + \varepsilon_{i,j}$	6.59%	13.65
12	$s(depth_{i,j}) + \varepsilon_{i,j}$	82.4%	2.65
13	$f(year_j) + \varepsilon_{i,j}$	81.1%	2.76
14	$f(month_{i,j}) + \varepsilon_{i,j}$	0.0000%	14.45
15	$s(X_{i,j},Y_{i,j,})+s(depth_{i,j})+f(nb\_hauls_{i,j}) + \varepsilon_{i,j}$	68.3%	1.05
16	$s(X_{i,j}, Y_{i,j}) + s(depth_{i,j}) + f(month_j) + \varepsilon_{i,j}$	68.1%	1.04
	Model (tw)	**% Deviance**	**REML**
17	$s(X_{i,j}, Y_{i,j}) + s(depth_{i,j}) + f(month_j) + \varepsilon_{i,j}$	64.9%	3040.4
18	$\boldsymbol{s(X_{i,j}, Y_{i,j}) + s(depth_{i,j}) + \varepsilon_{i,j}}$	**64.6%**	**3038.3**

The best model apparently result in model number 16, but the final plot is underfitted. We selected the model number 18, data identity, family Tweedie, link log, depth range 10-100 m.

The model summary is reported in Table 3.1.3.5.c and indicates the significance of the geographical position, depth and year. The residuals of the model and the q-q plot, reported in Figure 3.1.3.5.A show right skewed distribution.

The estimation of the splines was significant (Table 3.1.3.5.c and Figure 3.1.3.5.B).

Table 3.1.3.5.c – Summary of the estimates, GVC and deviance explained of the best GAM for *S. solea* in GSA 17.

****

family: tw

link : log
transformation: identity
****
-- Summary of the model --

Family: Tweedie(p=1.432)
Link function: log

Formula:
response ~ s(year) + s(X, Y) + s(depth)

Parametric coefficients:
Estimate Std. Error t value Pr(>|t|)
(Intercept) 3.75351 0.03253 115.4 <2e-16 ***

Signif. codes: 0 '***' 0.001 '**' 0.01 '*' 0.05 '.' 0.1 ' ' 1

Approximate significance of smooth terms:
edf Ref.df F p-value
s(year) 4.213 9 37.96 <2e-16 ***
s(X,Y) 20.835 29 22.50 <2e-16 ***
s(depth) 6.806 9 30.87 <2e-16 ***

Signif. codes: 0 '***' 0.001 '**' 0.01 '*' 0.05 '.' 0.1 ' ' 1

R-sq.(adj) = 0.588 Deviance explained = 64.6%
-REML = 3038.3 Scale est. = 5.8009 n = 899

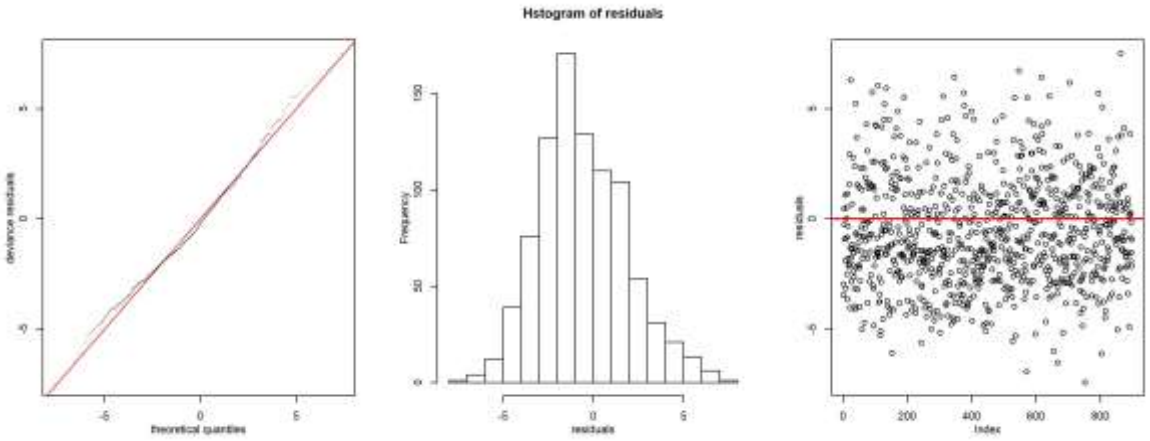

Figure 3.1.3.5.A – Diagnostic plots of residuals for *S. solea* in GSA 17.

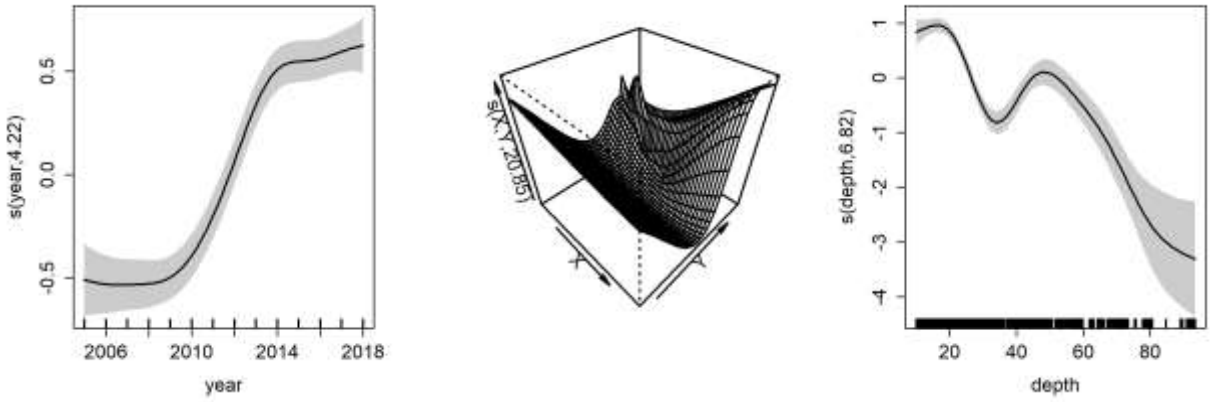

Figure 3.1.3.5.B – Splines of the best model for *S. solea* in GSA 17.

Only the points of the predictive grid corresponding to a depth comprised in the 10 - 100 m range were selected. The grid points were also linked to the values of the other variables included in the best GAM and useful to predict the model in the standardized conditions: year and number of hauls.

In Figure 3.1.3.5.C the comparison is reported between the original indices estimated on rough data according to Souplet (1996) and the indices estimated on the predicted

results, predicted over the grid with the corresponding confidence intervals (Figure 3.1.3.5.C left). The prediction was also done on the original haul positions (Figure 3.1.3.5.C right).

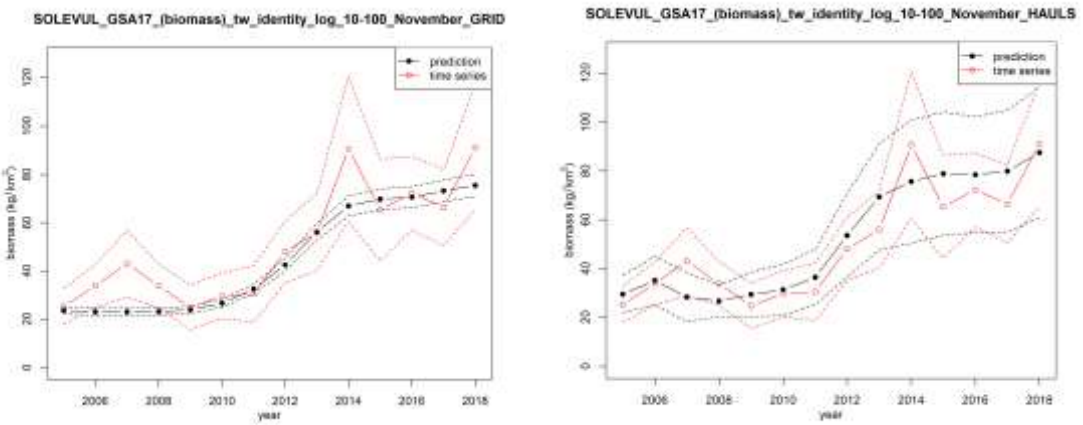

Figure 3.1.3.5.C – Comparison between the original and standardized biomass indices of *S. solea* in GSA 17 predicted on the grid (left) and on the haul positions (right).

3.2 GSA18 – Southern Adriatic Sea

3.2.1 Ranking of the species from MEDITS survey

In the following Table 3.2.1.a, it is reported the ranking obtained for the commercial species represented in the MEDITS survey. Considering a cumulative percentage of 90%, 24 species were considered. To these, the two red shrimps, which are also important in the GSA, have been added, thus for a total of 26 species.

Table 3.2.1.a – Ranking of MEDITS species selected for the GSA18.

Species	GSA18 MEDITS CODE	CUMULATIVE %
Mullus barbatus	MULLBAR	18
Merluccius merluccius	MERLMER	31
Illex coindetii	ILLECOI	42
Spicara flexuosa	SPICFLE	50
Trachurus trachurus	TRACTRA	55
Parapenaeus longirostris	PAPELON	59
Spicara smaris	SPICSMA	63
Apitrigla cuculus	ASPICUC	66
Loligo vulgaris	LOLIVUL	68
Phicis blennoides	PHYIBLE	71
Micromesistius potassou	MICMPOU	73
Pagellus erythrinus	PAGEERY	75
Helicolenus dactylopterus	HELIDAC	76
Bothus podas	BOTHPOD	78
Trachurus mediterraneus	TRACMED	80
Lophius budegassa	LOPHBUD	81
Eledone cirrhosa	ELEDCIR	83
Octopus vulgaris	OCTOVUL	84
Pagellus acarne	PAGEACA	85
Boops boops	BOOPBOO	87
Todaropsis eblanae	TODIEBL	88
Pagellus bogaraveo	PAGEBOG	89
Allotheutis media	ALLOMED	90
Conger conger	CONGCON	90
Aristaeomorpha foliacea	ARISFOL	91

Aristeus antennatus	ARITANT	92

3.2.2 Analysis of trawl survey data with BioIndex

BioIndex (version2.1.2) was carried out to derive all the indicators provided by the software and described in the Methods section. The outputs are provided in an Excel file and a selection is summarized in terms of trend significance and ranges in Table 3.2.2.a. The extended outputs in terms of tables of indicators, plots and raster files are reported on the sharepoint (WP4-Integrated platform/Activity 4.3-BSTAT/D4.3.1Spatial distribution of marine species).

The trends of abundance, biomass and positive hauls are increasing for about 50% of the examined species (Table 3.2.2.a). Most of the trends are stationary. In some situations decreasing trends of population structure are highlighted. For *Eledone cirrhosa* such trends are associated to a significant decreasing of the biomass index. For *Trachurus trachurus* instead the indices of population structure are decreasing, as possible consequence of abundance decreasing. For this species, the abundance is mainly associated to the first 2 age classes given that adult individuals, for their predominant pelagic behaviour, are less vulnerable to the MEDITS gear. Thus, a decreasing of abundance can be interpreted as a decrease of recruitment.

As regards the aggregation of recruits and spawners at spatial level, both recruits and spawners of *Aristaeomorpha foliacea* are mainly concentrated in the area of the Otranto channel, along the deep grounds of the Bari pit (Figure 3.2.2.A). Likewise for the spawners of *A. antennatus* (Figure 3.2.2.B).

Recruits and spawners of *P. longirostris* and *M. merluccius* are widespread in the GSA 18 (Figure 3.2.2.C-D), however higher abundance for both species were observed in the southern side of Albania coasts, between 100 and 200 m depth, and also in the southern costs of Italy, for *P. longirostris*, while on the northern ones for *M. merluccius*.

Recruits of *M. barbatus* (Figure 3.2.2.E) could be observed sporadically, given the usual period of the MEDITS survey. Both recruits and spawners can be observed on

both sides of the GSA, though recruits appear to be more abundant on the west side and spawners on the east one.

The recruits aggregation of *I. coindetii* (Figure 3.2.2.F) is very wide and partially overlaps with the spawning aggregations that mainly occur along the eastern side of the Otranto Channel between 100 and 200 m depth.

In the GSA18 both nursery areas and spawning aggregation of common pandora were localised in the western side along the coast of Apulia region, while the recruits are mostly located in the area of the Otranto Channel (Figure 3.2.2.G).

In the GSA18 nursery and adult aggregations of *E. cirrhosa* are mainly localized along the western side of the GSA, where the recruits aggregation is in overlap with aggregation area of adult females (figure 3.2.2.H)

Table 3.2.2.a – Summary table of the principal indicators calculated by BioIndex for all the species analysed in GSA18.

SPECIES	depth range	ABUNDANCE (n/km^2)	CV ABUNDANCE	BIOMASS (kg/km^2)	CV BIOMASS	Positive hauls	50th perc. (mm)	CV 50th perc.	95th perc. (mm)	CV 95th perc.	ABUNDANCE TREND	BIOMASS TREND	Positive hauls	50th perc. TREND	95th perc. TREND
ALLOMED	10-200	180.47 - 5193.64	0.1643 - 0.4752	0.47 - 13.275	0.123 - 0.409	26.67 - 68.89	NA	NA	NA	NA	↔	↔	↔	NA	NA
ARISFOL	200-800	17.36 - 420.89	0.135 - 0.485	0.292 - 8.947	0.164 - 0.589	8.33 - 20.22	26.4 - 46.6	0.006 - 0.147	43.7 - 62.6	0.006 - 0.165	↗	↗	↗	↔	↔
ARITANT	200-800	0 - 479.19	0.266 - 1.036	0 - 12.381	0.261 - 1.036	0 - 15.56	27.2 - 45.2	0.006 - 0.255	38.8 - 59	0.003 - 0.116	↗	↗	↗	↔	↔
ASPICUC	10-800	5.04 - 659.13	0.186 - 0.597	0.269 - 13.739	0.204 - 0.718	8.04 - 56.67	101.3 - 167.2	0.002 - 0.121	169.6 - 217.4	0.001 - 0.014	↗	↗	↔	↔	↔
BOOPBOO	10-200	51.86 - 557.06	0.198 - 0.73	1.882 - 13.191	0.201 - 0.673	14.44 - 56.67	124.6 - 165.1	0.001 - 0.009	167.8 - 199.2	0.002 - 0.009	↔	↔	↔	↔	↔
BOTHPOD	10-200	0 - 1221.63	0.571 - 1.037	0 - 26.385	0.572 - 1.037	0 - 7.06	NA	NA	NA	NA	↔	↗	↔	NA	NA
CONGCON	10-800	2.06 - 14.38	0.196 - 0.402	0.325 - 3.734	0.242 - 0.807	8.89 - 33.33	NA	NA	NA	NA	↔	↔	↔	NA	NA
ELEDCIR	10-200	16.55 - 164.33	0.128 - 0.485	1.224 - 42.651	0.137 - 0.433	25.56 - 55.56	34.6 - 110.8	0.004 - 0.066	63.8 - 147.3	0.002 - 0.042	↔	↘	↔	↘	↘
HELIDAC	10-800	33.07 - 359.91	0.166 - 0.456	1.761 - 15.639	0.199 - 0.658	30 - 54.44	64 - 190.9	0.002 - 0.335	186.1 - 271.8	0.003 - 0.058	↔	↔	↔	↔	↔
ILLECOI	10-800	11.04 - 2058.41	0.094 - 0.484	0.556 - 56.036	0.093 - 0.389	20.83 - 83.53	55.3 - 136	0.001 - 0.088	104.6 - 193	0.001 - 0.064	↗	↗	↗	↔	↘
LOLIVUL	10-200	2.46 - 2053.19	0.239 - 0.589	0.427 - 17.806	0.206 - 0.92	6.94 - 56.25	32 - 140	0.002 - 0.092	64.7 - 209	0.001 - 0.119	↗	↗	↗	↔	↔
LOPHBUD	10-800	4.95 - 46.24	0.105 - 0.246	1.55 - 12.509	0.153 - 0.404	18.89 - 60	119.5 - 320	0.003 - 0.071	301 - 577	0.003 - 0.019	↔	↔	↔	↗	↔
MERLMER	10-800	168.56 - 1586.06	0.08 - 0.224	14.712 - 44.446	0.067 - 0.141	82.22 - 95.56	99.9 - 158.3	0.001 - 0.013	219.1 - 355.9	0.004 - 0.048	↔	↔	↔	↔	↔
MICMPOU	200-800	13.52 - 811.01	0.254 - 0.725	1.388 - 23.288	0.202 - 0.852	8.89 - 47.22	124.9 - 259.6	0.001 - 0.033	149.8 - 377	0.001 - 0.013	↔	↗	↔	↗	↔
MULLBAR	10-200	13.4 - 8458.83	0.166 - 0.618	0.693 - 108.778	0.164 - 0.527	13.89 - 70.59	53.2 - 155.5	0.001 - 0.048	135.9 - 226.8	0.001 - 0.035	↗	↗	↗	↔	↘
OCTOVUL	10-200	1.75 - 55.75	0.22 - 0.573	0.909 - 13.072	0.214 - 0.615	5.36 - 36.67	58.9 - 155	0.008 - 0.058	92.2 - 243	0.003 - 0.029	↗	↗	↗	↘	↘
PAGEACA	10-800	0.71 - 1401.31	0.328 - 0.993	0.025 - 8.901	0.332 - 0.959	3.57 - 37.78	72.3 - 249.2	0.0008 - 0.063	108.4 - 295.4	0.0004 - 0.086	↗	↗	↗	↘	↔
PAGEBOG	10-800	0.49 - 139.48	0.253 - 0.952	0.081 - 5.513	0.24 - 0.95	2.68 - 38.89	78.8 - 238.3	0.003 - 0.029	170.5 - 357.5	0.002 - 0.032	↗	↗	↗	↔	↔
PAGEERY	10-200	0.32 - 358.59	0.235 - 0.973	0.024 - 9.623	0.286 - 0.973	1.39 - 29.41	84 - 161.2	0.002 - 0.035	144 - 251	0.002 - 0.055	↗	↗	↗	↔	↔
PAPELON	10-800	12.63 - 3451.63	0.111 - 0.436	0.126 - 15.642	0.11 - 0.427	12.5 - 88.76	16.4 - 28.6	0.004 - 0.128	26.8 - 39.7	0.006 - 0.113	↗	↗	↗	↘	↔
PHYIBLE	10-800	19.84 - 365.2	0.115 - 0.338	2.468 - 14.069	0.12 - 0.287	31.11 - 57.78	104.8 - 208.4	0.002 - 0.032	252.1 - 446.5	0.006 - 0.071	↔	↗	↔	↔	↗
SPICFLE	10-200	0.29 - 3921.15	0.257 - 1.02	0.016 - 42.836	0.279 - 1.02	0.89 - 43.33	71.9 - 162.5	0 - 0.019	126 - 194.7	0.001 - 0.064	↗	↗	↗	↘	↘
SPICSMA	10-200	22.41 - 4502.81	0.209 - 0.982	0.359 - 56.831	0.216 - 0.965	21.11 - 48.89	73.2 - 134.9	0 - 0.017	111.3 - 173.5	0.001 - 0.019	↔	↔	↔	↔	↔
TODIEBL	200-800	3.05 - 345.19	0.209 - 1	0.609 - 28.648	0.217 - 1	15.28 - 47.78	NA	NA	NA	NA	↗	↗	↗	NA	NA
TRACMED	10-200	2.46 - 1034.94	0.197 - 0.826	0.36 - 10.848	0.173 - 0.662	4.44 - 56.18	69.2 - 260	0.001 - 0.023	92.7 - 348.5	0.001 - 0.02	↗	↗	↗	↘	↘
TRACTRA	10-200	685.08 - 22972.32	0.171 - 0.451	7.462 - 182.304	0.14 - 0.558	54.44 - 76.39	63.7 - 126.5	0.0003 - 0.002	91.8 - 185.1	0.0002 - 0.07	↘	↔	↔	↗	↗

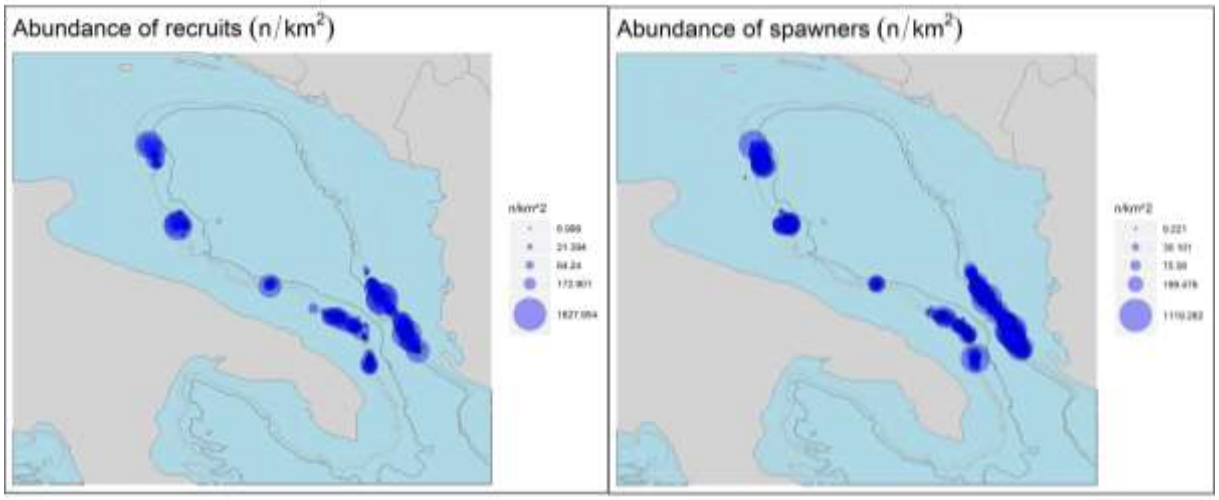

Figure 3.2.2.A – Spatial distribution of recruits and spawners of *A. foliacea* for GSA 18 during the time series 2014-2018.

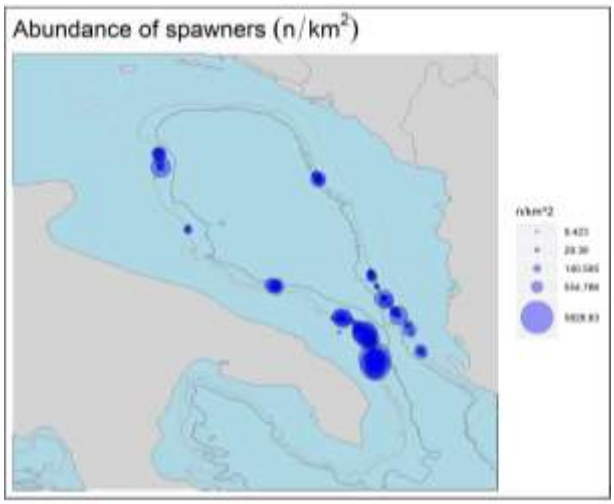

Figure 3.2.2.B – Spatial distribution of spawners of *A. antennatus* for GSA 18 during the time series 2014-2018.

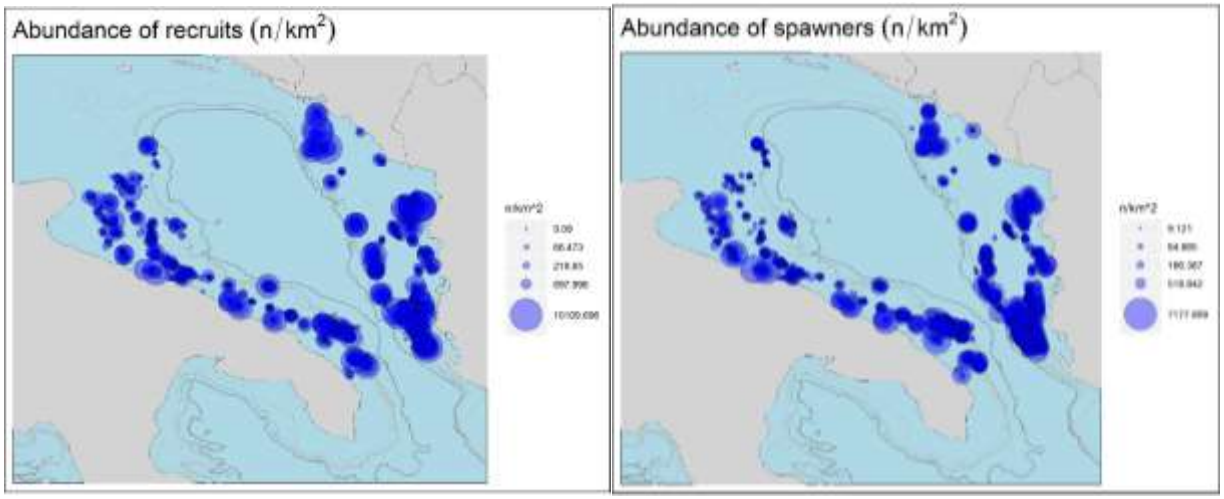

Figure 3.2.2.C – Spatial distribution of recruits and spawners of *P. longirostris* for GSA 18 during the time series 2014-2018.

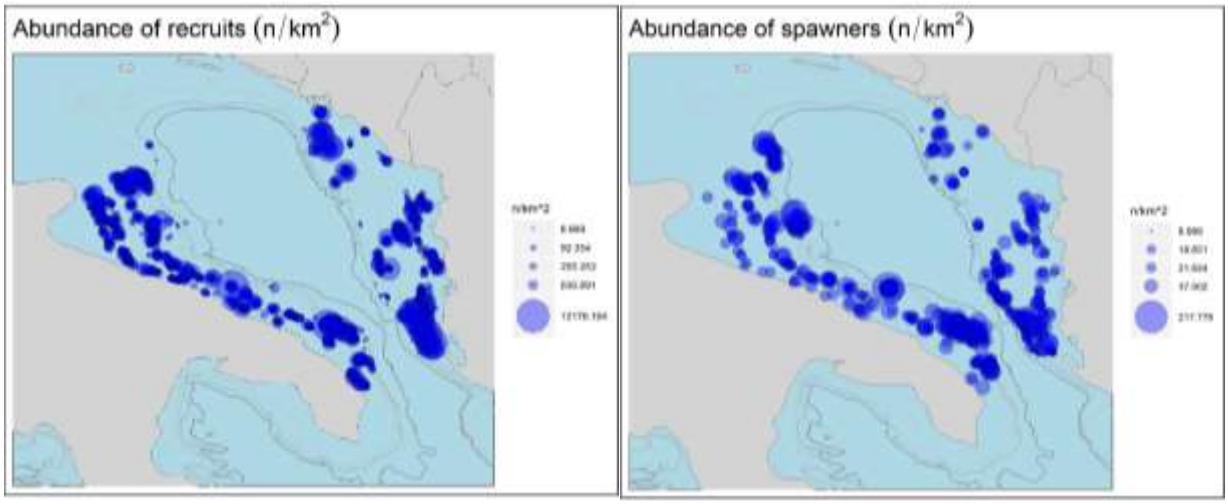

Figure 3.2.2.D – Spatial distribution of recruits and spawners of *M. merluccius* for GSA 18 during the time series 2014-2018.

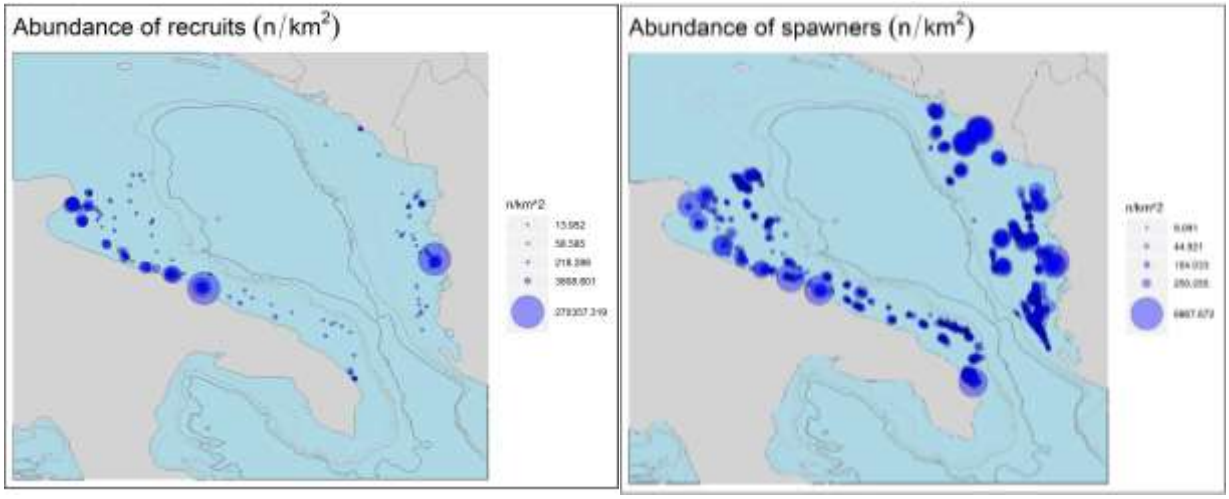

Figure 3.2.2.E – Spatial distribution of recruits and spawners of *M. barbatus* for GSA 18 during the time series 2014-2018.

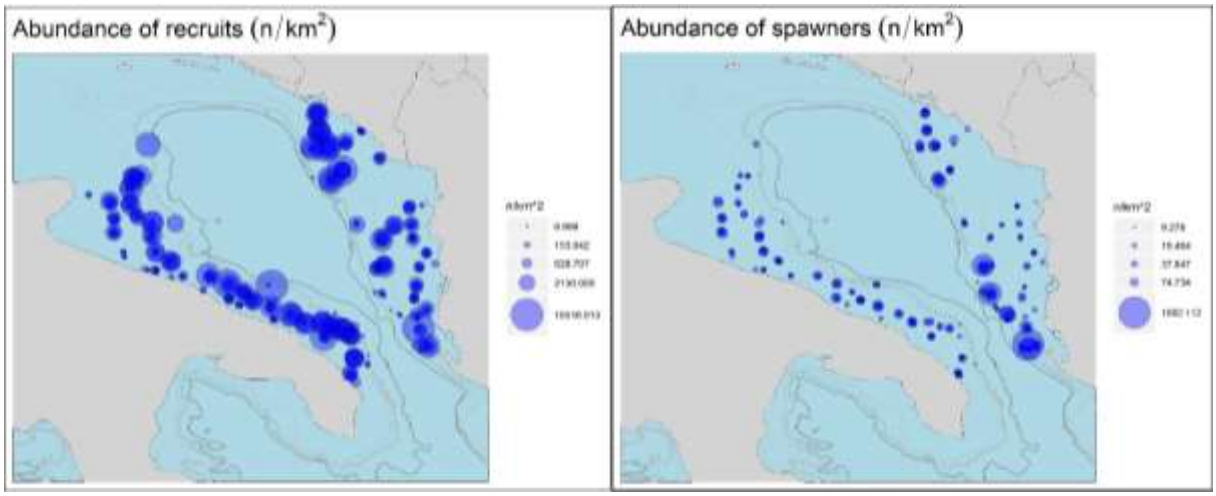

Figure 3.2.2.F – Spatial distribution of recruits and spawners of *I. coindetii* for GSA 18 during the time series 2014-2018.

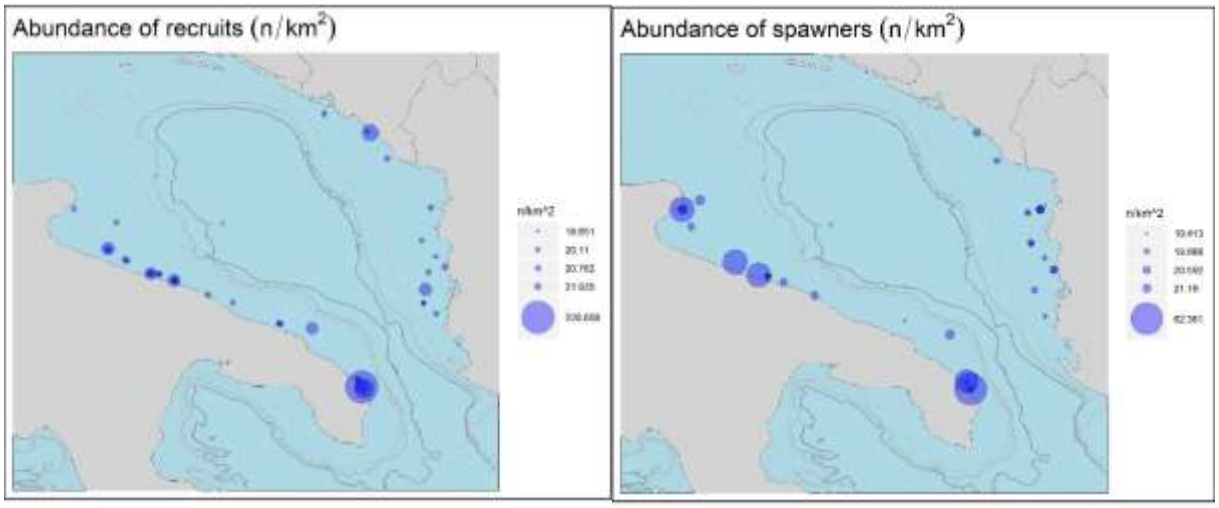

Figure 3.2.2.G – Spatial distribution of recruits and spawners of *P. erythrinus* for GSA 18 during the time series 2014-2018.

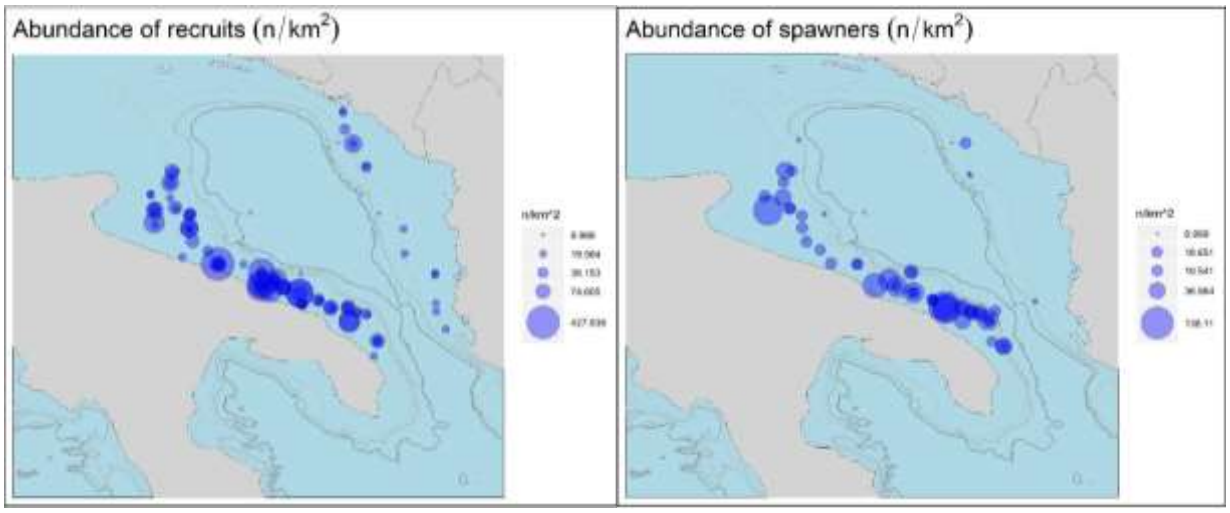

Figure 3.2.2.H – Spatial distribution of recruits and spawners of *E. cirrhosa* for GSA 18 during the time series 2014-2018.

3.2.3 Standardization of trawl survey data with BioStand

BioStand (version2.1.2) was carried out to standardize the data described in Data section for the following selected species: *M. merluccius, M. barbatus, P. longirostris, A. foliacea,* and *I. coindetii*. For all the species, the Gaussian, quasi-Poisson and Tweedie distributions were explored and logarithmic, square root and inverse transformations of data.

3.2.3.1. *Merluccius merluccius*

The analysis was performed using data from MEDITS survey conducted in the period between the 1994 and 2018, focusing on the bathymetrical range 10-800 m.

The presence of correlations among the explanatory variables was tested using the Pearson's correlation coefficients (Table 3.2.3.1.a). The correlation matrix shows a correlation coefficient of -0.55 for latitude and longitude while, for these two variables VIF values of 1.56 (longitude) and 1.46 (latitude) were estimated. Being the VIF values lower than the threshold value (3), no collinearity was detected between these variables. Among the other variables no significant correlations were found.

Table 3.2.3.1.a - Correlation table among the quantitative explanatory variables explored for *M. merluccius* in GSA 18.

	year	**month**	**hour**	**Y**	**X**	**depth**
year		0.41	0	0.05	0.1	0.01
month	0.41		0	0.01	0.12	0.01
hour	0	0		0.02	-0.01	-0.11
Y	0.05	0.01	0.02		-0.55	-0.17
X	0.1	0.12	-0.01	-0.55		0.27
depth	0.01	0.01	-0.11	-0.17	0.27	

The explanatory variables considered are the year, month, depth, hour, latitude, longitude, sampling intensity (expressed as number of hauls, defined as a factor). The list of the most relevant models explored is reported in Table 3.2.3.1.b; in bold the best performing model is reported. The best model was estimated using the quasi-Poisson family distribution, assuming a logarithmic link function.

Table 3.2.3.1.b – Selection of the models explored for *M. merluccius* in GSA 18 (biomass index kg/km^2). In bold the best performing model is reported. Quasi-Poisson family distribution, assuming a logarithmic link function.

Model	**% Deviance**	**GCV**
$f(year_j) + \varepsilon_{i,j}$	9.79%	24.64
$f(year_j) + s(depth_{i,j}) + \varepsilon_{i,j}$	27.50%	19.99
$f(year_j) + s(X_{i,j},Y_{i,j}) + s(depthi,j) + \varepsilon_{i,j}$	36.28%	18.10
$f(year_j) + s(X_{i,j},Y_{i,j}) + s(depthi,j) + f(month_j) + \varepsilon_{i,j}$	36.62%	18.07
$f(year_j) + s(X_{i,j},Y_{i,j}) + s(depthi,j) + f(month_j) + f(hour_j) + \varepsilon_{i,j}$	36.62%	18.07
$f(year_j) + s(X_{i,j},Y_{i,j}) + s(depthi,j) + f(month_j) + f(vessel_j) + \varepsilon_{i,j}$	36.62%	18.07
$f(year_j) + s(X_{i,j},Y_{i,j}) + s(depthi,j) + f(month_j) + f(nb\_hauls_j) + \varepsilon_{i,j}$	36.62%	18.07
$\mathbf{f(year_j) + s(X_{i,j},Y_{i,j},by=month) + s(depth_{i,j}) + \varepsilon_{i,j}}$	**35.85%**	**18.24**

The model summary is reported in Table 3.2.3.1.c and indicates the significance of the geographical position, the year and the month of the survey. The residuals of the model and the q-q plot, reported in Figure 3.2.3.1.A show a slightly skewed distribution.

The estimation of the splines and factors was found in any cases significant (Table 3.2.3.1.c and Figure 3.2.3.1.B).

Table 3.2.3.1.c – Summary of the estimates, GVC and deviance explained of the best GAM for *M. merluccius* in GSA 18.

Parametric coefficients:

```
                Estimate Std. Error t value Pr(>|t|)
factor(year)1994   3.7457     0.3491  10.728  < 2e-16 ***
factor(year)1995   3.9704     0.3456  11.488  < 2e-16 ***
factor(year)1996   3.8942     0.3537  11.010  < 2e-16 ***
factor(year)1997   3.7947     0.3692  10.279  < 2e-16 ***
factor(year)1998   3.3333     0.3308  10.077  < 2e-16 ***
factor(year)1999   3.3291     0.4114   8.092 9.42e-16 ***
factor(year)2000   3.2510     0.3307   9.829  < 2e-16 ***
factor(year)2001   3.1577     0.3425   9.219  < 2e-16 ***
factor(year)2002   3.3293     0.4032   8.256 2.51e-16 ***
factor(year)2003   3.1572     0.3736   8.450  < 2e-16 ***
factor(year)2004   3.4945     0.3708   9.425  < 2e-16 ***
factor(year)2005   4.2561     0.4137  10.287  < 2e-16 ***
factor(year)2006   3.8625     0.3665  10.539  < 2e-16 ***
factor(year)2007   3.8204     0.5172   7.387 2.09e-13 ***
factor(year)2008   3.9117     0.3626  10.787  < 2e-16 ***
factor(year)2009   4.0730     0.3407  11.955  < 2e-16 ***
factor(year)2010   3.5878     0.3690   9.723  < 2e-16 ***
factor(year)2011   3.1944     0.3743   8.534  < 2e-16 ***
factor(year)2012   3.6421     0.3686   9.880  < 2e-16 ***
factor(year)2013   3.6302     0.3703   9.803  < 2e-16 ***
factor(year)2014   3.4328     0.4208   8.159 5.53e-16 ***
factor(year)2015   2.9753     0.3997   7.443 1.39e-13 ***
factor(year)2016   3.2191     0.4164   7.731 1.58e-14 ***
factor(year)2017   4.0450     0.5171   7.823 7.85e-15 ***
factor(year)2018   3.5310     0.3848   9.176  < 2e-16 ***
---
Signif. codes:  0 ‘***’ 0.001 ‘**’ 0.01 ‘*’ 0.05 ‘.’ 0.1 ‘ ’ 1

Approximate significance of smooth terms:
              edf Ref.df     F p-value
s(depth)    7.108      9 26.674  <2e-16 ***
s(X,Y):month 25.356     30  7.965  <2e-16 ***
---
Signif. codes:  0 ‘***’ 0.001 ‘**’ 0.01 ‘*’ 0.05 ‘.’ 0.1 ‘ ’ 1

R-sq.(adj) =  0.316   Deviance explained = 35.8%
```

GCV = 18.237 Scale est. = 19.808   n = 2336

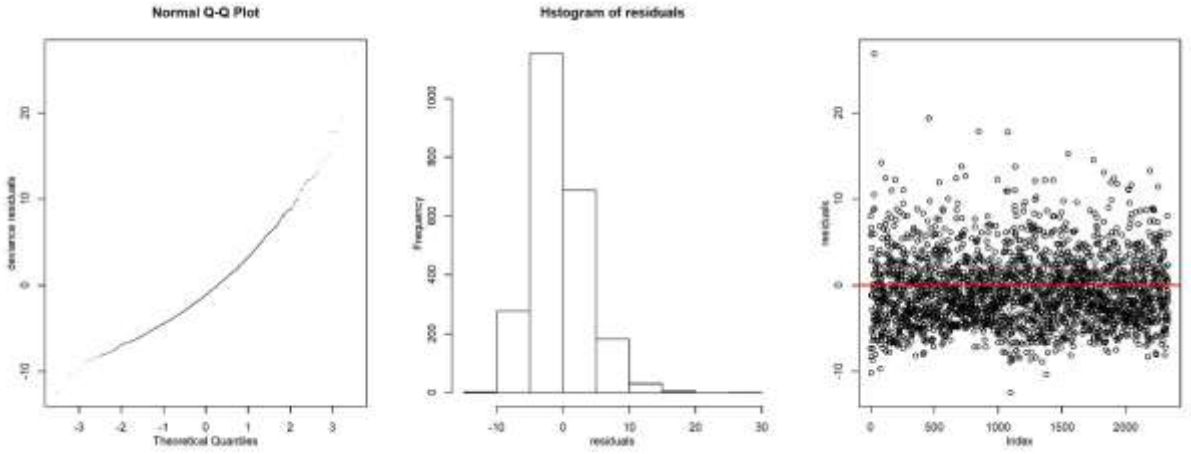

Figure 3.2.3.1.A – Diagnostic plots of residuals for *M. merluccius* in GSA 18.

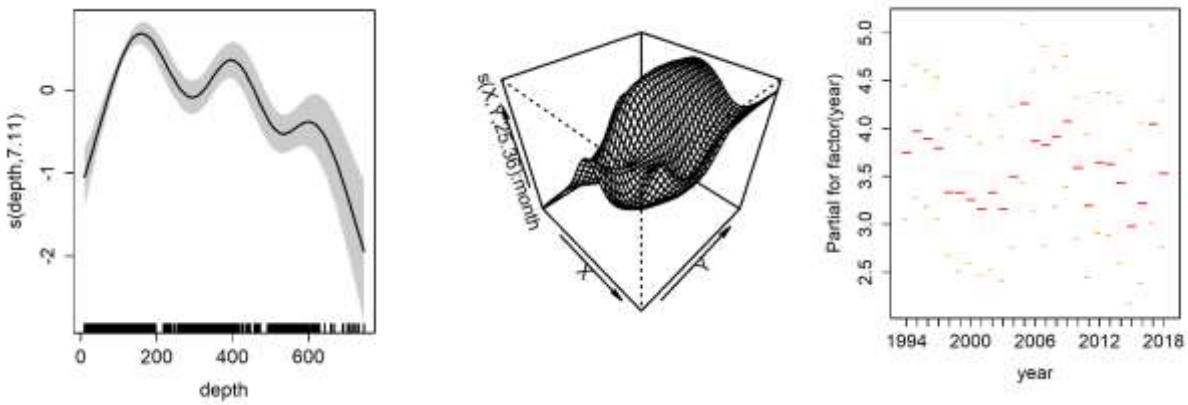

Figure 3.2.3.1.B – Splines and factors of the best model for *M. merluccius* in GSA 18.

Only the points of the predictive grid corresponding to a depth comprised in the 10-800 m range were selected. The grid points were also linked to the values of the other

variables included in the best GAM and useful to predict the model in the standardized conditions: year and month (for standardization was used July).

In Figure 3.2.3.1.C the comparison is reported between the original indices estimated on rough data according to Souplet (1996) and the indices estimated on the predicted results, predicted over the grid with the corresponding confidence intervals (Figure 3.2.3.1.C left). The prediction was also done on the original haul positions (Figure 3.2.3.1.C right).

The indices estimated by the model shows a good level of agreement between the original biomass index and the standardizations, especially on the original hauls positions. Indeed, the values predicted on the grid positions return an index generally higher than the original one, even if the overall trend between the two series is consistent.

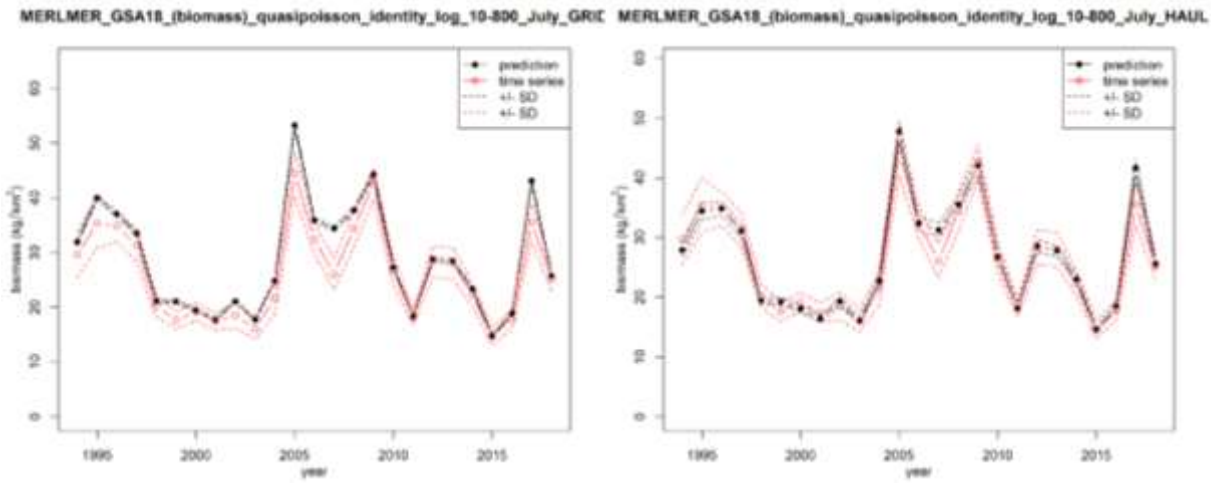

Figure 3.2.3.1.C – Comparison between the original and standardized biomass indices of *M. merluccius* in GSA 18 predicted on the grid (left) and on the haul positions (right).

3.2.3.2. *Mullus barbatus*

The analysis was performed using data from MEDITS survey conducted in the period between the 1994 and 2018, focusing on the bathymetrical range 10-200 m.

The presence of correlations among the explanatory variables was tested using the Pearson's correlation coefficients (Table 3.2.3.2.a). The correlation matrix shows a correlation coefficient of -0.46 for latitude and longitude while, for these two variables VIF values of 1.3 (longitude) and 1.4 (latitude) were estimated. Being the VIF values lower than the threshold value (3), no collinearity was detected between these variables. Among the other variables no significant correlations were found.

Table 3.2.3.2.a - Correlation table among the quantitative explanatory variables explored for *M. barbatus* in GSA 18.

	year	**month**	**hour**	**Y**	**X**	**depth**
year		0.43	0.02	0.02	0.14	0
month	0.43		0.02	0.01	0.14	0.02
hour	0.02	0.02		0.05	0	0.03
Y	0.02	0.01	0.05		-0.46	-0.27
X	0.14	0.14	0	-0.46		0.34
depth	0	0.02	0.03	-0.27	0.34	

The explanatory variables considered are the year, month, depth, hour, latitude, longitude, sampling intensity (expressed as number of hauls, defined as a factor). The list of the most relevant models explored is reported in Table 3.2.3.2.b; in bold the best performing model is reported. The best model was estimated using the Gaussian family distribution, applying a log-transformation on the data and assuming an identity link function.

Table 3.2.3.2.b – Selection of the models explored for *M. barbatus* in GSA 18 (biomass index kg/km^2). In bold the best performing model is reported. Gaussian family distribution, applying a log-transformation on the data and assuming an identity link function.

Model	**% Deviance**	**GCV**
$f(year_j) + \varepsilon_{i,j}$	61.14%	2.00
$f(year_j) + s(X_{i,j}) + \varepsilon_{i,j}$	70.48%	1.54
$f(year_j) + s(Y_{i,j}) + \varepsilon_{i,j}$	65.29%	1.81
$f(year_j) + s(X_{i,j},Y_{i,j}) + \varepsilon_{i,j}$	75.53%	1.32
$\mathbf{f(year_j) + s(X_{i,j},Y_{i,j}) + s(depth_{i,j}) + \varepsilon_{i,j}}$	**77.72%**	**1.22**

The model summary is reported in Table 3.2.3.2.c and indicates the significance of the geographical position and year. The residuals of the model and the q-q plot, reported in Figure 3.2.3.2.A show a quite normal distribution.
The estimation of the splines was found in any cases significant although the wide confidence intervals in factor variable (Table 3.2.3.2.c and Figure 3.2.3.2.B).

Table 3.2.3.2.c – Summary of the estimates, GVC and deviance explained of the best GAM for *M. barbatus* in GSA 18.

	Estimate	Std. Error	t value	Pr(>|t|)	
factor(year)1994	0.8068	0.1510	5.344	1.04e-07	***
factor(year)1995	0.6439	0.1499	4.294	1.86e-05	***
factor(year)1996	0.8687	0.1253	6.934	5.97e-12	***
factor(year)1997	0.7728	0.1244	6.213	6.67e-10	***
factor(year)1998	0.8750	0.1241	7.051	2.66e-12	***
factor(year)1999	1.5074	0.1242	12.139	< 2e-16	***
factor(year)2000	1.2140	0.1241	9.781	< 2e-16	***
factor(year)2001	1.3079	0.1242	10.535	< 2e-16	***
factor(year)2002	0.9988	0.1354	7.376	2.63e-13	***
factor(year)2003	1.1099	0.1355	8.194	5.22e-16	***

```
factor(year)2004   1.1297    0.1355   8.336  < 2e-16 ***
factor(year)2005   1.7009    0.1354  12.567  < 2e-16 ***
factor(year)2006   1.3180    0.1351   9.752  < 2e-16 ***
factor(year)2007   1.8664    0.1354  13.789  < 2e-16 ***
factor(year)2008   1.9017    0.1312  14.496  < 2e-16 ***
factor(year)2009   1.6373    0.1366  11.983  < 2e-16 ***
factor(year)2010   1.1355    0.1356   8.375  < 2e-16 ***
factor(year)2011   1.0767    0.1359   7.924 4.34e-15 ***
factor(year)2012   2.2151    0.1359  16.303  < 2e-16 ***
factor(year)2013   2.5903    0.1360  19.043  < 2e-16 ***
factor(year)2014   2.3435    0.1359  17.239  < 2e-16 ***
factor(year)2015   2.1353    0.1370  15.592  < 2e-16 ***
factor(year)2016   2.2320    0.1370  16.286  < 2e-16 ***
factor(year)2017   3.0796    0.1419  21.696  < 2e-16 ***
factor(year)2018   2.1897    0.1379  15.876  < 2e-16 ***
---
Signif. codes:  0 '***' 0.001 '**' 0.01 '*' 0.05 '.' 0.1 ' ' 1

Approximate significance of smooth terms:
           edf Ref.df     F p-value
s(X,Y)   27.133     29 32.10  <2e-16 ***
s(depth)  6.013      9 16.86  <2e-16 ***
---
Signif. codes:  0 '***' 0.001 '**' 0.01 '*' 0.05 '.' 0.1 ' ' 1

R-sq.(adj) =  0.559   Deviance explained = 77.7%
GCV = 1.2185  Scale est. = 1.1399 n = 1618
```

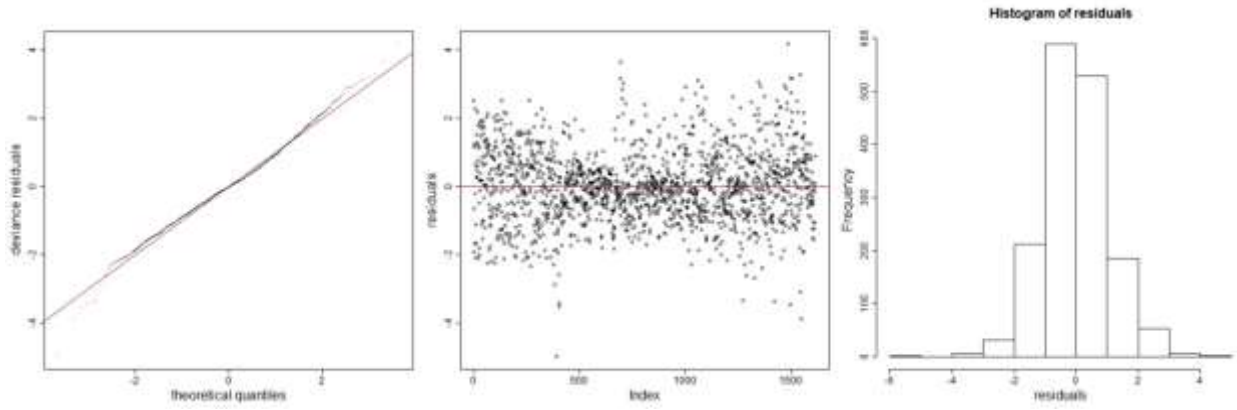

Figure 3.2.3.2.A – Diagnostic plots of residuals for *M. barbatus* in GSA 18.

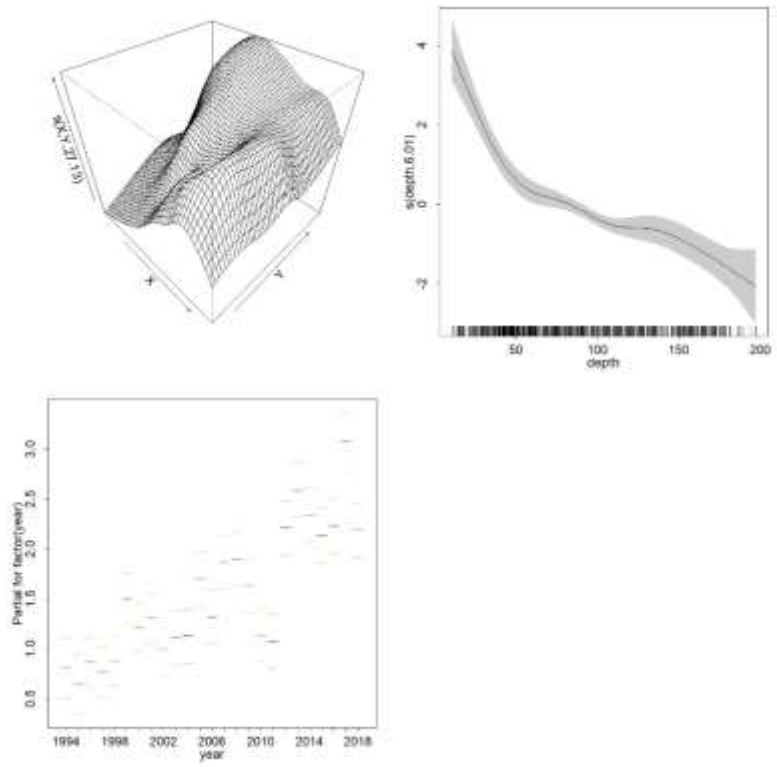

Figure 3.2.3.2.B – Splines of the best model for *M. barbatus* in GSA 18.

Only the points of the predictive grid corresponding to a depth comprised in the 10-200 m range were selected. The grid points were also linked to the values of the other variables included in the best GAM and useful to predict the model in the standardized conditions: year and number of hauls (for standardization was used a unique reference value in the study area since 2002).

In Figure 3.2.3.2.C the comparison is reported between the original indices estimated on rough data according to Souplet (1996) and the indices estimated on the predicted results, predicted over the grid with the corresponding confidence intervals (Figure

3.2.3.2.C left). The prediction was also done on the original haul positions (Figure 3.2.3.2.C right).

The indices estimated by the model shows a higher agreement between the original biomass index and the standardization on the grid. Indeed, the values predicted on the haul positions return an index generally lower than the original one, even if the overall trend between the two series is consistent.

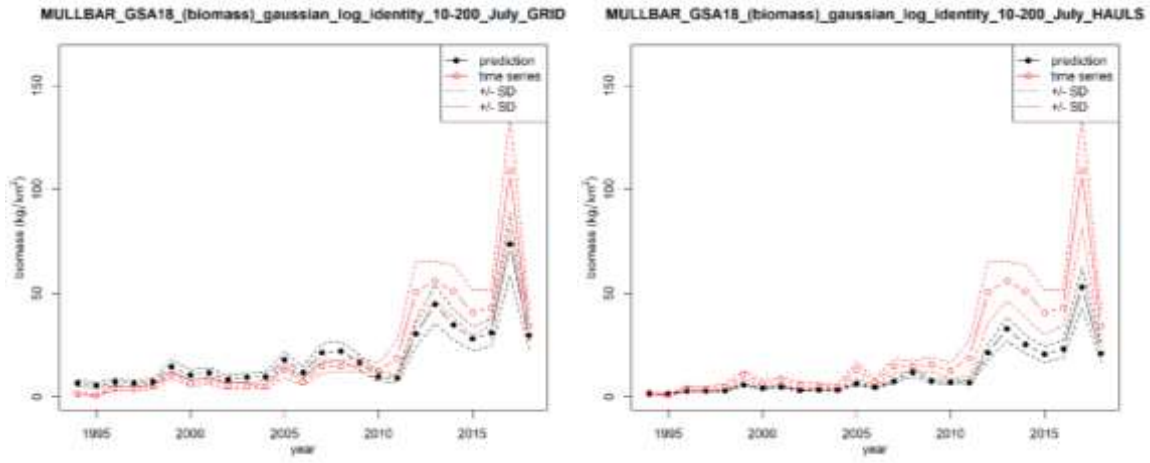

Figure 3.2.3.2.C – Comparison between the original and standardized biomass indices of *M. barbatus* in GSA 18 predicted on the grid (left) and on the haul positions (right).

3.2.3.3 *Parapenaeus longirostris*

The analysis was performed using data from MEDITS survey conducted in the period between the 1994 and 2018, focusing on the bathymetrical range 10-800 m.
The presence of correlations among the explanatory variables was tested using the Pearson's correlation coefficients (Table 3.2.3.3.a). The correlation matrix shows a correlation coefficient of -0.55 for latitude and longitude while, for these two variables VIF values of 1.56 (longitude) and 1.46 (latitude) were estimated. Being the VIF values lower than the threshold value (3), no collinearity was detected between these variables. Among the other variables no significant correlations were found.

Table 3.2.3.3.a - Correlation table among the quantitative explanatory variables explored for *P. longirostris* in GSA 18.

	year	**month**	**hour**	**Y**	**X**	**depth**
year		0.41	0	0.05	0.1	0.01
month	0.41		0	0.01	0.12	0.01
hour	0	0		0.02	-0.01	-0.11
Y	0.05	0.01	0.02		-0.55	-0.17
X	0.1	0.12	-0.01	-0.55		0.27
depth	0.01	0.01	-0.11	-0.17	0.27	

The explanatory variables considered are the year, month, depth, hour, latitude, longitude, sampling intensity (expressed as number of hauls, defined as a factor). The list of the most relevant models explored is reported in Table 3.2.3.3.b; in bold the best performing model is reported. The best model was estimated using the quasi-Poisson family distribution, assuming a logarithmic link function.

Table 3.2.3.8 – Selection of the models explored for *P. longirostris* in GSA 18 (biomass index kg/km^2). In bold the best performing model is reported. Quasi-Poisson family distribution, assuming a logarithmic link function.

Model	% Deviance	GCV
$f(year_j) + \varepsilon_{i,j}$	18.20%	10.66
$f(year_j) + s(X_{i,j},Y_{i,j}) + \varepsilon_{i,j}$	41.82%	7.85
$f(year_j) + s(X_{i,j},Y_{i,j}) + s(depth_{i,j}) + \varepsilon_{i,j}$	51.27%	6.64
$f(year_j) + s(X_{i,j},Y_{i,j}) + s(depth_{i,j}) + f(hour_j) + \varepsilon_{i,j}$	51.57%	6.62
$f(year_j) + s(X_{i,j},Y_{i,j},by=vessel) + s(depth_{i,j}) + f(hour_j) + \varepsilon_{i,j}$	52.72%	6.57
$f(year_j) + s(X_{i,j},Y_{i,j},by=month + s(depth_{i,j}) + f(hour_j) + \varepsilon_{i,j}$	52.03%	6.53
$f(year_j) + s(X_{i,j},Y_{i,j},by=nb\_hauls + s(depth_{i,j}) + f(hour_j) + \varepsilon_{i,j}$	**55.07%**	**6.29**

The model summary is reported in Table 3.2.3.3.c and indicates the significance of the geographical position, the year, hour and sampling intensity. The residuals of the model and the q-q plot, reported in Figure 3.2.3.3.A show a slightly skewed distribution. The estimation of the splines and factors was found in any cases significant (Table 3.2.3.3.c and Figure 3.2.3.3.B).

Table 3.2.3.9 – Summary of the estimates, GVC and deviance explained of the best GAM for *P. longirostris* in GSA 18.

Parametric coefficients:

	Estimate	Std. Error	t value	Pr(>|t|)	
factor(year)1994	-2.60749	1.28340	-2.032	0.042300	*
factor(year)1995	-1.75802	1.00371	-1.752	0.079994	.
factor(year)1996	0.28228	0.29496	0.957	0.338656	
factor(year)1997	-0.54012	0.33124	-1.631	0.103118	
factor(year)1998	0.13020	0.30302	0.430	0.667473	

```
factor(year)1999 -0.58124    0.33643  -1.728 0.084183 .
factor(year)2000 -0.38557    0.32429  -1.189 0.234572
factor(year)2001  0.13741    0.30168   0.455 0.648800
factor(year)2002  1.05807    0.15363   6.887 7.36e-12 ***
factor(year)2003  1.26559    0.14131   8.956  < 2e-16 ***
factor(year)2004  1.52920    0.12296  12.436  < 2e-16 ***
factor(year)2005  1.82807    0.11001  16.617  < 2e-16 ***
factor(year)2006  1.46898    0.12746  11.525  < 2e-16 ***
factor(year)2007  0.69178    0.18099   3.822 0.000136 ***
factor(year)2008  1.46028    0.12295  11.877  < 2e-16 ***
factor(year)2009  1.45736    0.12816  11.372  < 2e-16 ***
factor(year)2010  1.12100    0.14824   7.562 5.74e-14 ***
factor(year)2011  0.92310    0.16364   5.641 1.90e-08 ***
factor(year)2012  1.21634    0.14409   8.442  < 2e-16 ***
factor(year)2013  0.25915    0.22801   1.137 0.255843
factor(year)2014  1.12349    0.15074   7.453 1.29e-13 ***
factor(year)2015  0.22882    0.22918   0.998 0.318182
factor(year)2016  1.90924    0.10697  17.848  < 2e-16 ***
factor(year)2017  2.33392    0.09411  24.799  < 2e-16 ***
factor(year)2018  2.05314    0.10082  20.364  < 2e-16 ***
---
Signif. codes:  0 ‘***’ 0.001 ‘**’ 0.01 ‘*’ 0.05 ‘.’ 0.1 ‘ ’ 1

Approximate significance of smooth terms:
                    edf Ref.df     F p-value
s(X,Y):n_haul112 hauls 20.4393     29  5.412  <2e-16 ***
s(X,Y):n_haul72 hauls   0.9386     29  0.087  0.0855 .
s(X,Y):n_haul90 hauls  28.3087     29 13.290  <2e-16 ***
s(depth)                7.7679      9 25.862  <2e-16 ***
---
Signif. codes:  0 ‘***’ 0.001 ‘**’ 0.01 ‘*’ 0.05 ‘.’ 0.1 ‘ ’ 1

R-sq.(adj) =  0.335   Deviance explained = 55.1%
GCV =  6.288  Scale est. = 8.9944    n = 2336
```

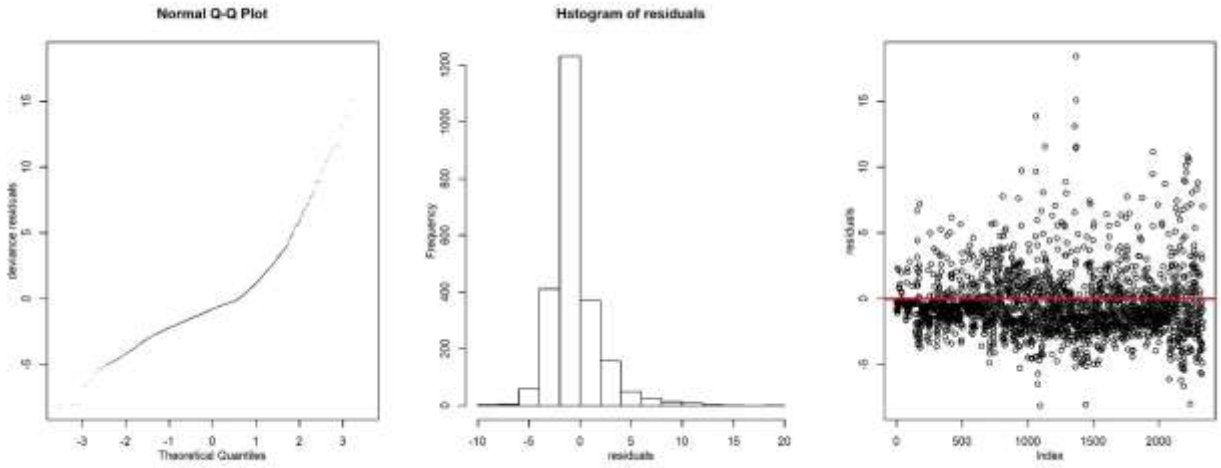

Figure 3.2.3.3.A – Diagnostic plots of residuals for *P. longirostris* in GSA 18.

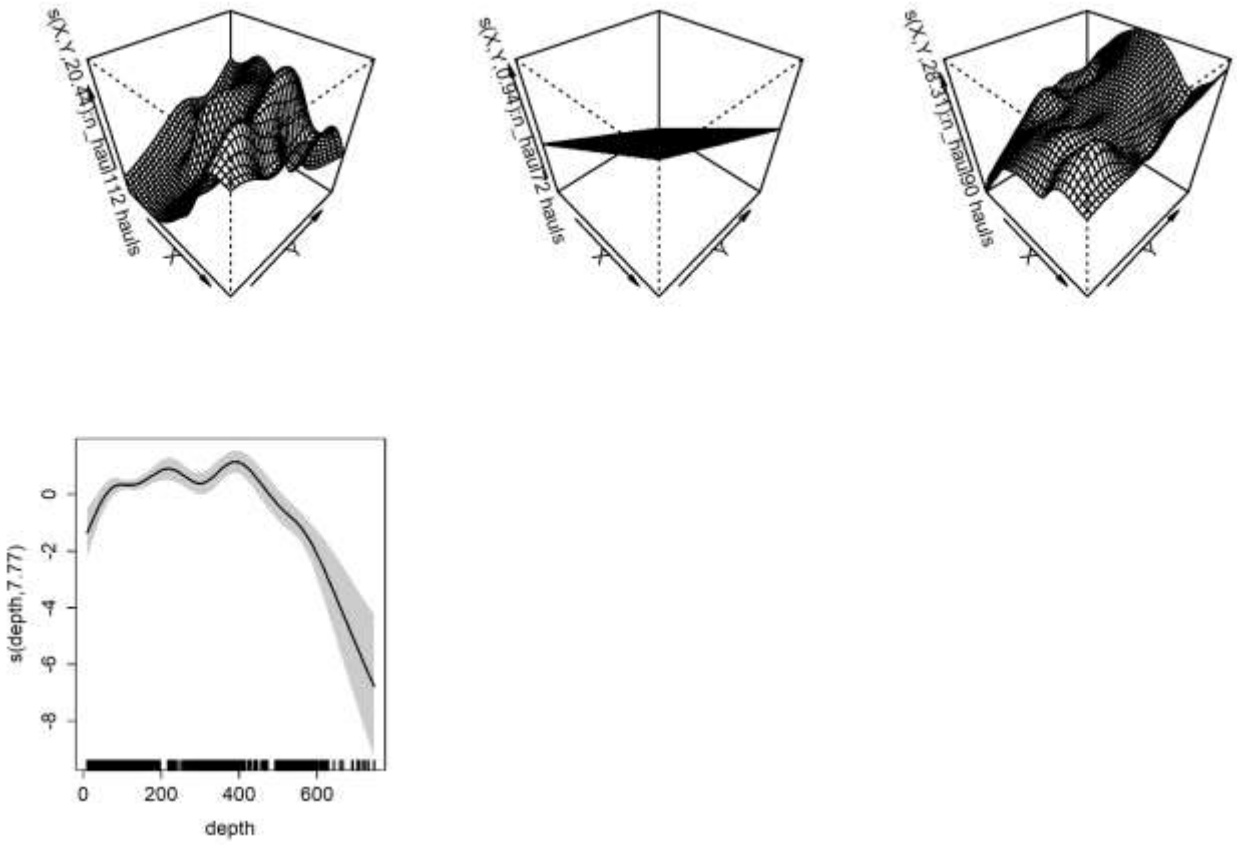

Figure 3.2.3.3.B – Splines and factors of the best model for *P. longirostris* in GSA 18.

Only the points of the predictive grid corresponding to a depth comprised in the 10-800 m range were selected. The grid points were also linked to the values of the other variables included in the best GAM and useful to predict the model in the standardized conditions: year and number of hauls (for standardization was used a unique reference value in the study area since 2002).

In Figure 3.2.3.3.C the comparison is reported between the original indices estimated on rough data according to Souplet (1996) and the indices estimated on the predicted results, predicted over the grid with the corresponding confidence intervals (Figure

3.2.3.3.C left). The prediction was also done on the original haul positions (Figure 3.2.3.3.C right).

The indices estimated by the model shows a good level of agreement between the original biomass index and the standardizations, especially on the original hauls positions. Indeed, the values predicted on the grid positions return an index generally lower than the original one, even if the overall trend between the two series is consistent.

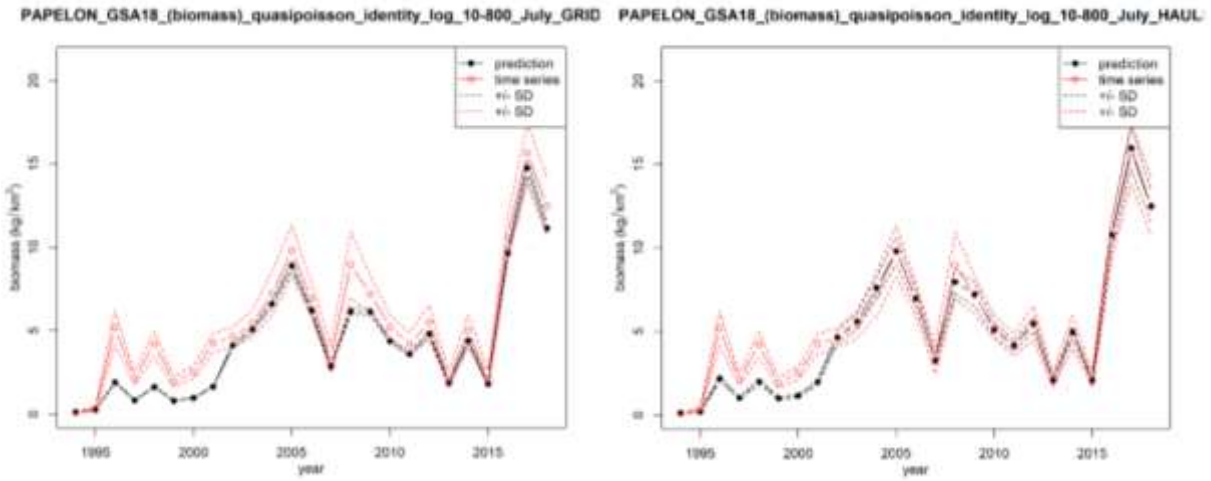

Figure 3.2.3.9 – Comparison between the original and standardized biomass indices of *P. longirostris* in GSA 18 predicted on the grid (left) and on the haul positions (right).

3.2.3.4 *Aristaeomorpha foliacea*

The analysis was performed using data from MEDITS survey conducted in the period between the 1996 and 2018, focusing on the bathymetrical range 200-800 m.

The presence of correlations among the explanatory variables was tested using the Pearson's correlation coefficients (Table 3.2.3.4.a). The correlation matrix shows a strong correlation coefficient of 0.8 for latitude and longitude also confirmed by the VIF coefficient that is 3 for both variables. For this reason, only longitude was retained.

Table 3.2.3.4.a - Correlation table among the quantitative explanatory variables explored for *A. foliacea* in GSA 18.

	year	**month**	**hour**	**Y**	**X**	**depth**
year		0.38	-0.06	0.11	0.03	0.1
month	0.38		-0.05	0	0.09	0.01
hour	-0.06	-0.05		-0.07	0.07	-0.08
Y	0.11	0	-0.07		-0.81	-0.05
X	0.03	0.09	0.07	-0.81		0
depth	0.1	0.01	-0.08	-0.05	0	

The explanatory variables considered are the year, month, depth, hour, longitude, sampling intensity (expressed as number of hauls, defined as a factor). The list of the most relevant models explored is reported in Table 3.2.3.4.b; in bold the best performing model is reported. The best model was estimated using the quasi-Poisson family distribution assuming a logarithm link function.

Table 3.2.3.4.b – Selection of the models explored for *A. foliacea* in GSA 18 (biomass index kg/km^2). In bold the best performing model is reported. Quasi-Poisson family distribution assuming a logarithm link function.

Model	% Deviance	GCV
$s(depth_{i,j}) + \varepsilon_{i,j}$	37.67%	6.80
$s(depth_{i,j}) + s(X_{i,j}) + \varepsilon_{i,j}$	47.65%	5.82
$s(depth_{i,j}) + s(X_{i,j}) + f(yeari,j) + \varepsilon_{i,j}$	56.52%	5.36
$s(depth_{i,j}, X_{i,j}) + f(year_{i,j}) + \varepsilon_{i,j}$	50.80%	6.17
$s(depth_{i,j}, Xi_{,j}, by=nb\_hauls) + f(year_{i,j}) + \varepsilon_{i,j}$	57.17%	5.61
$s(depth_{i,j}, by=nb\_hauls)\ s(X_{i,j}) + f(year_{i,j}) + \varepsilon_{i,j}$	57.01%	5.41
$s(depth_{i,j})\ s(X_{i,j}, by=nb\_hauls) + f(year_{i,j}) + \varepsilon_{i,j}$	59.56%	5.05
$s(depth_{i,j})\ s(X_{i,j}, Y_{i,j}, by=nb\_hauls) + f(year_{i,j}) + \varepsilon_{i,j}$	**64.1%**	**4.87**

The model summary is reported in the Table 3.2.3.4.c and indicates the significance of the sampling intensity, geographical position (longitude and depth) and year. The residuals of the model and the q-q plot reported in Figure 3.2.3.4.A show a skewed distribution.
The estimation of the splines was found in any cases significant although the wide confidence intervals in factor variable (Table 3.2.3.4.c and Figure 3.2.3.4.B).

Table 3.2.3.4.c – Summary of the estimates, REML and deviance explained of the best GAM for *A. foliacea* in GSA 18.

Parametric coefficients:

	Estimate	Std. Error	t value	Pr(>|t|)	
factor(year)1994	-1.70734	0.95182	-1.794	0.07331	.
factor(year)1995	-1.85039	0.98659	-1.876	0.06116	.
factor(year)1996	-0.65357	0.42184	-1.549	0.12178	
factor(year)1997	-0.24182	0.39821	-0.607	0.54389	

```
factor(year)1998 -0.83526    0.43556  -1.918  0.05559 .
factor(year)1999 -0.58023    0.41444  -1.400  0.16198
factor(year)2000 -0.67106    0.42710  -1.571  0.11662
factor(year)2001  0.22318    0.37730   0.592  0.55437
factor(year)2002  0.36689    0.26660   1.376  0.16923
factor(year)2003  0.44876    0.26155   1.716  0.08668 .
factor(year)2004  0.21832    0.27730   0.787  0.43139
factor(year)2005  0.70537    0.24422   2.888  0.00400 **
factor(year)2006  1.03039    0.22825   4.514 7.52e-06 ***
factor(year)2007 -0.45608    0.35814  -1.273  0.20330
factor(year)2008  0.08839    0.32798   0.270  0.78763
factor(year)2009  0.70567    0.24530   2.877  0.00415 **
factor(year)2010  0.03573    0.31819   0.112  0.91063
factor(year)2011  0.43585    0.28273   1.542  0.12366
factor(year)2012  0.23357    0.29594   0.789  0.43025
factor(year)2013  0.85844    0.24992   3.435  0.00063 ***
factor(year)2014  0.77619    0.25497   3.044  0.00243 **
factor(year)2015  0.76526    0.25792   2.967  0.00312 **
factor(year)2016  0.71182    0.25995   2.738  0.00634 **
factor(year)2017  1.07177    0.23820   4.499 8.05e-06 ***
factor(year)2018  0.66147    0.26916   2.458  0.01425 *
---
Signif. codes:  0 ‘***’ 0.001 ‘**’ 0.01 ‘*’ 0.05 ‘.’ 0.1 ‘ ’ 1

Approximate significance of smooth terms:
                       edf Ref.df     F  p-value
s(X,Y):n_haul112 hauls 1.046e+01     29 2.992 1.97e-15 ***
s(X,Y):n_haul72 hauls  6.647e-05     29 0.000    0.792
s(X,Y):n_haul90 hauls  1.833e+01     29 3.241 6.96e-13 ***
s(depth)               2.875e+00      9 7.240  < 2e-16 ***
---
Signif. codes:  0 ‘***’ 0.001 ‘**’ 0.01 ‘*’ 0.05 ‘.’ 0.1 ‘ ’ 1

R-sq.(adj) =  0.499   Deviance explained = 64.1%
GCV = 4.8772  Scale est. = 5.6798    n = 718
```

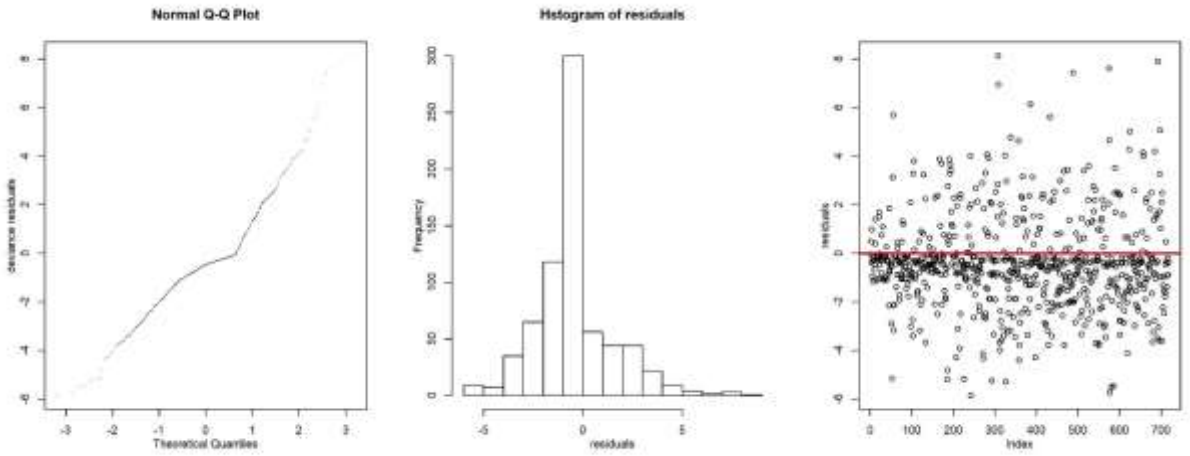

Figure 3.2.3.4.A– Diagnostic plots of residuals for *A. foliacea* in GSA 18.

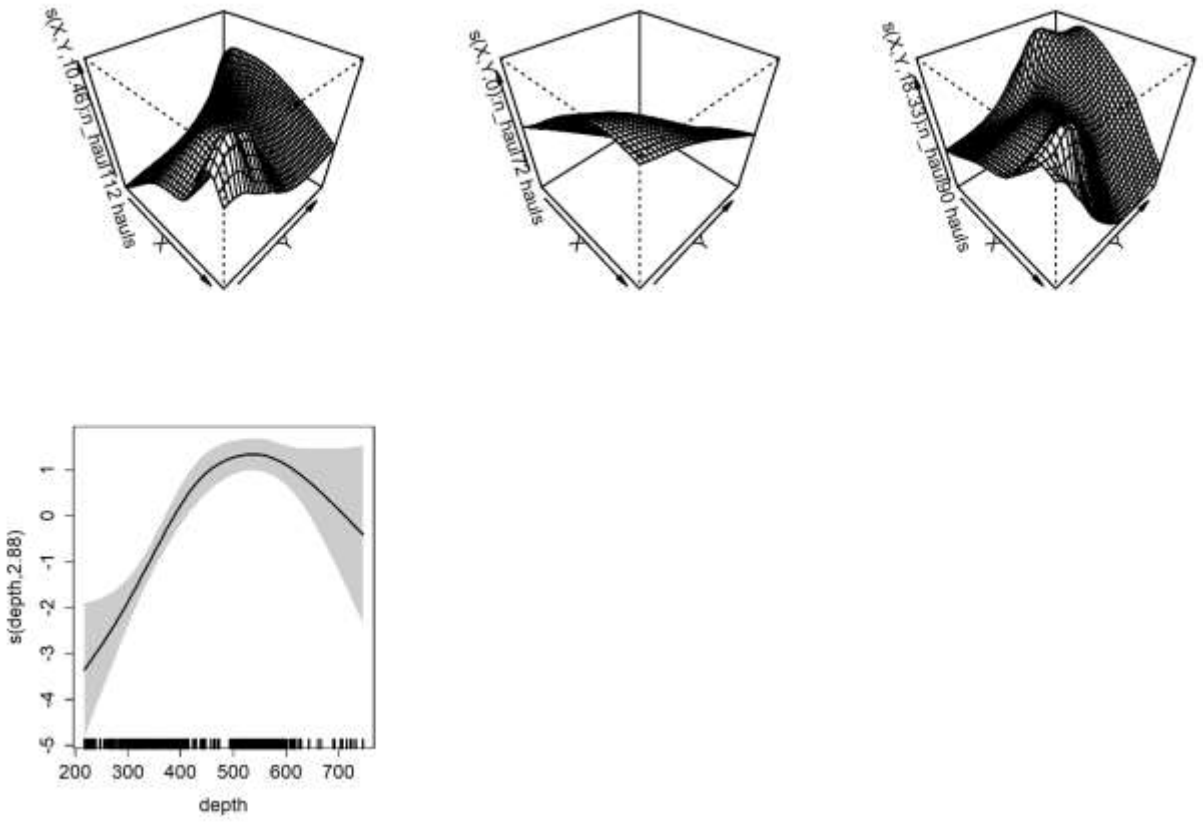

Figure 3.2.3.4.B – Splines of the best model for *A. foliacea* in GSA 18.

Only the points of the predictive grid corresponding to a depth comprised in the 200-800 m range were selected. The grid points were also linked to the values of the other variables included in the best GAM and useful to predict the model in the standardized conditions: year and number of hauls (for standardization a unique reference value was used in the study area since 2002).

In Figure 3.2.3.4.C the comparison is reported between the original indices estimated on rough data according to Souplet (1996) and the indices estimated on the predicted results, predicted over the grid with the corresponding confidence intervals (Figure

3.2.3.4.C left). The prediction was also done on the original haul positions (Figure 3.2.3.4.C right).

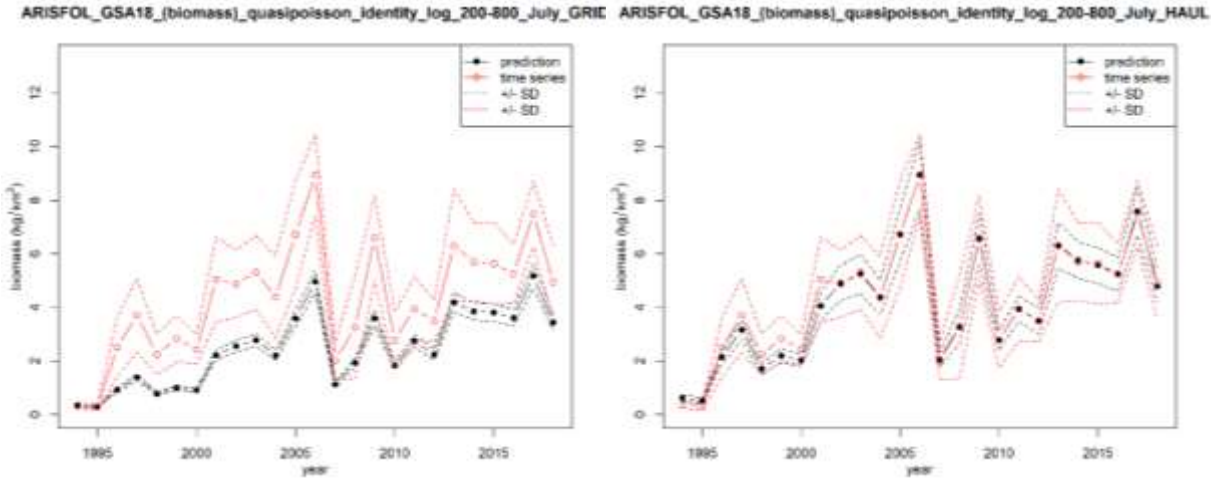

Figure 3.2.3.4.C – Comparison between the original and standardized biomass indices of *A. foliacea* in GSA 18 predicted on the grid (left) and on the haul positions (right).

3.2.3.5. *Illex coindetii*

The analysis was performed using data from MEDITS survey conducted in the period between the 1994 and 2018, focusing on the bathymetrical range 10-200 m.

The presence of correlations among the explanatory variables was tested using the Pearson's correlation coefficients (Table 3.2.3.5.a). The correlation matrix shows a correlation coefficient of -0.46 for latitude and longitude while, for these two variables VIF values of 1.4 (longitude) and 1.3 (latitude) were estimated. Being the VIF values lower than the threshold value (3), no collinearity was detected between these variables. Among the other variables no significant correlations were found.

Table 3.2.3.5.a - Correlation table among the quantitative explanatory variables explored for *I. coindetii* in GSA 18.

	year	**month**	**X**	**Y**	**depth**	**hour**
year		0.43	0.14	0.02	0.00	0.02
month	0.43		0.14	0.01	0.02	0.02
X	0.14	0.14		-0.46	0.34	0.00
Y	0.02	0.01	-0.46		-0.27	0.05
depth	0.00	0.02	0.34	-0.27		0.03
hour	0.02	0.02	0.00	0.05	0.03	

The explanatory variables considered are the year, month, depth, hour, latitude, longitude, sampling intensity (expressed as number of hauls, defined as a factor). The list of the most relevant models explored is reported in Table 3.2.3.5.b; in bold the best performing model is reported. The best model was estimated using the quasi-Poisson family distribution, assuming a logarithmic link function.

Table 3.2.3.5.b – Selection of the models explored for *I. coindetii* in GSA 18 (biomass index kg/km^2). In bold the best performing model is reported. Quasi-Poisson family distribution, assuming a logarithmic link function.

Model	% Deviance	GCV
$f(year_j) + \varepsilon_{i,j}$	21.34%	22.40025
$f(year_j) + s(X_{i,j},Y_{i,j}) + \varepsilon_{i,j}$	51.85%	14.42025
$f(year_j) + s(X_{i,j},Y_{i,j}) + s(depth_{i,j}) + \varepsilon_{i,j}$	55.17%	13.42322
$\mathbf{f(year_j) + s(X_{i,j},Y_{i,j}) + s(depth_{i,j}) + f(hour_j,bs="cc") + \varepsilon_{i,j}}$	56.01%	13.28828

The model summary is reported in Table 3.2.3.5.c and indicates the significance of the geographical position, the hour and the year. The residuals of the model and the q-q plot, reported in Figure 3.2.3.5.A show a quite normal distribution.

The estimation of the splines and factors was found in any cases significant (Table 3.2.3.5.c and Figure 3.2.3.5.B).

Table 3.2.3.5.c – Summary of the estimates, GVC and deviance explained of the best GAM for *I. coindetii* in GSA 18.

Parametric coefficients:

	Estimate	Std. Error	t value	Pr(>|t|)	
factor(year)1994	-1.02135	0.73809	-1.384	0.16663	
factor(year)1995	0.82215	0.29532	2.784	0.00544	**
factor(year)1996	1.03288	0.24157	4.276	2.02e-05	***
factor(year)1997	0.57436	0.30007	1.914	0.05579	.
factor(year)1998	0.97842	0.24691	3.963	7.75e-05	***
factor(year)1999	2.14122	0.14093	15.194	< 2e-16	***
factor(year)2000	1.97353	0.15454	12.771	< 2e-16	***
factor(year)2001	2.46451	0.12041	20.467	< 2e-16	***
factor(year)2002	1.63855	0.18854	8.691	< 2e-16	***

```
factor(year)2003  1.62388    0.18862   8.609  < 2e-16 ***
factor(year)2004  2.13323    0.14571  14.640  < 2e-16 ***
factor(year)2005  2.85548    0.10945  26.090  < 2e-16 ***
factor(year)2006  1.69967    0.18192   9.343  < 2e-16 ***
factor(year)2007  2.81788    0.11110  25.364  < 2e-16 ***
factor(year)2008  2.77205    0.10575  26.214  < 2e-16 ***
factor(year)2009  3.04496    0.09946  30.614  < 2e-16 ***
factor(year)2010  2.57919    0.11769  21.916  < 2e-16 ***
factor(year)2011  1.96095    0.15414  12.722  < 2e-16 ***
factor(year)2012  2.57971    0.11545  22.345  < 2e-16 ***
factor(year)2013  2.54157    0.11621  21.870  < 2e-16 ***
factor(year)2014  2.60584    0.11441  22.777  < 2e-16 ***
factor(year)2015  2.30223    0.13028  17.671  < 2e-16 ***
factor(year)2016  2.73171    0.10940  24.969  < 2e-16 ***
factor(year)2017  2.56742    0.12022  21.355  < 2e-16 ***
factor(year)2018  2.48691    0.11844  20.996  < 2e-16 ***
---
Signif. codes:  0 ‘***’ 0.001 ‘**’ 0.01 ‘*’ 0.05 ‘.’ 0.1 ‘ ’ 1

Approximate significance of smooth terms:
          edf Ref.df      F  p-value
s(X,Y)   21.777    29 10.770  < 2e-16 ***
s(depth)  5.577     9 13.468  < 2e-16 ***
s(hour)   5.453     8  2.869 0.000192 ***
---
Signif. codes:  0 ‘***’ 0.001 ‘**’ 0.01 ‘*’ 0.05 ‘.’ 0.1 ‘ ’ 1

R-sq.(adj) =  0.383   Deviance explained =   56%
GCV =  13.29  Scale est. = 16.088    n = 1618
```

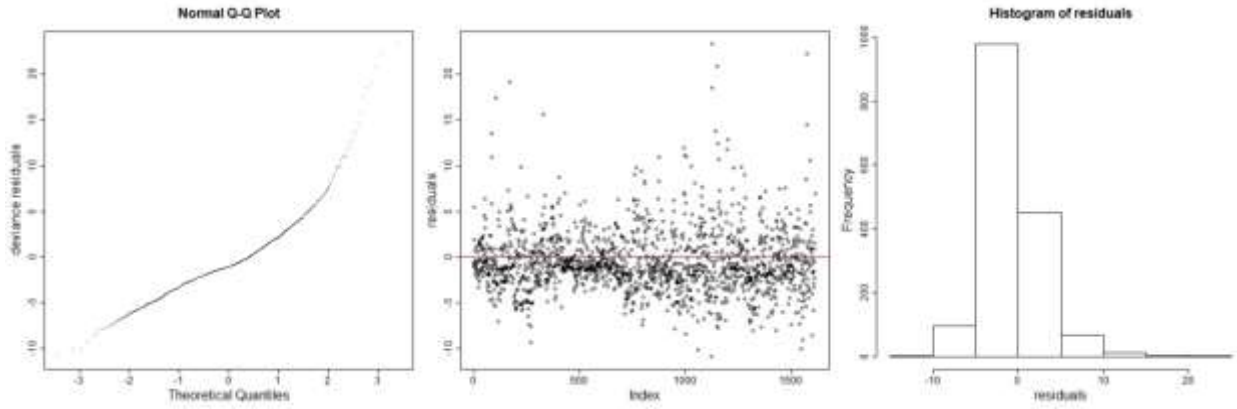

Figure 3.2.3.5.A – Diagnostic plots of residuals for *I. coindetii* in GSA 18.

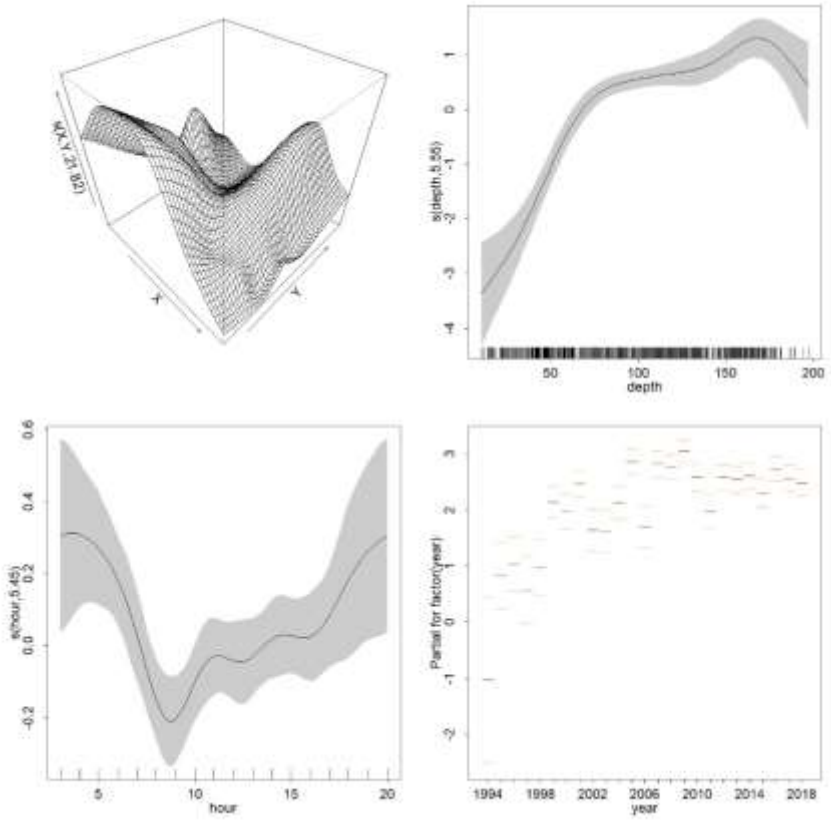

Figure 3.2.3.5.B – Splines and factors of the best model for *I. coindetii* in GSA 18.

Only the points of the predictive grid corresponding to a depth comprised in the 10-200 m range were selected. The grid points were also linked to the values of the other variables included in the best GAM and useful to predict the model in the standardized conditions: year and hour (for standardization was used 12:00).

In Figure 3.2.3.5.C the comparison is reported between the original indices estimated on rough data according to Souplet (1996) and the indices estimated on the predicted results, predicted over the grid with the corresponding confidence intervals (Figure 3.2.3.5.C left). The prediction was also done on the original haul positions (Figure 3.2.3.5.C right).

The indices estimated by the model shows a higher agreement between the original biomass index and the standardization, especially on the hauls positions. Indeed, the values predicted on the grid return in the last years an index generally lower than the original one, even if the overall trend between the two series is consistent.

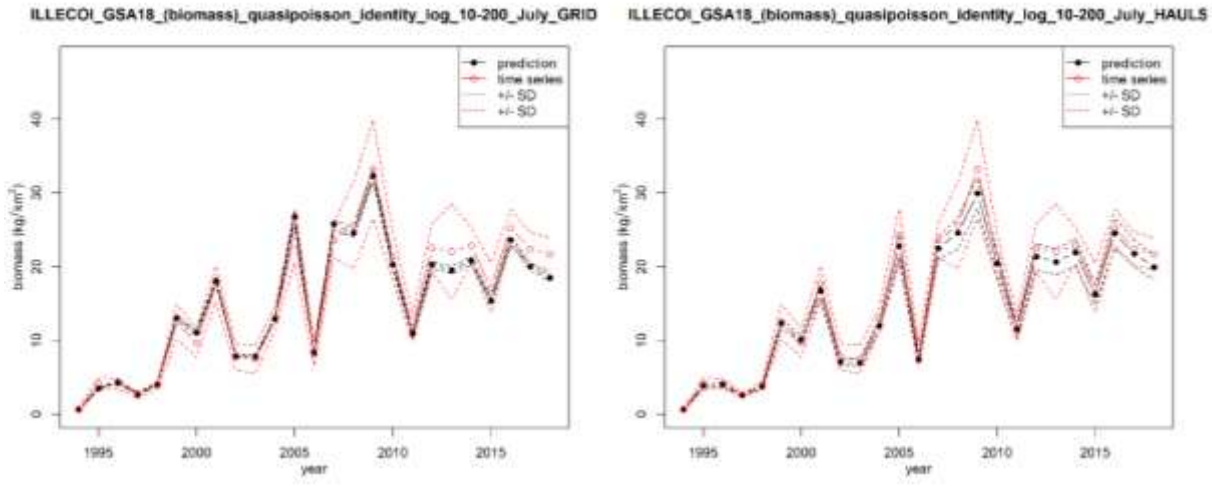

Figure 3.2.3.5.C – Comparison between the original and standardized biomass indices of *I. coindetii* in GSA 18 predicted on the grid (left) and on the haul positions (right).

3.3 GSA19 – Western Ionian Sea

3.3.1 Ranking of the species from MEDITS survey

In the following Table 3.3.1.a, it is reported the ranking obtained for the commercial species represented in the MEDITS survey. Considering a cumulative percentage of 90%, 13 species were considered. However, other 5 species were added to their commercial importance in the GSA, resulting in 18 species.

Table 3.2.1.a – Ranking of MEDITS species selected for the GSA19.

Species	GSA19 MEDITS CODE	CUMULATIVE %
Mullus barbatus	MULLBAR	19.4
Pagellus acarne	PAGEACA	33.5
Trachurus trachurus	TRACTRA	47.2
Merluccius merluccius	MERLMER	58.6
Parapenaeus longirostris	PAPELON	66.8
Illex coindetii	ILLECOI	72.9
Phycis blennoides	PHYIBLE	76.9
Pagellus erythrinus	PAGEERY	80.3
Micromesistius poutassou	MICMPOU	83.3
Aristeus antennatus	ARITANT	85.6
Trachurus mediterraneus	TRACMED	87.2
Aristaeomorpha foliacea	ARISFOL	88.8
Lophius budegassa	LOPHBUD	90.1
Pagellus bogaraveo	PAGEBOG	91.3
Helicolenus dactylopterus	HELIDAC	94.4
Eledone cirrhosa	ELEDCIR	97.8
Nephrops norvegicus	NEPRNOR	99.6
Galeus melastomus	GALUMEL	-

3.3.2 Analysis of trawl survey data with BioIndex

BioIndex (version2.1.2) was carried out to derive all the indicators provided by the software and described in the Methods section. The outputs are provided in an Excel file and a selection is summarized in terms of trend significance and ranges in Table 3.3.2.a. The extended outputs in terms of tables of indicators, plots and raster files are reported on the sharepoint (WP4-Integrated platform/Activity 4.3-BSTAT/D4.3.1Spatial distribution of marine species).

The trends of biomass index are increasing for about 50% of the examined species along the time series of MEDITS data (1994-2018) (Table 3.3.2.a). The abundance index and the number of positive hauls are increasing for about 30% of the examined species during the same time series. Decreasing trends in abundance, biomass and positive hauls are highlighted for *Nephrops norvegicus*. Decreasing trends in length at 50th percentile are point out for *Mullus barbatus*, *Merluccius merluccius*, *Parapenaeus longirostris* and Pagellus *bogaraveo.*

Concerning the aggregation of recruits and spawners at spatial level, the stock of giant red shrimps *A. foliacea* occurred with higher abundance values of recruits on the fishing grounds along Apulian coasts and along the southern coast of Calabrian region, and with higher abundance values of spawners on grounds between Santa Maria di Leuca and Otranto, and along southern coast of Calabrian region (Figure 3.3.2.A).

The stock of the blue and red shrimps *A. antennatus* occurred with the higher abundance values of recruits on the fishing grounds off Gallipoli and along Calabrian costs, whilst the higher abundance values of spawners were recorded along Apulian and Calabrian coasts (Figure 3.3.2.B).

The stock of deep-water rose shrimp *P. longirostris* occurred with higher abundance values of recruits on the fishing grounds off Otranto and S. Maria di Leuca, and along the eastern and south-eastern coast of Calabrian region. On the other hand, spawners occurred with higher abundance values on bathyal grounds from Otranto to Taranto along Apulian and Calabrian coasts and off south-eastern Sicily (Figure 3.3.2.C).

The European hake *M. merluccius* occurred with higher abundance values of recruits on the fishing grounds along eastern Sicily coasts. On the other hand, spawners occurred with higher abundance values along Apulian and Calabrian coasts as well as along eastern Sicily (Figure 3.3.2.D).

The red mullet *M. barbatus* occurred with higher abundance values of recruits and spawners on the fishing grounds off Otranto and along Lucania and Calabrian coasts as well as off eastern Sicily (Figure 3.3.2.E).

The broadtail shortfin squid *I. coindetii* occurred with the higher abundance values of recruits on the fishing grounds off Otranto and off north-eastern Calabrian region whereas the higher abundance values of spawners occurred on grounds off southern part of Apulian region (both Adriatic and Ionian Sea) and along southern Calabrian coasts (Figure 3.3.2.F).

The Norway lobster *Nephrops norvegicus* occurred with higher abundance values of recruits on the fishing grounds off Porto Cesareo (Apulia) and with higher values of abundance of spawners on grounds off Apulian region as well off eastern and southern Calabrian region (Figure 3.3.2.G).

Table 3.3.2.a - Summary table of the principal indicators calculated by BioIndex for all the species analysed in GSA19.

Species	Depth range	abundance n/km^2	CV abundance	biomass (kg/km^2)	CV biomass (kg/km^2)	Positive hauls	50th perc	CV 50th perc	95th perc	CV 95th perc	Abundance trend	Biomass trend	Positive hauls	50 th perc trend	95th perc trend
MULLBAR	10-200	152-14623	0.20-0.90	6.14-210.15	0.24-0.88	18.92-42.86	66.8-143.8	0.0003-0.0026	121.6-192.2	0.0003-0.0060	↗	↗	↗	↘	↔
PAGEACA	10-200	6-15445	0.32-1.00	0.22-188.40	0.32-0.98	6.76-42.86	49.9-162.5	0.003-0.0173	89.5-189.5	0.0003-0.0110	↗	↗	↗	↔	↔
TRACTRA	10-200	805-53987	0.26-0.83	12.11-248.09	0.22-0.76	18.92-45.95	59.7-138.4	0.0002-0.0450	74.8-180.5	0.0000-0.0039	↔	↔	↔	↔	↔
MERLMER	10-800	154-1632	0.19-0.80	10.59-36.20	0.12-0.33	45.71-72.86	88.5-212.1	0.0012-0.0137	145.5-363.0	0.0017-0.0338	↗	↔	↔	↘	↔
PAPELON	10-800	520-4646	0.16-0.35	3.28-18.84	0.13-0.41	28.38-67.14	17.8-23.2	0.0025-0.0278	26.1-31.0	0.0041-0.0213	↗	↗	↔	↘	↔
ILLECOI	10-800	15-879	0.20-0.59	0.70-35.17	0.17-0.61	17.57-80.00	58.0-134.5	0.0015-0.0712	115.0-190.2	0.0021-0.0442	↗	↗	↗	↔	↘
PHYIBLE	10-800	43-874	0.14-0.30	1.49-14.79	0.10-0.33	50.00-68.57	86.3-175.4	0.0015-0.0606	118.2-386.5	0.0027-0.1007	↔	↔	↔	↗	↔
PAGEERY	10-200	11-2514	0.25-0.64	0.58-35.11	0.26-0.54	6.76-28.57	73.8-172.5	0.0007-0.0258	133.00-248.20	0.0016-0.0165	↗	↗	↗	↔	↔
MICMPOU	10-800	16-6941	0.23-0.87	1-56	0.24-0.73	14.29-41.89	96.5-249.4	0.0004-0.0192	112.0-334.5	0.0002-0.0371	↔	↔	↘	↔	↔
ARITANT	200-800	156-774	0.09-0.39	3.02-13.05	0.09-0.35	21.43-45.71	26.2-41.5	0.0091-0.055	42.2-56.4	0.0061-0.0578	↔	↔	↔	↔	↔
TRACMED	10-200	14-2882	0.29-0.79	0.29-44.65	0.26-0.82	5.71-34.29	55.6-170.0	0.0006-0.059	102.4-319.2	0.0004-0.0629	↔	↔	↔	↔	↔
ARISFOL	200-800	21-1091	0.17-0.69	0.37-11.82	0.18-0.58	20.00-47.14	22.5-36.2	0.0040-0.0474	31.8-52.7	0.0066-0.6307	↔	↗	↔	↗	↔
LOPHBUD	10-800	5-108	0.14-0.54	1.49-8.10	0.16-0.66	16.22-61.43	78.6-345.0	0.0031-0.0727	233.0-561.5	0.0024-0.0391	↔	↔	↔	↔	↔
PAGEBOG	10-800	0-1606	0.31-0.96	0.00-10.26	0.21-0.96	0.00-51.43	63.5-220.0	0.0008-0.0320	98.8-284.0	0.0006-0.0354	↗	↗	↗	↘	↔
HELIDAC	10-800	8-1039	0.21-0.63	0.52-3.23	1.99-5.88	16.22-51.43	37.0-200.4	0.0013-0.1267	52.1-254.9	0.0009-0.0602	↔	↗	↔	↔	↔
ELEDCIR	10-800	2-88	0.17-0.57	0.32-6.67	0.22-0.88	6.76-34.29	22.5-105.0	0.0054-0.1276	68.2-146.0	0.0033-0.0638	↔	↔	↔	↔	↔
NEPRNOR	10-800	4-207	0.25-0.57	0.20-2.38	0.22-0.59	14.29-43.24	24.2-39.2	0.0185-0.2465	39.5-58.7	0.0250-0.1634	↘	↘	↘	↗	↔
GALUMEL	10-800	27-300	0.12-0.41	5.10-43.20	0.13-0.46	12.16-48.57	265.0-419.7	0.0021-0.046	463.6-519.5	0.0019-0.0268	↔	↗	↔	↗	↗

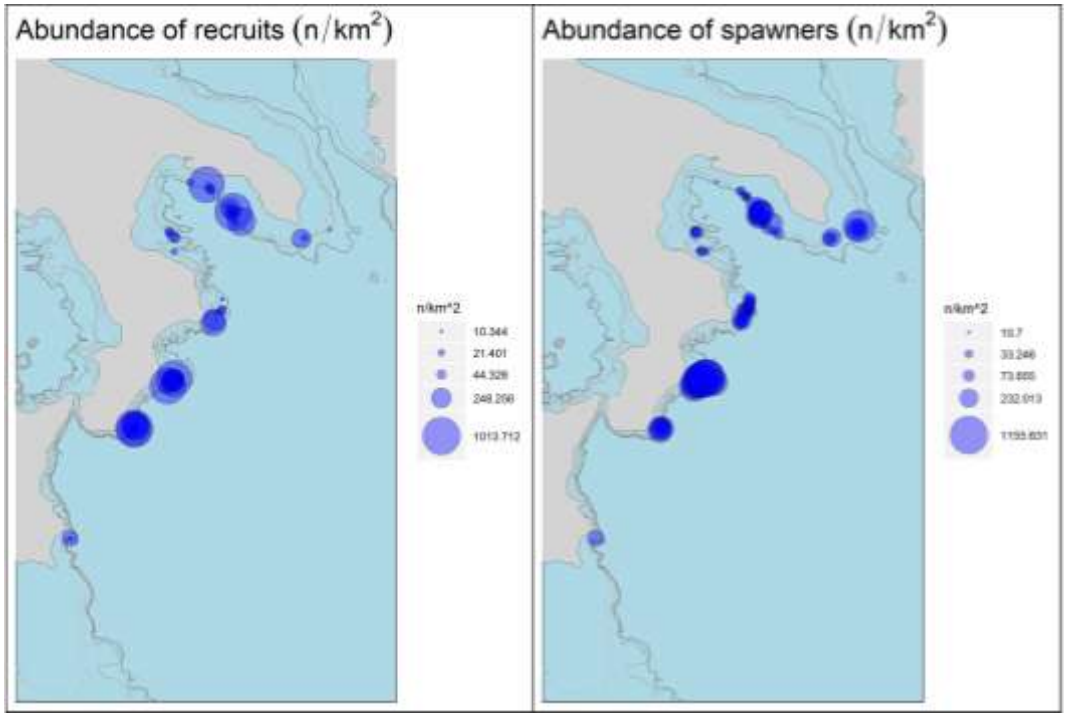

Figure 3.3.2.A – Bubble plot of the abundance of recruits and spawners by hauls of *A. foliacea* in the GSA19 during time series 2014-2018.

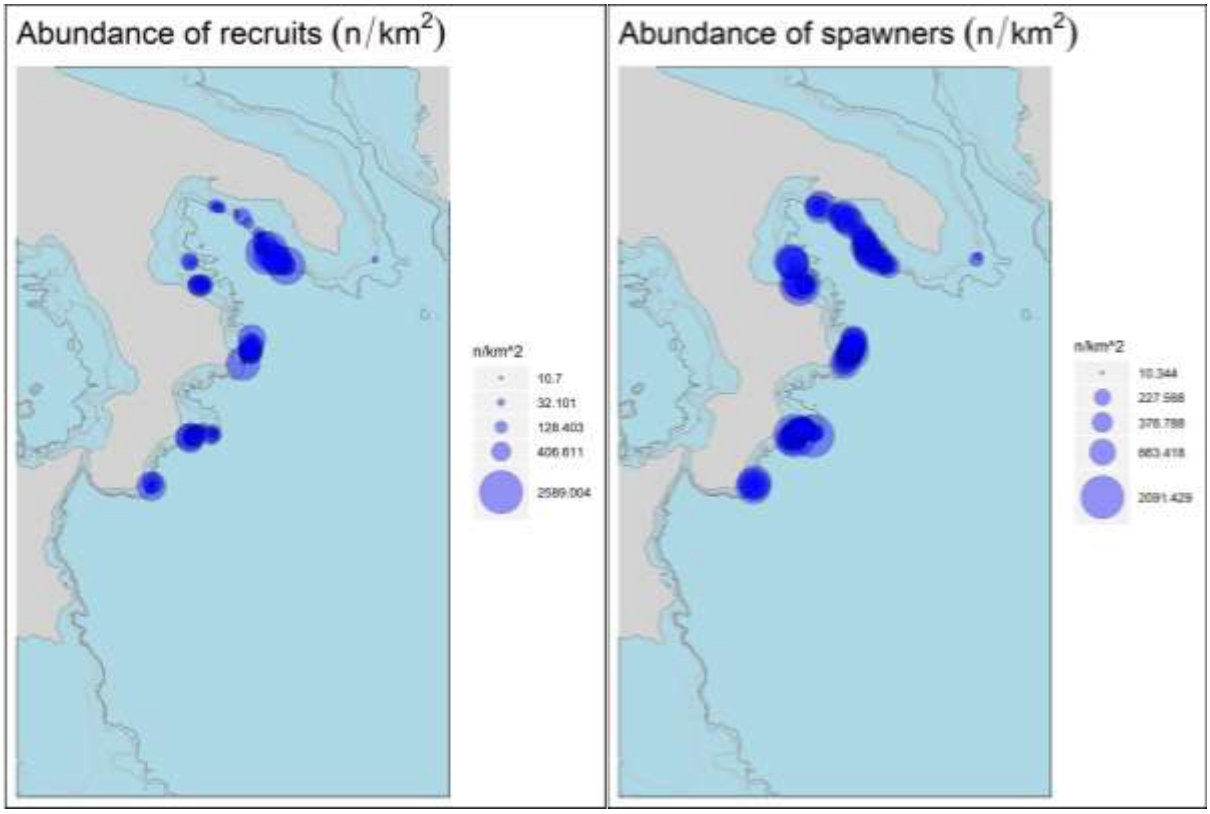

Figure 3.3.2.B – Bubble plot of the abundance of recruits and *A. antennatus* in the GSA19 during time series 2014-2018.

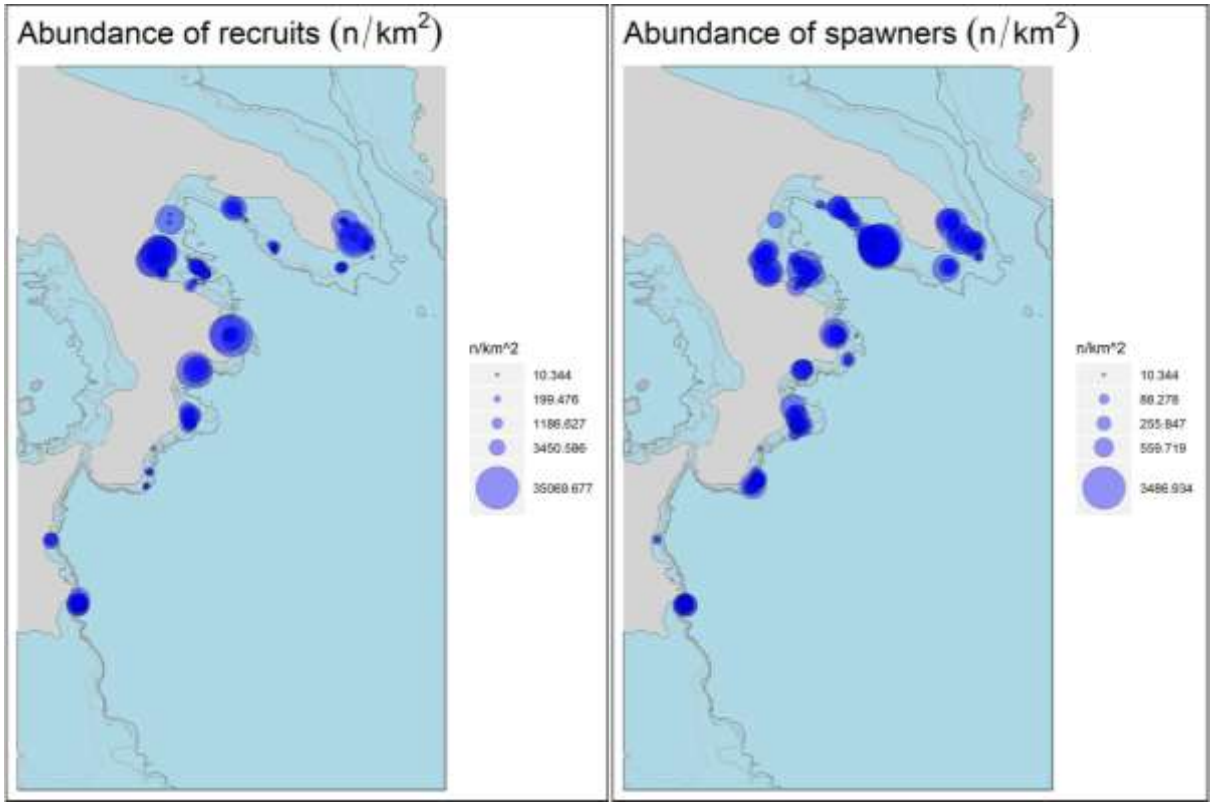

Figure 3.3.2.C – Bubble plot of the abundance of recruits and *P. longirostris* in the GSA19 during time series 2014-2018.

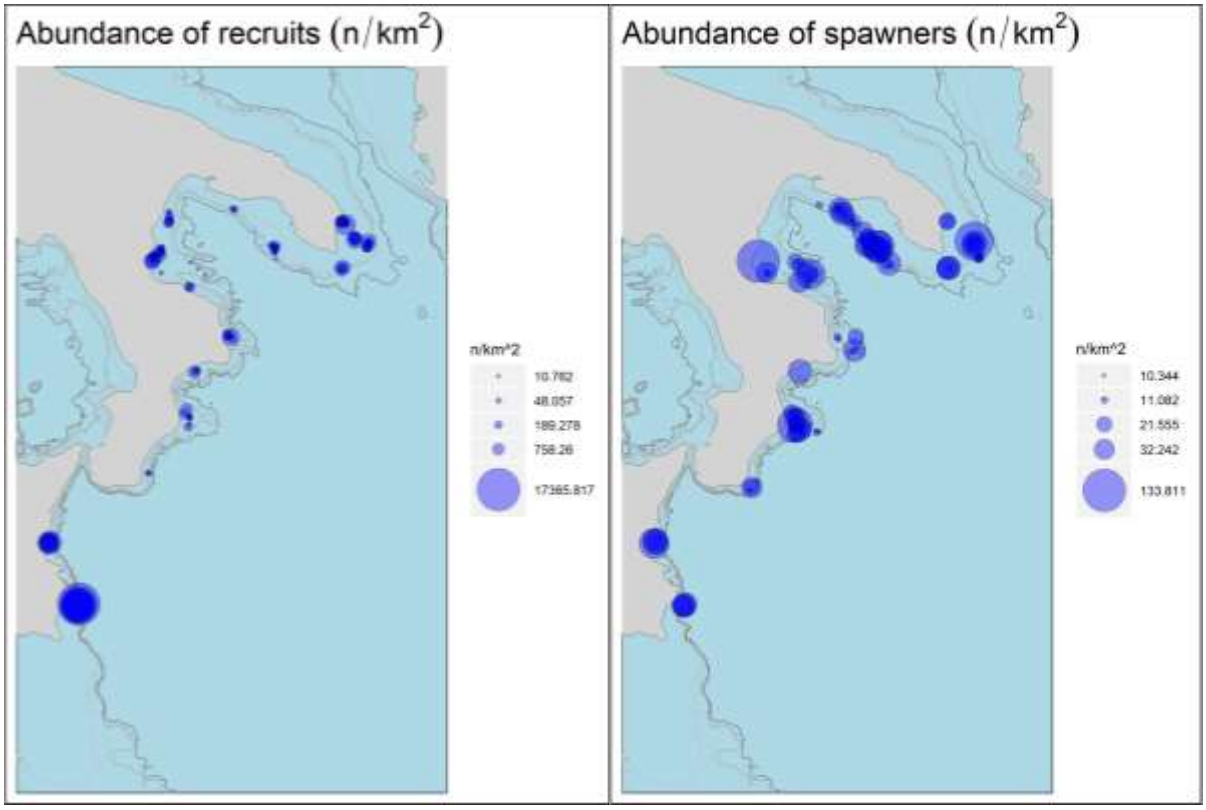

Figure 3.3.2.D – Bubble plot of the abundance of recruits and spawners by hauls of *M. merluccius* in the GSA19 during time series 2014-2018.

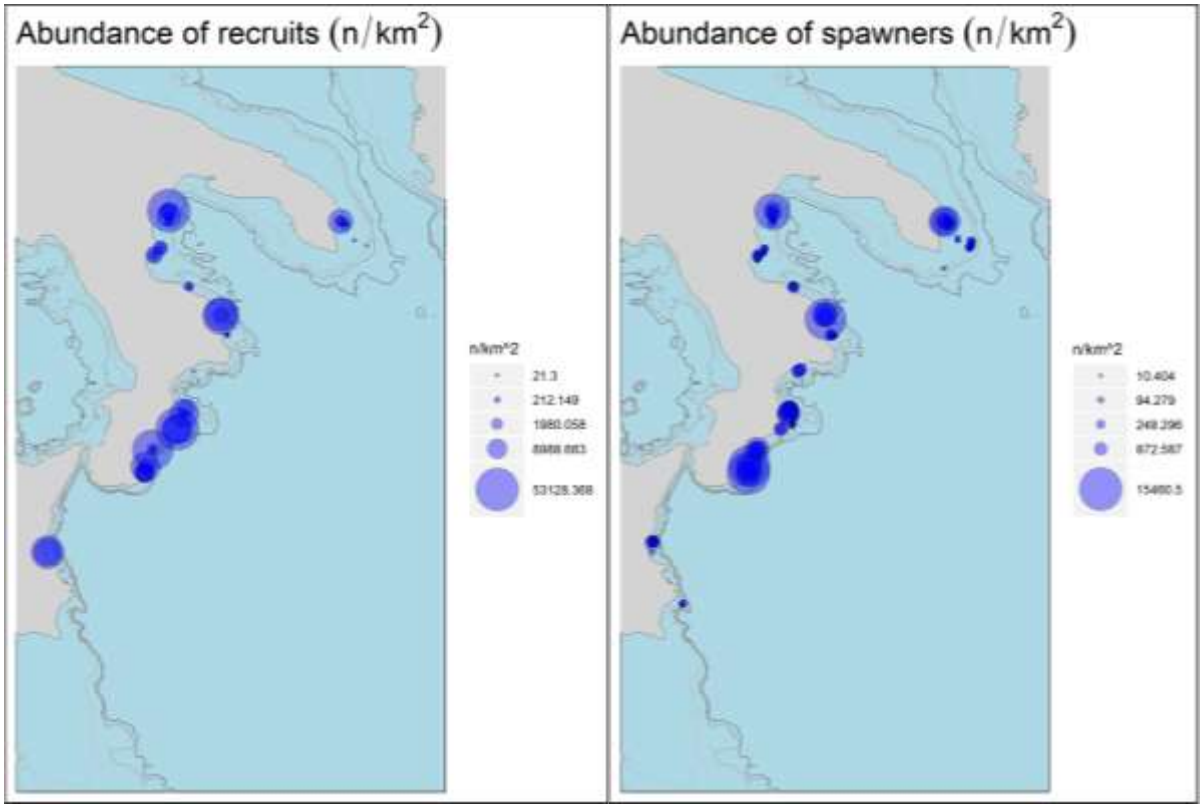

Figure 3.3.2.D – Bubble plot of the abundance of recruits and spawners by hauls of *M. barbatus* in the GSA19 during time series 2014-2018.

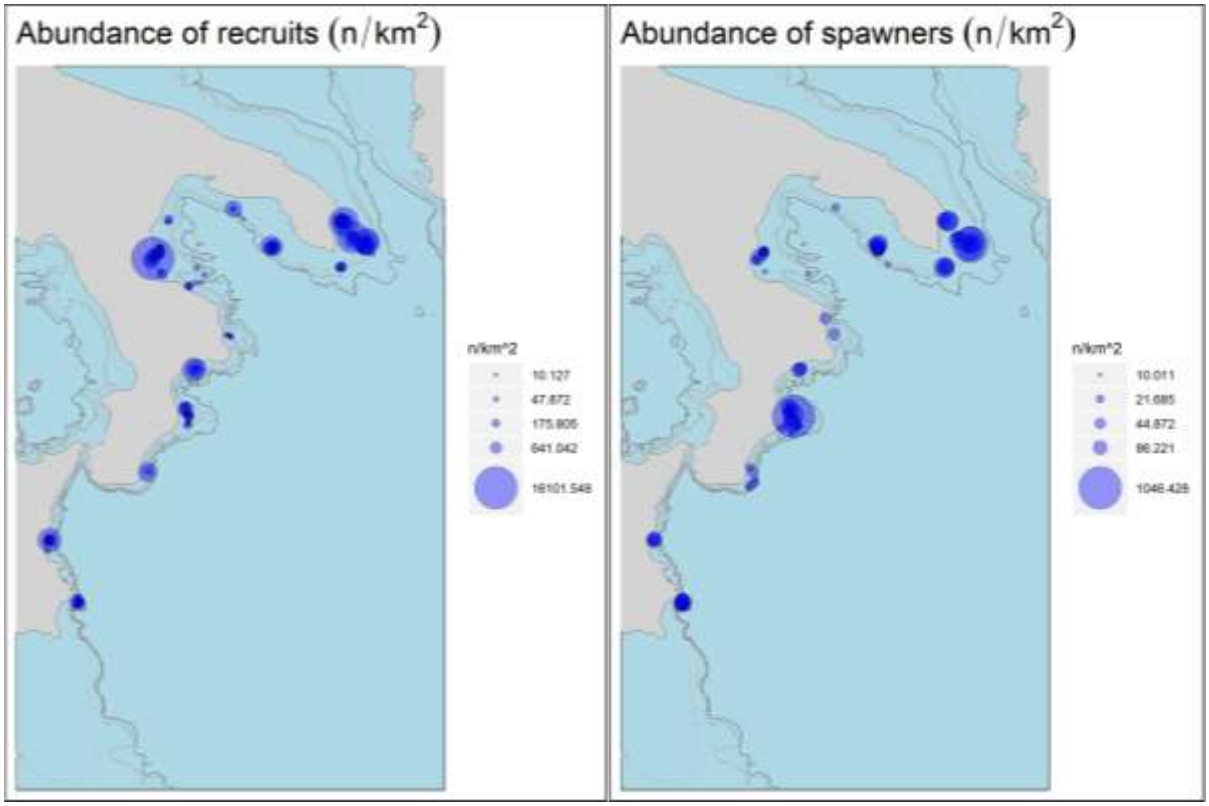

Figure 3.3.2.F – Bubble plot of the abundance of recruits and spawners by hauls of *I. coindetii* in the GSA19 during time series 2014-2018.

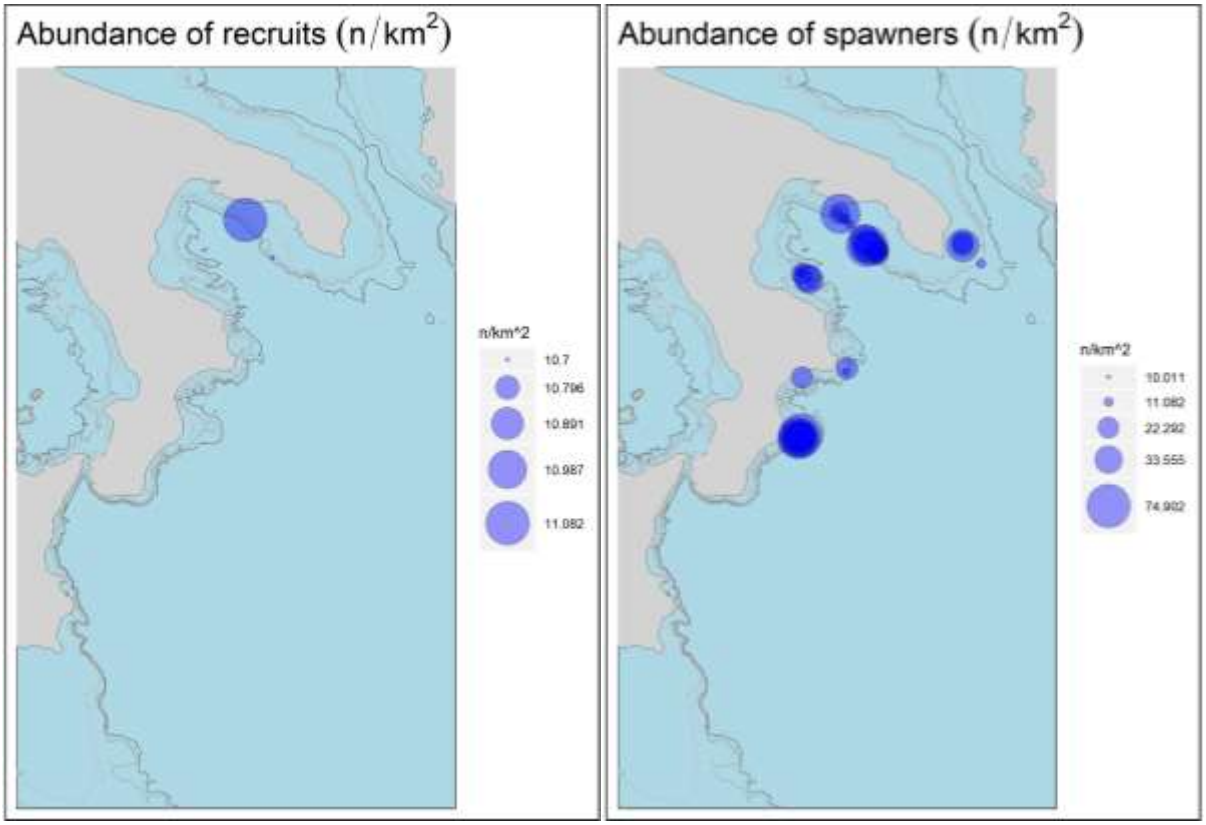

Figure 3.3.2.G - Bubble plot of the abundance of recruits and spawners by hauls of *N. norvegicus* in the GSA19 during time series 2014-2018.

3.3.3 Standardization of trawl survey data with BioStand

BioStand (version 2.1.2) was carried out to standardize the data described in Data section for the following selected species: *A. foliacea*, *P. longirostris, M. merluccius, M. barbatus, I. coindetii.* For all species, the Gaussian, quasi-Poisson and Tweedie distributions were explored with logarithmic, square root and identity transformations data.

3.3.3.1. *Aristaeomorpha foliacea*

The analysis was performed using data from MEDITS survey conducted in the period between the 1994 and 2018, focusing on the bathymetrical range 200-800 m.

The presence of correlations among the explanatory variables was tested using the Pearson's correlation coefficients (Table 3.3.3.1.a). The correlation matrix shows a strong correlation coefficient of 0.81 for latitude and longitude also confirmed by the VIF coefficient that is 3 for the longitude. For this reason, only latitude was retained. Among the other variables no significant correlations were found.

Table 3.2.3.1.a - Correlation table among the quantitative explanatory variables explored for *A. foliacea* in GSA 19.

	year	**month**	**hour**	**Y**	**X**	**depth**
year		0.55	0.07	-0.02	0.02	0.02
month	0.55		0.00	-0.01	0.00	-0.01
hour	0.07	0.00		0.04	0.06	-0.03
Y	-0.02	-0.01	0.04		0.81	0.12
X	0.02	0.00	0.06	0.81		0.22
depth	0.02	-0.01	-0.03	0.12	0.22	

The explanatory variables considered are the year, month, depth, hour, latitude, longitude. The list of the most relevant models explored is reported in Table 3.3.3.1.b. The best model was estimated using the Tweedie family distribution, assuming a logarithm link function e no transformation of data.

Table 3.3.3.1.b – Selection of the models explored for *A. foliacea* in GSA 19 (biomass index kg/km²). The best performing model is reported in bold.

	Model (Gaussian, transf: sqrt)	**% Deviance**	**GCV**
1	$s(Y_{i,j}) + \varepsilon_{i,j}$	3.33%	4.22
2	$s(depth_{i,j}) + \varepsilon_{i,j}$	11.3%	3.84
3	$s(Y_{i,j}) + s(depth_{i,j}) + \varepsilon_{i,j}$	11.5%	3.84
4	$s(Y_{i,j}) + s(depth_{i,j}) + f(year_{,j}) + \varepsilon_{i,j}$	59.1%	1.93
5	$s(Y_{i,j}) + s(depth_{i,j}) + f(year_{,j}) + f(month_{,j}) + \varepsilon_{i,j}$	59.4%	1.94
	Model (Gaussian, transf: log)	**% Deviance**	**GCV**
6	$s(Y_{i,j}) + \varepsilon_{i,j}$	3.26%	1.87
7	$s(depth_{i,j}) + \varepsilon_{i,j}$	11.9%	1.70
8	$s(Y_{i,j}) + s(depth_{i,j}) + \varepsilon_{i,j}$	11.9%	1.70
9	$s(Y_{i,j}) + s(depth_{i,j}) + f(year_{,j}) + \varepsilon_{i,j}$	62.4%	0.79
10	$s(Y_{i,j}) + s(depth_{i,j}) + f(year_{,j}) + f(month_{,j}) + \varepsilon_{i,j}$	62.6%	0.79
	Model (Tweedie, no transf)	**% Deviance**	**REML**
11	$\mathbf{s(depth_{i,j}) + f(year_{,j}) + \varepsilon_{i,j}}$	**41.2%**	**1641.3**
12	$s(Y_{i,j}) + s(depth_{i,j}) + f(year_{,j}) + \varepsilon_{i,j}$	41.9%	1639.7
13	$s(Y_{i,j}) + s(depth_{i,j}) + f(year_{,j}) + f(month_{,j}) + \varepsilon_{i,j}$	42.5%	1631.9

Although the highest value of Deviance explained was associated to the model 10, the best model in terms of better fitting the observation data is the model 11. The model summary indicates the significance of the depth and the year (Table 3.3.3.1.c). The residuals of the model and the q-q plot reported in Figure 3.3.3.1.A show a skewed distribution.

The estimation of the splines was found in any cases significant although the wide confidence intervals in factor variables (Table 3.3.3.1.c. and Figure 3.3.3.1.B).

Table 3.3.3.1.c – Summary of the estimates, deviance explained and GCV of the best GAM for *A. foliacea* in GSA 19.

****
family: tw
link : log
transformation: identity
****
-- Summary of the model --

Family: Tweedie(p=1.593)
Link function: log

Formula:
response ~ s(depth) + factor(year) + 0

Parametric coefficients:

	Estimate	Std. Error	t value	Pr(>|t|)	
factor(year)1994	-0.80230	0.31308	-2.563	0.010524	*
factor(year)1995	-0.20374	0.27439	-0.743	0.457926	
factor(year)1996	-0.27507	0.27466	-1.002	0.316805	
factor(year)1997	-1.22394	0.32611	-3.753	0.000184	***
factor(year)1998	-1.24241	0.33331	-3.727	0.000203	***
factor(year)1999	-0.85498	0.31867	-2.683	0.007408	**
factor(year)2000	0.27699	0.25446	1.089	0.276604	
factor(year)2001	-0.01675	0.26650	-0.063	0.949894	
factor(year)2002	0.65389	0.25592	2.555	0.010753	*
factor(year)2003	1.84107	0.20078	9.169	< 2e-16	***
factor(year)2004	1.29566	0.22184	5.841	6.88e-09	***
factor(year)2005	1.77075	0.20284	8.730	< 2e-16	***
factor(year)2006	0.96960	0.24136	4.017	6.30e-05	***
factor(year)2007	-1.48181	0.39525	-3.749	0.000187	***
factor(year)2008	0.70515	0.25239	2.794	0.005300	**
factor(year)2009	0.07104	0.29067	0.244	0.806956	
factor(year)2010	0.25702	0.27568	0.932	0.351380	
factor(year)2011	0.37845	0.26974	1.403	0.160901	
factor(year)2012	1.11387	0.23492	4.741	2.41e-06	***
factor(year)2013	1.83238	0.20411	8.977	< 2e-16	***
factor(year)2014	0.83821	0.24492	3.422	0.000644	***
factor(year)2015	1.14521	0.23187	4.939	9.09e-07	***

```
factor(year)2016  2.09151    0.19152  10.921  < 2e-16 ***
factor(year)2017  2.19595    0.18979  11.570  < 2e-16 ***
factor(year)2018  0.98149    0.23839   4.117 4.13e-05 ***
---
Signif. codes:  0 ‘***’ 0.001 ‘**’ 0.01 ‘*’ 0.05 ‘.’ 0.1 ‘ ’ 1

Approximate significance of smooth terms:
         edf Ref.df     F p-value
s(depth) 5.066      9 43.25  <2e-16 ***
---
Signif. codes:  0 ‘***’ 0.001 ‘**’ 0.01 ‘*’ 0.05 ‘.’ 0.1 ‘ ’ 1

R-sq.(adj) =  0.269   Deviance explained = 41.2%
-REML = 1641.3  Scale est. = 3.9404    n = 1107
```

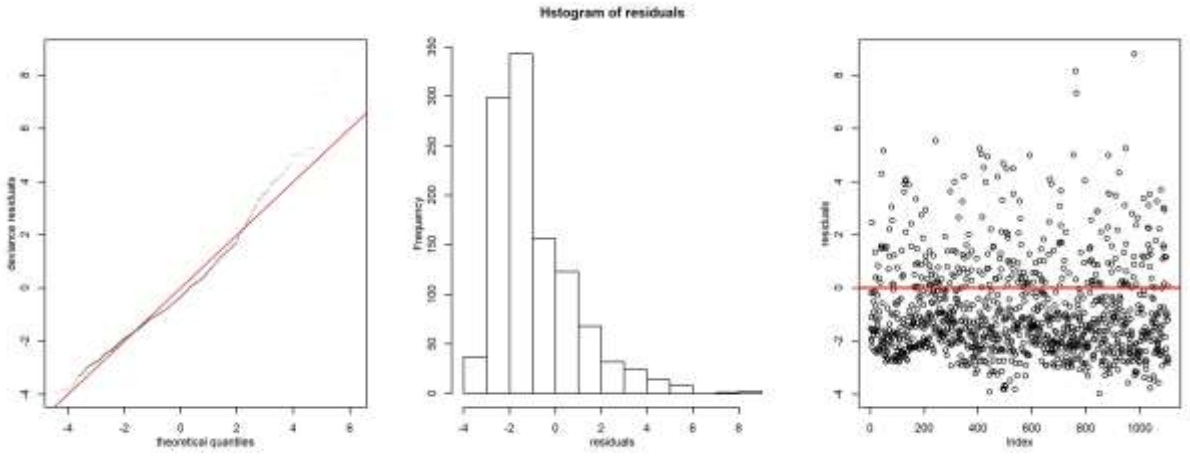

Figure 3.3.3.1.A– Diagnostic plots of residuals for *A. foliacea* in GSA 19.

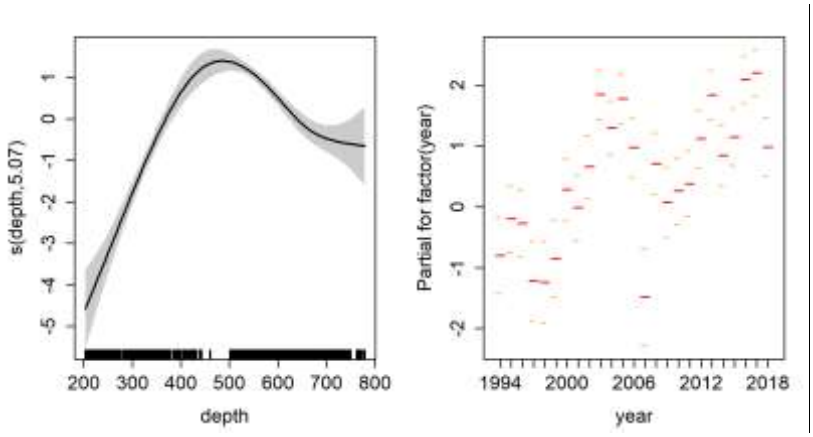

Figure 3.3.3.1.B – Splines of the best model for *A. foliacea* in GSA 19.

Only the points of the predictive grid corresponding to a depth comprised in the 200-800 m range were selected. The grid points were also linked to the values of the other variables included in the best GAM and useful to predict the model in the standardized conditions: year.

In Figure 3.3.3.1.C, the comparison is reported between the original indices estimated on rough data according to Souplet (1996) and the indices estimated on the predicted results, predicted over the grid with the corresponding confidence intervals (Figure 3.3.3.1.C left). The prediction was also done on the original haul positions (Figure 3.3.3.1.C right).

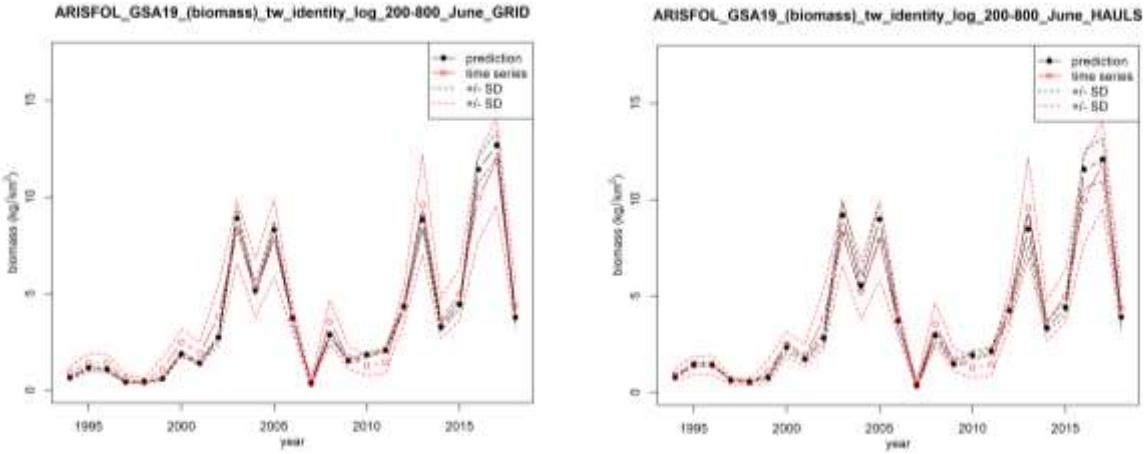

Figure 3.3.3.1.C – Comparison between the original and standardized biomass indices of *A. foliacea* in GSA 19 predicted on the grid (left) and on the haul positions (right).

3.3.3.2. *Parapenaeus longirostris*

The analysis was performed using data from MEDITS survey conducted in the period between the 1994 and 2018, focusing on the bathymetrical range 10-800 m.

The presence of correlations among the explanatory variables was tested using the Pearson's correlation coefficients (Table 3.3.3.2.a). The correlation matrix shows a correlation coefficient of 0.77 for latitude and longitude, nonetheless the VIF coefficient is lower than 3 for both the variables. Among the other variables no significant correlations were found.

Table 3.3.3.2.a - Correlation table among the quantitative explanatory variables explored for *P. longirostris* in GSA 19.

	year	**month**	**hour**	**Y**	**X**	**depth**
year		0.55	0.11	-0.01	0.00	-0.01
month	0.55		-0.01	0.00	0.00	-0.02
hour	0.11	-0.01		-0.05	-0.04	-0.07
Y	-0.01	0.00	-0.05		0.77	0.09
X	0.00	0.00	-0.04	0.77		0.24
depth	-0.01	-0.02	-0.07	0.09	0.24	

The explanatory variables considered are the year, month, depth, hour, latitude, longitude. The list of the most relevant models explored is reported in Table 3.3.3.2.b. The best model was estimated using the Gaussian family distribution, applying a square-transformation on the data and assuming an identity link function.

Table 3.3.3.2.b – Selection of the models explored for *P. longirostris* in GSA 19 (biomass index kg/km^2). The best performing model is reported in bold.

	Model (Gaussian, transf: sqrt)	% Deviance	GCV
1	$s(Y_{i,j}) + \varepsilon_{i,j}$	10.4	6.11
2	$s(depth_{i,j}) + \varepsilon_{i,j}$	39.7	4.09
3	$s(Y_{i,j}) + s(depth_{i,j}) + \varepsilon_{i,j}$	40.7	4.06
4	$s(Y_{i,j}) + s(depth_{i,j}) + f(year_{,j}) + \varepsilon_{i,j}$	72.9	1.93
5	$s(Y_{i,j}) + s(depth_{i,j}) + f(year_{,j}) + f(month_{,j}) + \varepsilon_{i,j}$	73.7	1.89
6	$s(X_{i,j}) + s(depth_{i,j}) + f(year_{,j}) + f(month_{,j}) + \varepsilon_{i,j}$	73.8	1.89
7	$\mathbf{s(X_{i,j}, Y_{i,j}) + s(depth_{i,j}) + f(year_{,j}) + \varepsilon_{i,j}}$	**75.7**	**1.79**
	Model (Gaussian, transf: log)	**% Deviance**	**GCV**
6	$s(Y_{i,j}) + \varepsilon_{i,j}$	11.4	2.31
7	$s(depth_{i,j}) + \varepsilon_{i,j}$	42.0	1.50
8	$s(Y_{i,j}) + s(depth_{i,j}) + \varepsilon_{i,j}$	42.9	1.50
9	$s(Y_{i,j}) + s(depth_{i,j}) + f(year_{,j}) + \varepsilon_{i,j}$	78.2	0.60
10	$s(Y_{i,j}) + s(depth_{i,j}) + f(year_{,j}) + f(month_{,j}) + \varepsilon_{i,j}$	78.6	0.59
11	$s(X_{i,j}) + s(depth_{i,j}) + f(year_{,j}) + f(month_{,j}) + \varepsilon_{i,j}$	78.8	0.58
12	$s(X_{i,j}, Y_{i,j}) + s(depth_{i,j}) + f(year_{,j}) + \varepsilon_{i,j}$	80.4	0.55
	Model (Tweedie, no transf)	**% Deviance**	**REML**
13	$s(X_{i,j}, Y_{i,j}) + \varepsilon_{i,j}$	25.8	2823.7
14	$s(depth_{i,j}) + \varepsilon_{i,j}$	54.2	2507.3
15	$s(Y_{i,j}) + s(depth_{i,j}) + \varepsilon_{i,j}$	56.4	2498.0
16	$s(Y_{i,j}) + s(depth_{i,j}) + f(year_{,j}) + \varepsilon_{i,j}$	65.5	2406.8
17	$s(Y_{i,j}) + s(depth_{i,j}) + f(year_{,j}) + f(month_{,j}) + \varepsilon_{i,j}$	65.9	2398.8
18	$s(X_{i,j}, Y_{i,j}) + s(depth_{i,j}) + f(year_{,j}) + \varepsilon_{i,j}$	68.8	2388.5
19	$s(X_{i,j}, Y_{i,j}) + s(depth_{i,j}) + f(year_{,j}) + f(month) + \varepsilon_{i,j}$	69.3	2378.9

Although the best model resulted apparently the model 12, the prediction underestimate the data so the model selected is the model number 7. The underestimation of model 12 probably is because the bathymetric range of distribution of the species is not properly those chosen.

The model summary indicates the significance of the geographical position (latitude, longitude and depth) and year (Table 3.3.3.2.c). The residuals of the model and the q-q plot reported in Figure 3.3.3.2.A show a skewed distribution. The estimation of the splines was found in any cases significant although the wide confidence intervals in factor variable (Table 3.3.3.2.c. and Figure 3.3.3.2.B).

Table 3.3.3.2.c – Summary of the estimates, deviance explained and GCV of the best GAM for *P. longirostris* in GSA 19.

Parametric coefficients:

	Estimate	Std. Error	t value	Pr(>|t|)	
factor(year)1994	1.2209	0.1541	7.922	4.16e-15	***
factor(year)1995	1.2074	0.1529	7.896	5.09e-15	***
factor(year)1996	0.9212	0.1526	6.038	1.91e-09	***
factor(year)1997	1.2335	0.1526	8.081	1.20e-15	***
factor(year)1998	1.2971	0.1518	8.547	< 2e-16	***
factor(year)1999	0.8404	0.1514	5.550	3.30e-08	***
factor(year)2000	0.7980	0.1514	5.270	1.53e-07	***
factor(year)2001	0.6702	0.1513	4.430	1.00e-05	***
factor(year)2002	1.1311	0.1555	7.274	5.28e-13	***
factor(year)2003	1.1606	0.1555	7.463	1.33e-13	***
factor(year)2004	1.2570	0.1554	8.088	1.13e-15	***
factor(year)2005	1.1668	0.1554	7.511	9.37e-14	***
factor(year)2006	1.1997	0.1554	7.722	1.92e-14	***
factor(year)2007	1.0589	0.1554	6.816	1.29e-11	***
factor(year)2008	1.4126	0.1554	9.091	< 2e-16	***
factor(year)2009	1.7348	0.1554	11.161	< 2e-16	***
factor(year)2010	1.7561	0.1553	11.305	< 2e-16	***
factor(year)2011	1.2723	0.1553	8.190	5.02e-16	***
factor(year)2012	1.4621	0.1555	9.404	< 2e-16	***
factor(year)2013	1.5881	0.1556	10.206	< 2e-16	***
factor(year)2014	1.4332	0.1554	9.222	< 2e-16	***
factor(year)2015	2.0332	0.1554	13.080	< 2e-16	***
factor(year)2016	1.9746	0.1554	12.704	< 2e-16	***
factor(year)2017	2.4764	0.1555	15.924	< 2e-16	***
factor(year)2018	2.6461	0.1555	17.021	< 2e-16	***

Signif. codes: 0 ‘***’ 0.001 ‘**’ 0.01 ‘*’ 0.05 ‘.’ 0.1 ‘ ’ 1

Approximate significance of smooth terms:

	edf	Ref.df	F	p-value	
s(X,Y)	25.12	29	9.17	<2e-16	***
s(depth)	6.50	9	156.09	<2e-16	***

Signif. codes: 0 ‘***’ 0.001 ‘**’ 0.01 ‘*’ 0.05 ‘.’ 0.1 ‘ ’ 1

R-sq.(adj) = 0.648 Deviance explained = 75.7%
GCV = 1.787 Scale est. = 1.6851 n = 1782

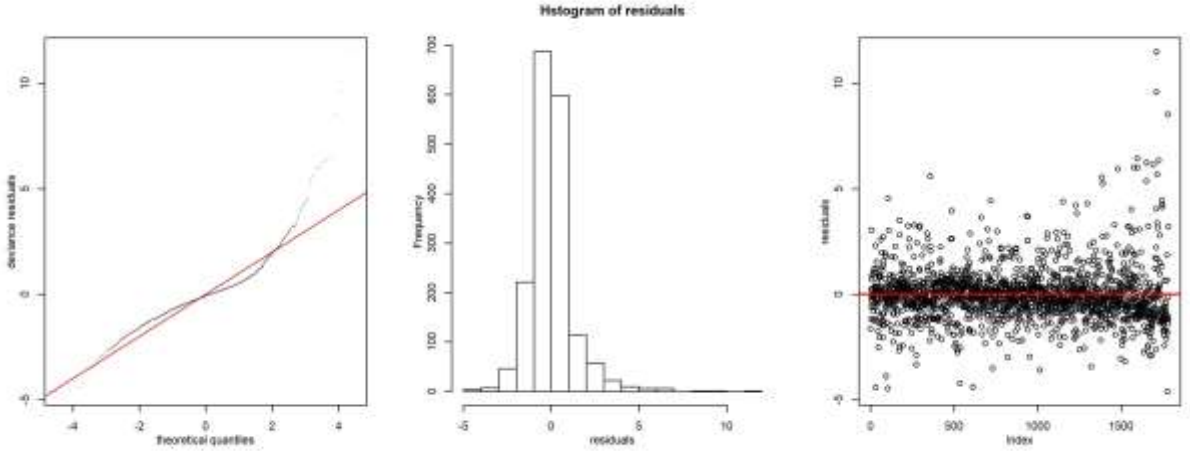

Figure 3.3.3.2.A– Diagnostic plots of residuals for *P. longirostris* in GSA 19.

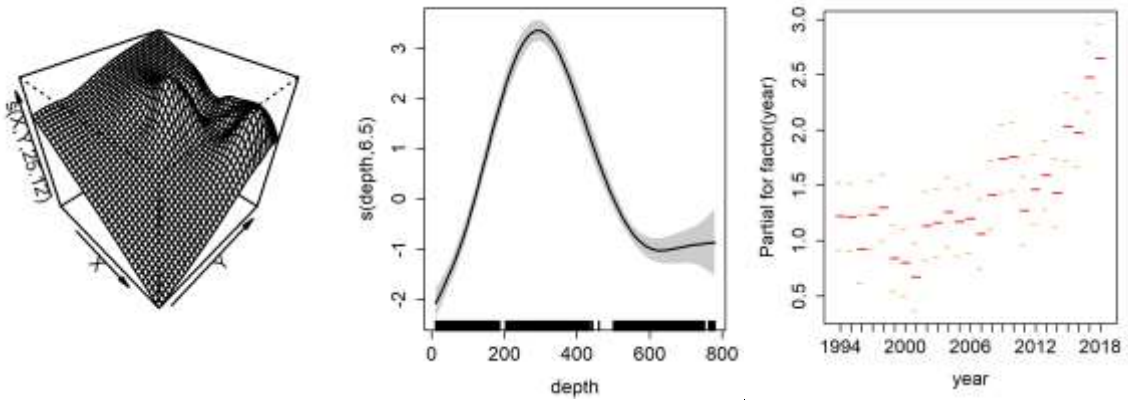

Figure 3.3.3.2.B – Splines of the best model for *P. longirostris* in GSA 19.

The points of the predictive grid corresponding to a depth comprised in the 10-800 m range were selected. The grid points were also linked to the values of the other

variables included in the best GAM and useful to predict the model in the standardized conditions: year.

In Figure 3.3.3.2.C, the comparison is reported between the original indices estimated on rough data according to Souplet (1996) and the indices estimated on the predicted results, predicted over the grid with the corresponding confidence intervals (Figure 3.3.3.2.C left). The prediction was also done on the original haul positions (Figure 3.3.3.2.C right).

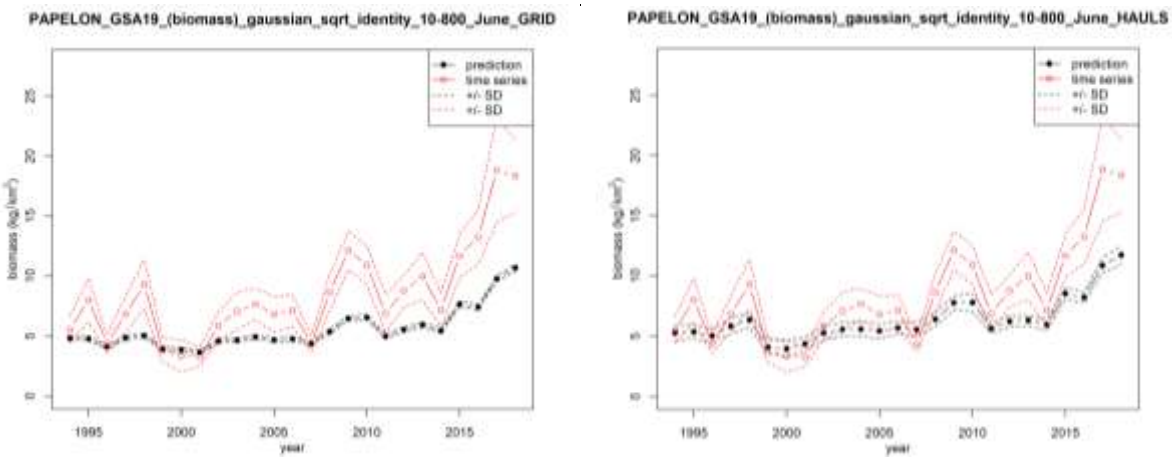

Figure 3.3.3.2.C – Comparison between the original and standardized biomass indices of *P. longirostris* in GSA 19 predicted on the grid (left) and on the haul positions (right).

3.3.3.3. *Merluccius merluccius*

The analysis was performed using data from MEDITS survey conducted in the period between the 1994 and 2018, focusing on the bathymetrical range 10-800 m.

The presence of correlations among the explanatory variables was tested using the Pearson's correlation coefficients (Table 3.3.3.3.a). The correlation matrix shows a correlation coefficient of 0.77 for latitude and longitude, nonetheless the VIF coefficient is lower than 3 for both the variables. Among the other variables no significant correlations were found.

Table 3.3.3.3.a - Correlation table among the quantitative explanatory variables explored for *M. merluccius* in GSA 19.

	year	**month**	**hour**	**Y**	**X**	**depth**
year		0.55	0.11	-0.01	0.00	-0.01
month	0.55		-0.01	0.00	0.00	-0.02
hour	0.11	-0.01		-0.05	-0.04	-0.07
Y	-0.01	0.00	-0.05		0.77	0.09
X	0.00	0.00	-0.04	0.77		0.24
depth	-0.01	-0.02	-0.07	0.09	0.24	

The explanatory variables considered are the year, month, depth, hour, latitude, longitude. The list of the most relevant models explored is reported in Table 3.3.3.3.b. The best model was estimated using the Tweedie family distribution assuming a logarithm link function.

Table 3.3.3.3.b – Selection of the models explored for *M. merluccius* in GSA 19 (biomass index kg/km^2). The best performing model is reported in bold.

	Model (Gaussian, transf: sqrt)	% Deviance	GCV
1	$s(X_{i,j}) + \varepsilon_{i,j}$	12.2	15.8
2	$s(depth_{i,j}) + \varepsilon_{i,j}$	18.9	14.6
3	$s(Y_{i,j}) + s(depth_{i,j}) + \varepsilon_{i,j}$	22.9	14.0
4	$s(Y_{i,j}) + s(depth_{i,j}) + f(year_j) + \varepsilon_{i,j}$	69.0	5.9
5	$s(Y_{i,j}) + s(depth_{i,j}) + f(year_j) + f(month_j) + \varepsilon_{i,j}$	69.1	5.9
6	$s(X_{i,j}) + s(depth_{i,j}) + f(year_j) + f(month_j) + \varepsilon_{i,j}$	69.0	5.9
7	$s(X_{i,j}, Y_{i,j}) + s(depth_{i,j}) + f(year_j) + \varepsilon_{i,j}$	70.5	5.7
	Model (Gaussian, transf: log)	**% Deviance**	**GCV**
6	$s(Y_{i,j}) + \varepsilon_{i,j}$	9.65	5.1
7	$s(depth_{i,j}) + \varepsilon_{i,j}$	18.0	4.6
8	$s(Y_{i,j}) + s(depth_{i,j}) + \varepsilon_{i,j}$	20.5	4.5
9	$s(Y_{i,j}) + s(depth_{i,j}) + f(year_j) + \varepsilon_{i,j}$	74.8	1.5
10	$s(Y_{i,j}) + s(depth_{i,j}) + f(year_j) + f(month_j) + \varepsilon_{i,j}$	74.9	1.5
11	$s(X_{i,j}) + s(depth_{i,j}) + f(year_j) + f(month_j) + \varepsilon_{i,j}$	74.8	1.5
12	$s(X_{i,j}, Y_{i,j}) + s(depth_{i,j}) + f(year_j) + \varepsilon_{i,j}$	75.8	1.5
	Model (Tweedie, no transf)	**% Deviance**	**REML**
13	$s(Y_{i,j}) + s(depth_{i,j}) + f(year_j) + \varepsilon_{i,j}$	41.9	3895.2
14	$s(Y_{i,j}) + s(depth_{i,j}) + f(year_j) + f(month_j) + \varepsilon_{i,j}$	42.2	3891.1
15	$\mathbf{s(X_{i,j}, Y_{i,j}) + s(depth_{i,j}) + f(year_j) + \varepsilon_{i,j}}$	**43.5**	**3889.1**
16	$s(X_{i,j}, Y_{i,j}) + s(depth_{i,j}) + f(year_j) + f(month) + \varepsilon_{i,j}$	43.7	3884.9

Although the best model apparently resulted the model 12, the prediction underestimate the data as well as the model 7. Thus, despite a lower percentage value of Deviance explained, the model selected to estimate the biomass of European hake in the GSA19 is the model number 15.

The model summary indicates the significance of the geographical position (latitude, longitude and depth) and year (Table 3.3.3.3.c). The residuals of the model and the q-q plot reported in Figure 3.3.3.3.A show a skewed distribution. The estimation of the splines was found in any cases significant although the wide confidence intervals in factor variable (Table 3.3.3.3.c. and Figure 3.3.3.3.B).

Table 3.3.3.3.c – Summary of the estimates, deviance explained and GCV of the best GAM for *M. merluccius* in GSA 19.

****

family: tw
link : log
transformation: identity
****
-- Summary of the model --

Family: Tweedie(p=1.412)
Link function: log

Formula:
response ~ s(X, Y) + s(depth) + factor(year) + 0

Parametric coefficients:

	Estimate	Std. Error	t value	Pr(>|t|)	
factor(year)1994	2.8598	0.1335	21.422	<2e-16	***
factor(year)1995	2.6005	0.1430	18.188	<2e-16	***
factor(year)1996	2.3512	0.1513	15.538	<2e-16	***
factor(year)1997	2.1371	0.1557	13.726	<2e-16	***
factor(year)1998	2.0670	0.1617	12.780	<2e-16	***
factor(year)1999	1.7053	0.1805	9.445	<2e-16	***
factor(year)2000	1.9632	0.1678	11.697	<2e-16	***
factor(year)2001	1.8073	0.1745	10.360	<2e-16	***
factor(year)2002	1.8130	0.1764	10.275	<2e-16	***
factor(year)2003	2.0306	0.1676	12.114	<2e-16	***
factor(year)2004	2.5195	0.1453	17.343	<2e-16	***
factor(year)2005	2.5184	0.1430	17.611	<2e-16	***
factor(year)2006	2.6756	0.1369	19.544	<2e-16	***
factor(year)2007	2.2092	0.1581	13.976	<2e-16	***
factor(year)2008	3.0108	0.1249	24.112	<2e-16	***
factor(year)2009	2.3949	0.1490	16.075	<2e-16	***
factor(year)2010	2.1662	0.1592	13.604	<2e-16	***
factor(year)2011	2.0453	0.1656	12.352	<2e-16	***
factor(year)2012	2.0318	0.1670	12.163	<2e-16	***
factor(year)2013	2.7336	0.1361	20.090	<2e-16	***
factor(year)2014	2.4999	0.1455	17.184	<2e-16	***
factor(year)2015	1.7804	0.1789	9.953	<2e-16	***
factor(year)2016	1.9227	0.1709	11.248	<2e-16	***

```
factor(year)2017   2.7964    0.1336  20.932   <2e-16 ***
factor(year)2018   2.6086    0.1402  18.602   <2e-16 ***
---
Signif. codes:  0 ‘***’ 0.001 ‘**’ 0.01 ‘*’ 0.05 ‘.’ 0.1 ‘ ’ 1

Approximate significance of smooth terms:
          edf Ref.df      F p-value
s(X,Y)   16.490     29  9.562  <2e-16 ***
s(depth)  7.595      9 31.894  <2e-16 ***
---
Signif. codes:  0 ‘***’ 0.001 ‘**’ 0.01 ‘*’ 0.05 ‘.’ 0.1 ‘ ’ 1

R-sq.(adj) =  0.375   Deviance explained = 43.5%
-REML = 3889.1  Scale est. = 7.5943    n = 1782
```

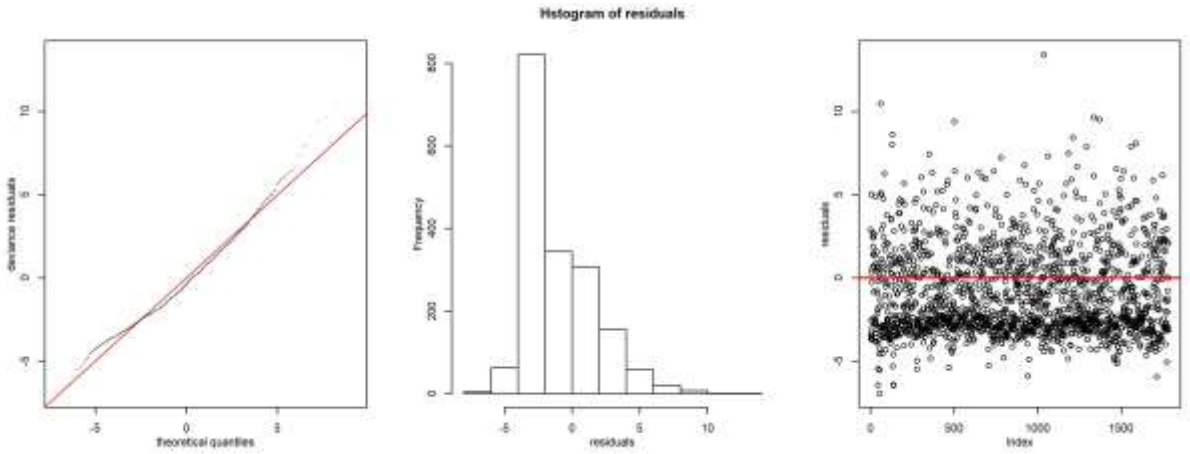

Figure 3.3.3.3.A– Diagnostic plots of residuals for *M. merluccius* in GSA 19.

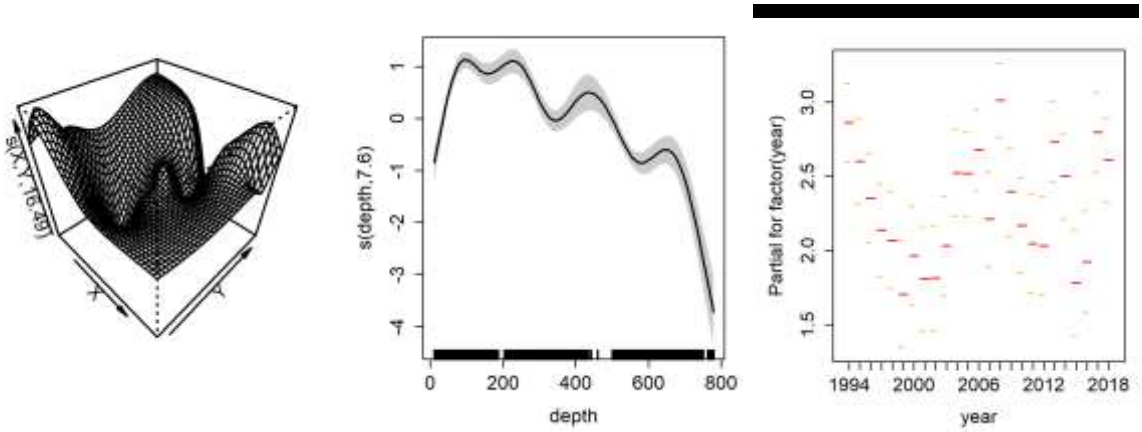

Figure 3.3.3.3.B – Splines of the best model for *M. merluccius* in GSA 19.

The points corresponding to a depth comprised in the 10-800 m range were selected. The grid points were also linked to the values of the other variables included in the best GAM and useful to predict the model in the standardized conditions: year.

In Figure 3.3.3.3.C, the comparison is reported between the original indices estimated on rough data according to Souplet (1996) and the indices estimated on the predicted results, predicted over the grid with the corresponding confidence intervals (Figure 3.3.3.3.C left). The prediction was also done on the original haul positions (Figure 3.3.3.3.C right).

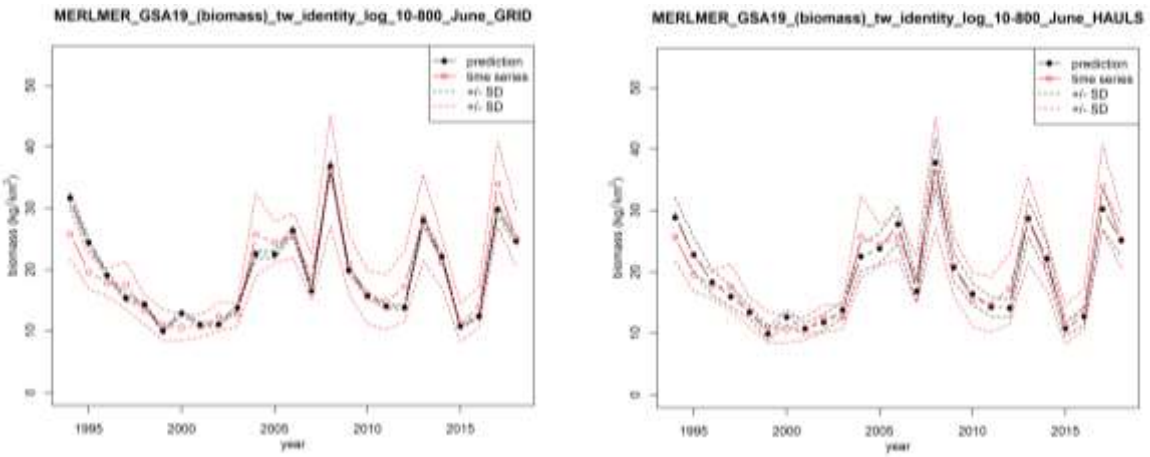

Figure 3.3.3.3.C – Comparison between the original and standardized biomass indices of *M. merluccius* in GSA 19 predicted on the grid (left) and on the haul positions (right).

3.3.3.4. *Mullus barbatus*

The analysis was performed using data from MEDITS survey conducted in the period between the 1994 and 2018, focusing on the bathymetrical range 10-200 m.

The presence of correlations among the explanatory variables was tested using the Pearson's correlation coefficients (Table 3.3.3.4.a). The correlation matrix shows a correlation coefficient of 0.75 for latitude and longitude, nonetheless the VIF coefficient is lower than 3 for both the variables. Among the other variables no significant correlations were found.

Table 3.3.3.4.a - Correlation table among the quantitative explanatory variables explored for *M. barbatus* in GSA 19.

	year	**month**	**hour**	**Y**	**X**	**depth**
year		0.55	0.15	0.01	-0.01	-0.06
month	0.55		-0.02	0.00	0.00	-0.02
hour	0.15	-0.02		-0.15	-0.11	-0.04
Y	0.01	0.00	-0.15		0.75	-0.06
X	-0.01	0.00	-0.11	0.75		0.19
depth	-0.06	-0.02	-0.04	-0.06	0.19	

The explanatory variables considered are the year, month, depth, hour, latitude, longitude. The list of the most relevant models explored is reported in Table 3.3.3.4.b. The best model was estimated using the Gaussian family distribution with a square root transformation of data assuming an identity link function.

Table 3.3.3.4.b – Selection of the models explored for *M. barbatus* in GSA 19 (biomass index kg/km^2). The best performing model is reported in bold.

	Model (Gaussian, transf: sqrt)	% Deviance	GCV
1	$s(Y_{i,j}) + \varepsilon_{i,j}$	12.3	53.1
2	$s(depth_{i,j}) + \varepsilon_{i,j}$	7.42	56.0
3	$s(Y_{i,j}) + s(depth_{i,j}) + \varepsilon_{i,j}$	13.5	52.3
4	$s(Y_{i,j}) + s(depth_{i,j}) + f(year_{,j}) + \varepsilon_{i,j}$	62.7	25.9
5	$s(Y_{i,j}) + s(depth_{i,j}) + f(year_{,j}) + f(month_{,j}) + \varepsilon_{i,j}$	63.4	25.8
6	$s(X_{i,j}) + s(depth_{i,j}) + f(year_{,j}) + f(month_{,j}) + \varepsilon_{i,j}$	58.4	29.4
7	$\mathbf{s(X_{i,j}, Y_{i,j}) + s(depth_{i,j}) + f(year_{,j}) + \varepsilon_{i,j}}$	**64.3**	**25.5**
	Model (Gaussian, transf: log)	**% Deviance**	**GCV**
6	$s(Y_{i,j}) + s(depth_{i,j}) + \varepsilon_{i,j}$	11.8	8.3
7	$s(Y_{i,j}) + s(depth_{i,j}) + f(year_{,j}) + \varepsilon_{i,j}$	80.3	2.1
8	$s(Y_{i,j}) + s(depth_{i,j}) + f(year_{,j}) + f(month_{,j}) + \varepsilon_{i,j}$	80.8	2.1
9	$s(X_{i,j}) + s(depth_{i,j}) + f(year_{,j}) + f(month_{,j}) + \varepsilon_{i,j}$	75.0	2.7
10	$s(X_{i,j}, Y_{i,j}) + s(depth_{i,j}) + f(year_{,j}) + \varepsilon_{i,j}$	82.7	1.9
	Model (Tweedie, no trasnf)	**% Deviance**	**REML**
11	$s(depth_{i,j}) + f(year_{,j}) + \varepsilon_{i,j}$	33.2	2045.5
12	$S(Y, depth) + f(year) + \varepsilon_{i,j}$	45.3	2008.4
13	$s(Y_{i,j}) + s(depth_{i,j}) + f(year_{,j}) + \varepsilon_{i,j}$	48.6	1989.1
14	$s(Y_{i,j}) + s(depth_{i,j}) + f(year_{,j}) + f(month_{,j}) + \varepsilon_{i,j}$	49.3	1982.9
15	$s(X_{i,j}, Y_{i,j}) + s(depth_{i,j}) + f(year_{,j}) + \varepsilon_{i,j}$	55.3	1970.2

Although the best model apparently resulted the model 10, the prediction underestimate the data, so the best model to estimate biomass of red mullet in GSA19 is the model 7.

The model summary indicates the significance of the depth and year (Table 3.3.3.4.c). The residuals of the model and the q-q plot reported in Figure 3.3.3.4.A show a skewed distribution. The estimation of the splines was found in any cases significant although the wide confidence intervals in factor variable (Table 3.3.3.4.c. and Figure 3.3.3.4.B).

Table 3.3.3.4.c – Summary of the estimates, deviance explained and GCV of the best GAM for *M. barbatus* in GSA 19.

****

family: gaussian
link : identity

transformation: sqrt
****
-- Summary of the model --

Family: gaussian
Link function: identity

Formula:
response ~ s(X, Y) + s(depth) + factor(year) + 0

Parametric coefficients:

	Estimate	Std. Error	t value	Pr(>|t|)	
factor(year)1994	2.5496	0.9360	2.724	0.006633	**
factor(year)1995	3.4098	0.9280	3.674	0.000259	***
factor(year)1996	2.5792	0.9282	2.779	0.005620	**
factor(year)1997	2.0920	0.9168	2.282	0.022825	*
factor(year)1998	3.3328	0.9141	3.646	0.000288	***
factor(year)1999	1.6821	0.9143	1.840	0.066288	.
factor(year)2000	2.3899	0.9145	2.613	0.009181	**
factor(year)2001	3.8856	0.9155	4.244	2.52e-05	***
factor(year)2002	4.0148	0.9135	4.395	1.30e-05	***
factor(year)2003	3.2894	0.9144	3.597	0.000347	***
factor(year)2004	4.6701	0.9145	5.107	4.35e-07	***
factor(year)2005	4.2204	0.9140	4.618	4.70e-06	***
factor(year)2006	4.0937	0.9135	4.481	8.81e-06	***
factor(year)2007	6.3627	0.9135	6.965	8.27e-12	***
factor(year)2008	5.9628	0.9136	6.527	1.38e-10	***
factor(year)2009	3.4952	0.9132	3.827	0.000142	***
factor(year)2010	4.5995	0.9134	5.036	6.22e-07	***
factor(year)2011	3.8747	0.9135	4.242	2.55e-05	***
factor(year)2012	4.6124	0.9137	5.048	5.84e-07	***
factor(year)2013	6.4075	0.9141	7.009	6.17e-12	***
factor(year)2014	9.6005	0.9139	10.505	< 2e-16	***
factor(year)2015	6.7072	0.9144	7.335	6.83e-13	***
factor(year)2016	5.2668	0.9140	5.762	1.30e-08	***
factor(year)2017	10.2834	0.9138	11.254	< 2e-16	***
factor(year)2018	9.1225	0.9141	9.980	< 2e-16	***

Signif. codes: 0 ‘***’ 0.001 ‘**’ 0.01 ‘*’ 0.05 ‘.’ 0.1 ‘ ’ 1

Approximate significance of smooth terms:
          edf Ref.df   F p-value
s(X,Y)   18.305   29 7.732 <2e-16 ***
s(depth) 1.414   9 3.078   9e-09 ***

Signif. codes: 0 ‘***’ 0.001 ‘**’ 0.01 ‘*’ 0.05 ‘.’ 0.1 ‘ ’ 1

R-sq.(adj) = 0.382   Deviance explained = 64.3%
GCV = 25.474 Scale est. = 22.455   n = 675

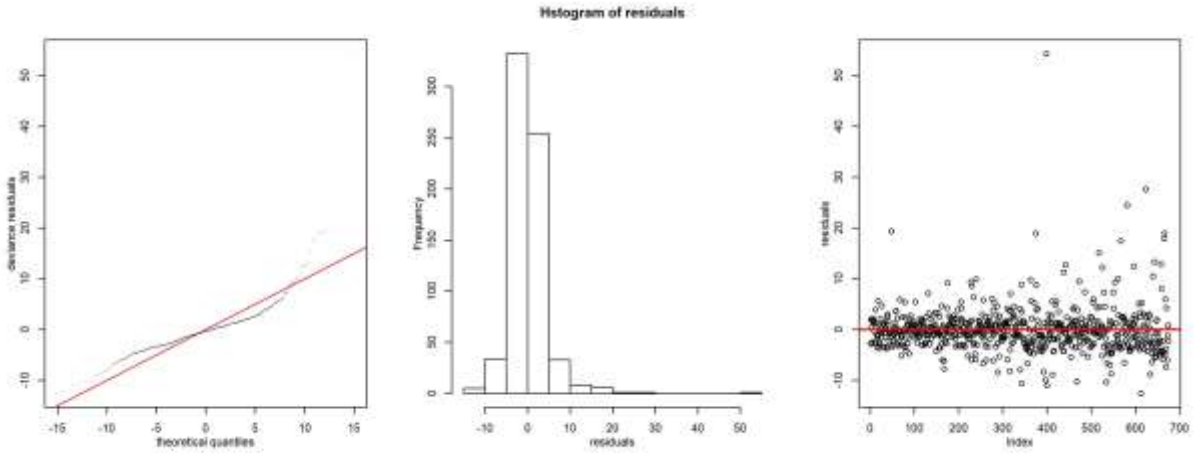

Figure 3.3.3.4.A– Diagnostic plots of residuals for *M. barbatus* in GSA 19.

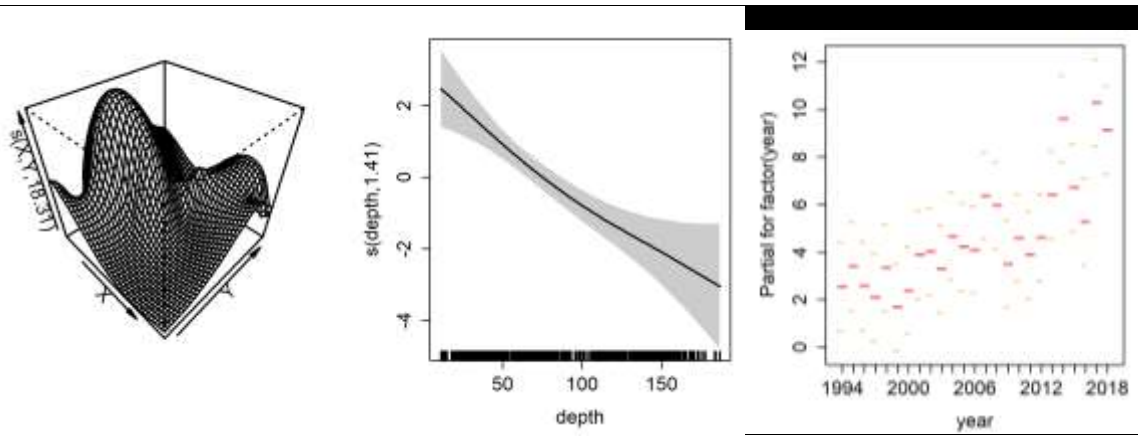

Figure 3.3.3.4.B – Splines of the best model for *M. barbatus* in GSA 19.

Only the points of the predictive grid corresponding to a depth comprised in the 10-200 m range were selected. The grid points were also linked to the values of the other variables included in the best GAM and useful to predict the model in the standardized conditions: year.

In Figure 3.3.3.4.C, the comparison is reported between the original indices estimated on rough data according to Souplet (1996) and the indices estimated on the predicted results, predicted over the grid with the corresponding confidence intervals (Figure 3.3.3.4.C left). The prediction was also done on the original haul positions (Figure 3.3.3.4.C right).

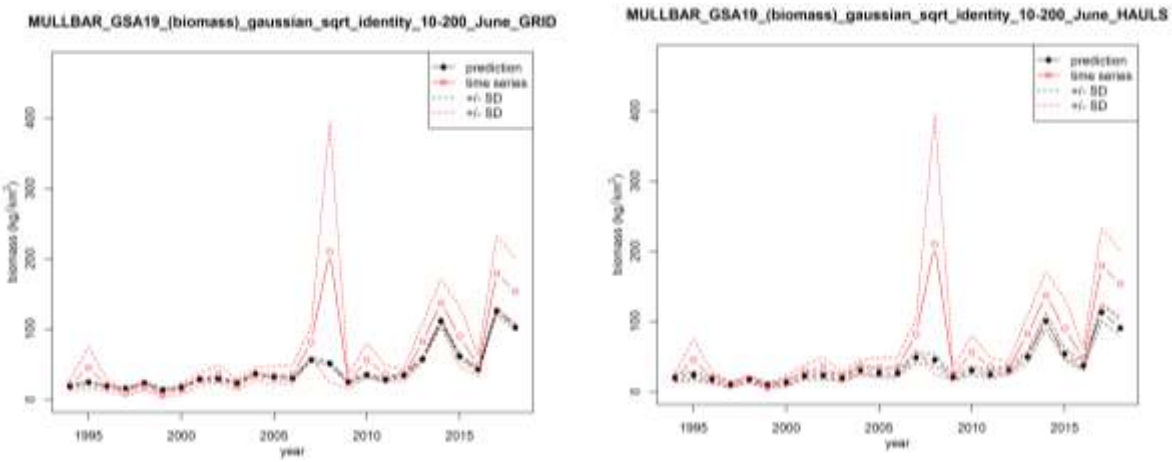

Figure 3.3.3.4.C – Comparison between the original and standardized biomass indices of *M. barbatus* in GSA 19 predicted on the grid (left) and on the haul positions (right).

3.3.3.5. *Illex coindetii*

The analysis was performed using data from MEDITS survey conducted in the period between the 1994 and 2018, focusing on the bathymetrical range 10-800 m.
The presence of correlations among the explanatory variables was tested using the Pearson's correlation coefficients (Table 3.3.3.5.a). The correlation matrix shows a correlation coefficient of 0.77 for latitude and longitude, nonetheless the VIF coefficient is lower than 3 for both the variables. Among the other variables no significant correlations were found.

Table 3.3.3.5.a - Correlation table among the quantitative explanatory variables explored for *I. coindetii* in GSA 19.

	year	**month**	**hour**	**Y**	**X**	**depth**
year		0.55	0.11	-0.01	0.00	-0.01
month	0.55		-0.01	0.00	0.00	-0.02
hour	0.11	-0.01		-0.05	-0.04	-0.07
Y	-0.01	0.00	-0.05		0.77	0.09
X	0.00	0.00	-0.04	0.77		0.24
depth	-0.01	-0.02	-0.07	0.09	0.24	

The explanatory variables considered are the year, month, depth, hour, latitude, longitude. The list of the most relevant models explored is reported in Table 3.3.3.5.b. The best model was estimated using the Tweedie family distribution, assuming a logarithmic link function and no transformation data.

Table 3.3.3.5.b – Selection of the models explored for M. barbatus in GSA 19 (biomass index kg/km2). The best performing model is reported in bold.

	Model (Gaussian, transf: sqrt)	% Deviance	GCV
1	$s(X_{i,j}) + \varepsilon_{i,j}$	11.4	6.8
2	$s(depth_{i,j}) + \varepsilon_{i,j}$	25.6	5.7
3	$s(X_{i,j}) + s(depth_{i,j}) + \varepsilon_{i,j}$	28.0	5.6
4	$s(X_{i,j}) + s(depth_{i,j}) + f(year_{,j}) + \varepsilon_{i,j}$	58.1	3.4
5	$s(X_{i,j}) + s(depth_{i,j}) + f(year_{,j}) + f(month_{,j}) + \varepsilon_{i,j}$	59.3	3.3
6	$s(X_{i,j}, Y_{i,j}) + s(depth_{i,j}) + f(year_{,j}) + \varepsilon_{i,j}$	59.3	3.4
	Model (Gaussian, transf: log)	**% Deviance**	**GCV**
7	$s(X_{i,j}) + s(depth_{i,j}) + \varepsilon_{i,j}$	31.4	8.3
8	$s(X_{i,j}) + s(depth_{i,j}) + f(year_{,j}) + \varepsilon_{i,j}$	68.7	0.8
9	$s(X_{i,j}) + s(depth_{i,j}) + f(year_{,j}) + f(month_{,j}) + \varepsilon_{i,j}$	69.3	0.8
10	$s(X_{i,j}, Y_{i,j}) + s(depth_{i,j}) + f(year_{,j}) + \varepsilon_{i,j}$	70.1	0.8
	Model (Tweedie, no transf)	**% Deviance**	**REML**
11	$s(depth_{i,j}) + f(year_{,j}) + \varepsilon_{i,j}$	53.2	2566.1
12	$s(X_{i,j}) + s(depth_{i,j}) + f(year_{,j}) + \varepsilon_{i,j}$	57.0	2539.6
13	$s(X_{i,j}) + s(depth_{i,j}) + f(year_{,j}) + f(month_{,j}) + \varepsilon_{i,j}$	58.4	2524.3
14	$\mathbf{s(X_{i,j}, Y_{i,j}) + s(depth_{i,j}) + f(year_{,j}) + \varepsilon_{i,j}}$	**60.2**	**2526.1**

Although the best model apparently resulted the model 7, the prediction underestimate the data, so there was selected the model 14 because it seems to better estimate the biomass indices of *I. coindetii* in the GSA19 rather than other models.

The model summary indicates the significance of the geographical position (latitude, longitude and depth) and year (Table 3.3.3.5.c). The residuals of the model and the q-q plot reported in Figure 3.3.3.5.A show a skewed distribution. The estimation of the splines was found in any cases significant although the wide confidence intervals in factor variable (Table 3.3.3.5.c. and Figure 3.3.3.5.B).

Table 3.3.3.5.c – Summary of the estimates, deviance explained and GCV of the best GAM for *I. coindetii* in GSA 19.

****
family: tw
link : log
transformation: identity

****
-- Summary of the model --

Family: Tweedie(p=1.52)
Link function: log

Formula:
response ~ s(X, Y) + s(depth) + factor(year) + 0

Parametric coefficients:

	Estimate	Std. Error	t value	Pr(>|t|)	
factor(year)1994	-1.63368	0.34567	-4.726	2.47e-06	***
factor(year)1995	-0.04609	0.23857	-0.193	0.846841	
factor(year)1996	-0.60282	0.26414	-2.282	0.022598	*
factor(year)1997	-0.37176	0.24357	-1.526	0.127127	
factor(year)1998	0.29856	0.21172	1.410	0.158670	
factor(year)1999	0.96586	0.18501	5.221	2.00e-07	***
factor(year)2000	0.09297	0.22651	0.410	0.681526	
factor(year)2001	-0.73195	0.27139	-2.697	0.007065	**
factor(year)2002	0.18923	0.22186	0.853	0.393817	
factor(year)2003	-1.22718	0.30905	-3.971	7.46e-05	***
factor(year)2004	-0.28997	0.24966	-1.161	0.245606	
factor(year)2005	0.70049	0.19679	3.560	0.000381	***
factor(year)2006	-0.01215	0.23080	-0.053	0.958027	
factor(year)2007	0.91725	0.18699	4.905	1.02e-06	***
factor(year)2008	2.19946	0.14127	15.570	< 2e-16	***
factor(year)2009	0.89305	0.18904	4.724	2.50e-06	***
factor(year)2010	0.53685	0.20596	2.607	0.009223	**
factor(year)2011	0.76209	0.19423	3.924	9.06e-05	***
factor(year)2012	0.13808	0.22399	0.616	0.537664	
factor(year)2013	1.25066	0.17606	7.104	1.77e-12	***
factor(year)2014	1.12924	0.18008	6.271	4.52e-10	***
factor(year)2015	0.72605	0.19791	3.669	0.000251	***
factor(year)2016	0.68842	0.19764	3.483	0.000508	***
factor(year)2017	1.04449	0.18306	5.706	1.36e-08	***
factor(year)2018	0.47920	0.20665	2.319	0.020518	*

Signif. codes: 0 ‘***’ 0.001 ‘**’ 0.01 ‘*’ 0.05 ‘.’ 0.1 ‘ ’ 1

Approximate significance of smooth terms:
```
          edf Ref.df     F p-value
s(X,Y)   18.044    29  7.127  <2e-16 ***
s(depth)  6.887     9 69.180  <2e-16 ***
```

Signif. codes: 0 ‘***’ 0.001 ‘**’ 0.01 ‘*’ 0.05 ‘.’ 0.1 ‘ ’ 1

R-sq.(adj) = 0.261   Deviance explained = 60.2%
-REML = 2526.1 Scale est. = 5.3644   n = 1782

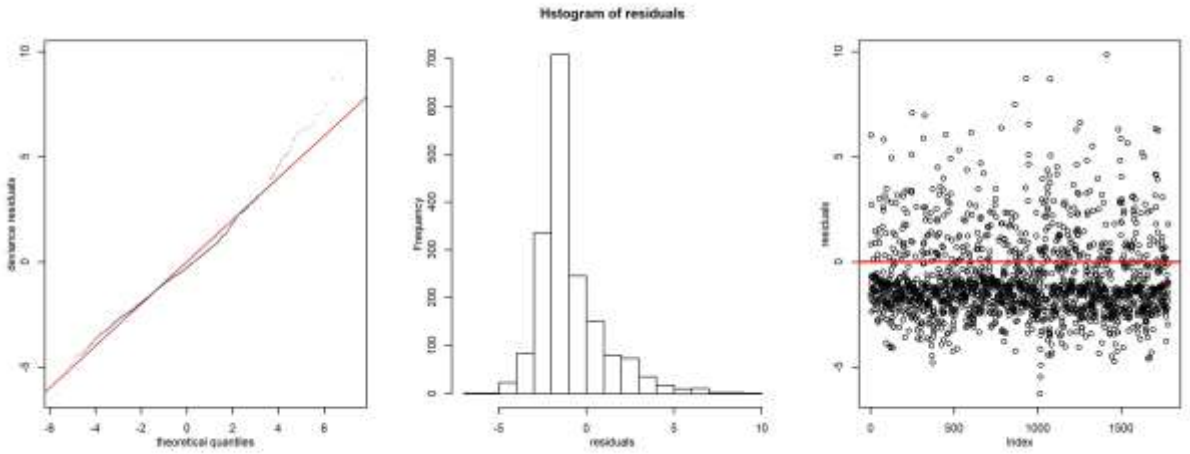

Figure 3.3.3.5.A– Diagnostic plots of residuals for *I. coindetii* in GSA 19.

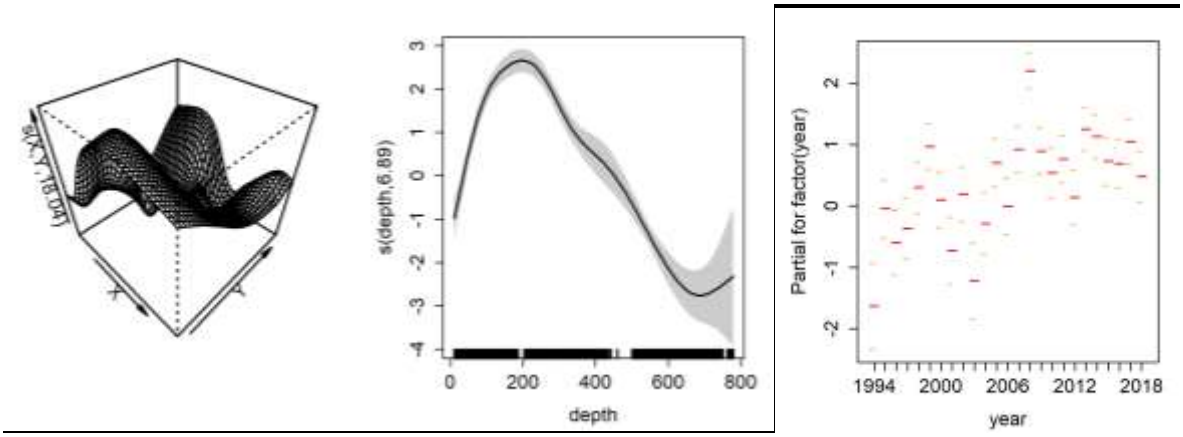

Figure 3.3.3.5.B – Splines of the best model for *I. coindetii* in GSA 19.

Only the points of the predictive grid corresponding to a depth comprised in the 10-800 m range were selected. The grid points were also linked to the values of the other variables included in the best GAM and useful to predict the model in the standardized conditions: year.

In Figure 3.3.3.5.C, the comparison is reported between the original indices estimated on rough data according to Souplet (1996) and the indices estimated on the predicted results, predicted over the grid with the corresponding confidence intervals (Figure 3.3.3.5.C left). The prediction was also done on the original haul positions (Figure 3.3.3.5.C right).

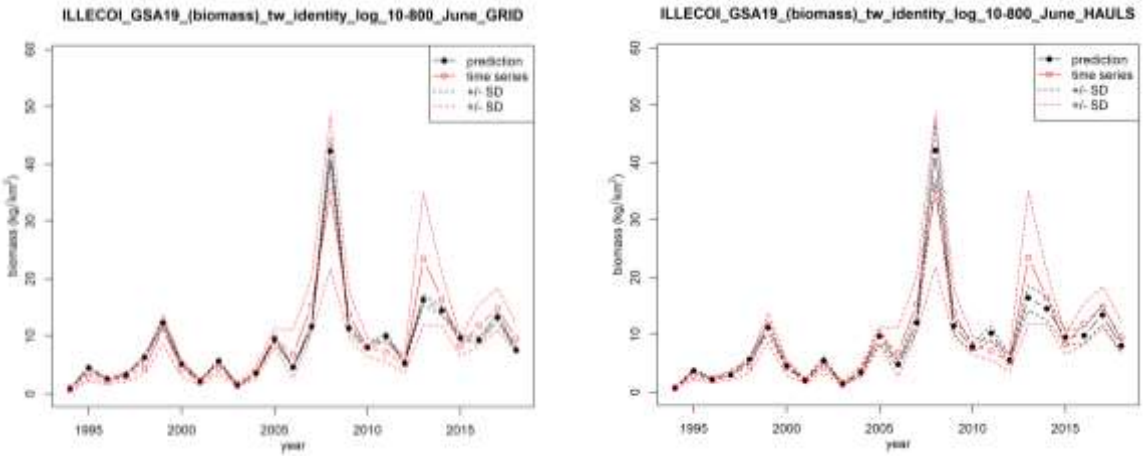

Figure 3.3.3.5.C – Comparison between the original and standardized biomass indices of *I. coindetii* in GSA 19 predicted on the grid (left) and on the haul positions (right).

3.4 Spatial distribution of abundance index in GSA17

The Laboratory of Marine Biology and Fishery of Fano was involved in the activity 4.3-BSTAT aimed to estimate the spatial distribution of abundance and biomass indices of interesting species in the GSA17. The species analyzed were selected according to the criteria detailed in the sub-section 2.2 and included 20 species such as three specie of cephalopods the musky octopus *Eledone moschata*, *I. coindetii* and the European squid *Loligo vulgaris,* the deep-water rose shrimp *P. longirostris* and mantis shrimp *Squilla mantis;* the bony fishes *B. boops*, *Cepola macrophthalma, Merlangius merlangius, M. merluccius, M. poutassou, M. barbatus, Pagellus erythrinus, Scorpaena notata, Serranus hepatus, T. trachurus, T. mediterraneus and Trisopterus minutus;* the cartilaginous fishes *Miliobatis aquilla, Raja clavata, Squalus acanthias.*

The study area covers the whole northern and central Adriatic Sea for a total surface of about 91300 km^2 and includes International Waters and Italian, Croatian and Slovenian Territorial Waters. The dataset used for the analysis was the MEDITS time-series for the period 1994-2018. First of all, species abundance indices per haul were estimated as number of individuals per km^2 (N/km^2), according to the swept-area method reported in the MEDITS protocol. Abundance indices per hauls were computed using the software ATrIS, and then, a metafile by species that contained georeferenced density indices per haul was produced.

For each species, a single bubble plot map of the observed MEDITS density indices was produced in order to visualize a preliminary analysis of abundance distribution. Overall, a total of 4267 hauls were plotted since, on average, about 170 hauls were sampled by year.

In order to obtain a global picture of the distribution area of species, metafiles with abundance index by hauls have been analyzed by geospatial method, using the entire set of available data and analysing all stations together.

Since the high number of stations and their distribution in space, where several points are clustered together, the interpolation technique IDW - Inverse Distance Weighted (Burrough and McDonnell, 1998) was used. The assumption of the IDW method is that the value of an attribute at some unvisited point is a distance-weighted average of data points occurring within a neighborhood surrounding the unvisited point; the

IDW method assigns a decreasing weight to points located at increasing distance from the interpolation point. The following parameters were used to carry out the interpolation:

• the exponent p of the distance to the denominator was set to 2; where p is the power that influences the way weights decrease with distance;

• the interpolation was carried out on a grid with cells with one nautical mile of resolution;

• the neighborhood radius where to search knowing points and surrounding the interpolation point was set to 5 miles.

Then, the grid with interpolated data was filtered by a mobile window (3 cells x 3 cells) and the mean value in the center of the window was calculated. Final map by species obtained for the time-frame 1994-2018 has a spatial resolution according to a grid with a horizontal resolution equals to 1/16˚ (ca. 6-7 km).

The summary of the results was reported below whereas the corresponding shapefile were provided in the sharepoint (Annex1).

Mullus barbatus - Red mullet is a migratory species, widely distributed throughout the whole Adriatic. Abundance is greatest along the western Adriatic coast during MEDITS survey performed in summer (Figure 3.4.A). Density is lower over 200m depth.

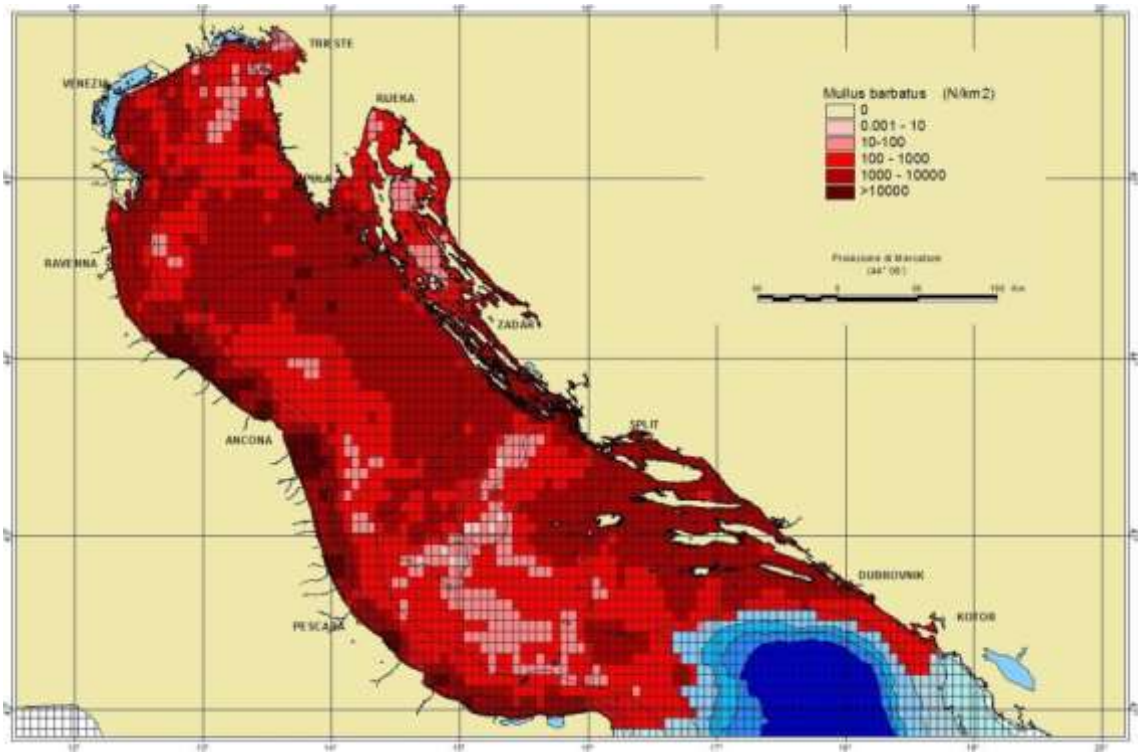

Figure 3.4.A – Spatial distribution of abundance of *M. barbatus* in the GSA17.

Illex coindetii - Broadtail shortfin squid is widely distribute throughout the northern and central Adriatic, mainly in areas deeper than 20m. It is mostly abundant in water deeper than 100m up to 200m in the central Adriatic (Figure 3.4.B).

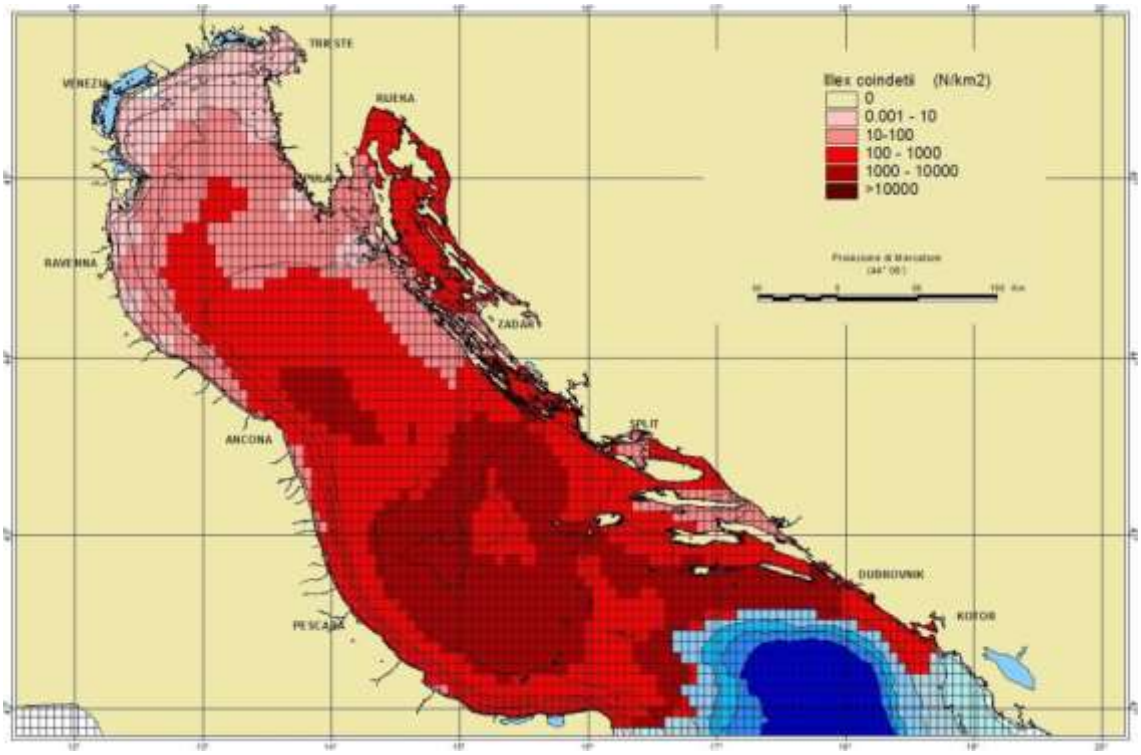

Figure 3.4.B – Spatial distribution of abundance of *I. coindetii* in the GSA17.

Merluccius merluccius - European hake is widely distributed in the whole basin with the exception of the northernmost area. Greatest abundance is steadily found in water deeper than 100 m in the central Adriatic and in the Kvarner Gulf in the northern Adriatic (Figure 3.4.C).

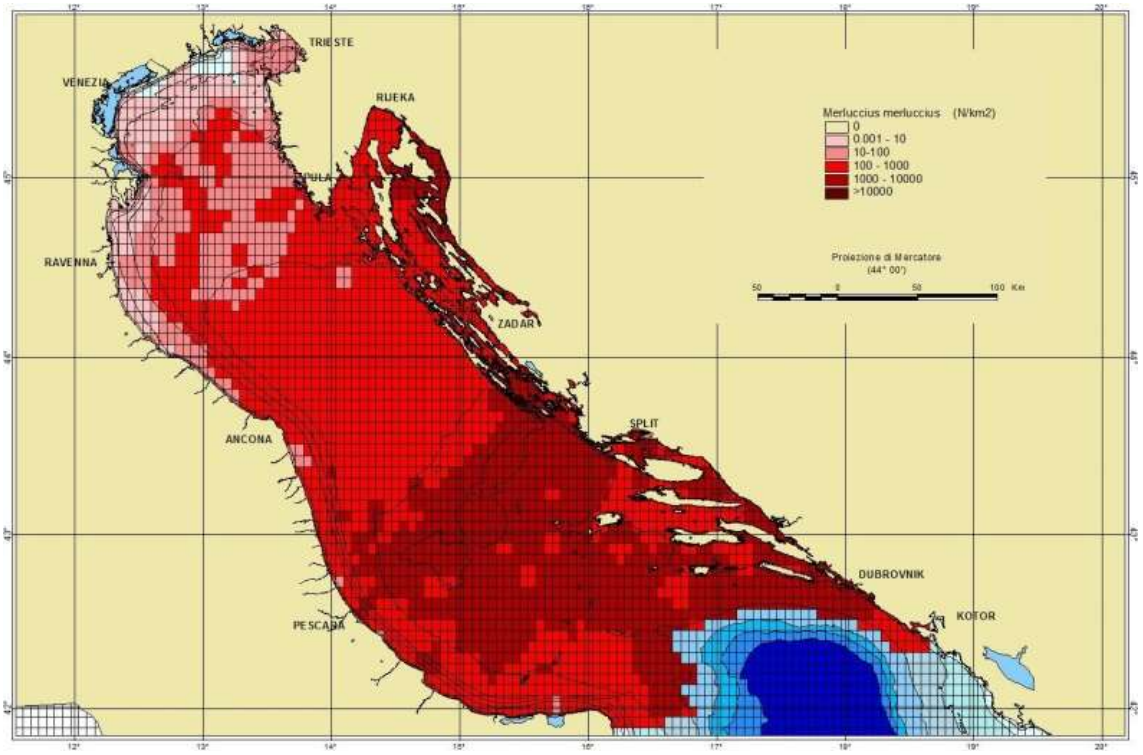

Figure 3.4.C – Spatial distribution of abundance of *M. merluccius* in the GSA17.

Micromesistius poutassou - Blue whiting is mainly distributed in the open central Adriatic with greatest abundances steadily found on silt and clay bottoms deeper than 130 m. Low abundance is also located off the northern Croatian coast and in the Kvarner Gulf (Figure 3.4.D).

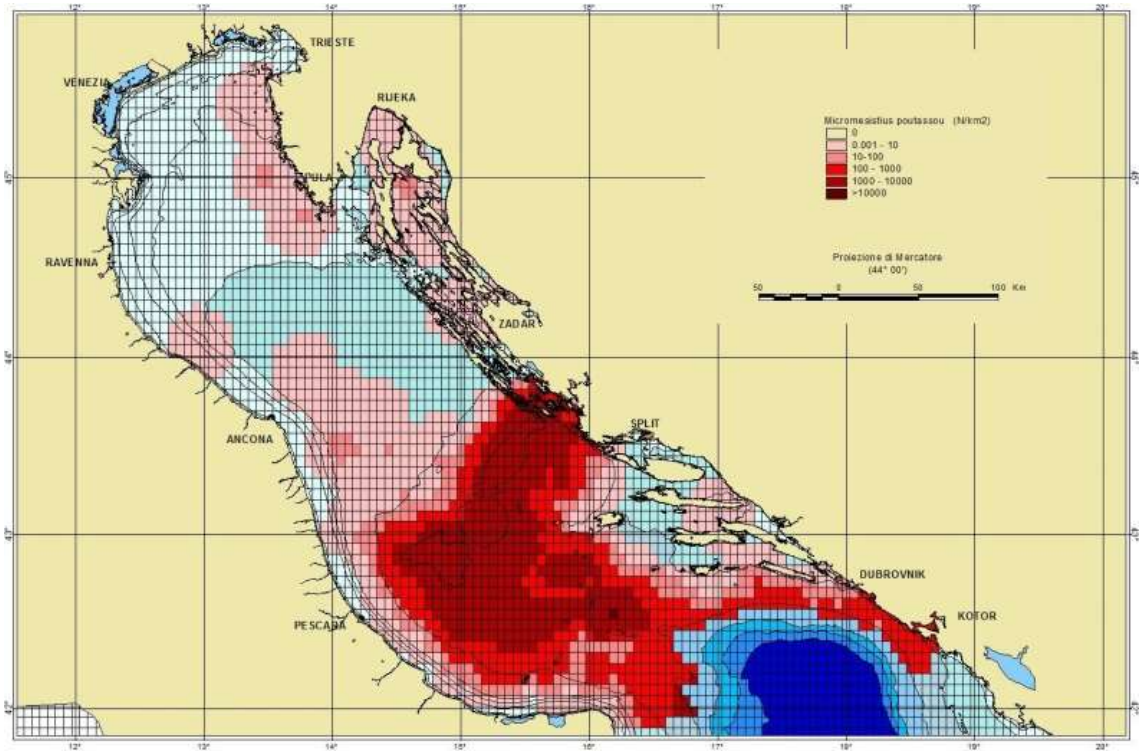

Figure 3.4.D – Spatial distribution of abundance of *M. poutassou* in the GSA17.

Merlangius merlangus - Whiting is widely distributed in shallow water of the north Adriatic and along the western coast (Figure 3.4.E). Greatest catches were steadily found in the northernmost part of the basin.

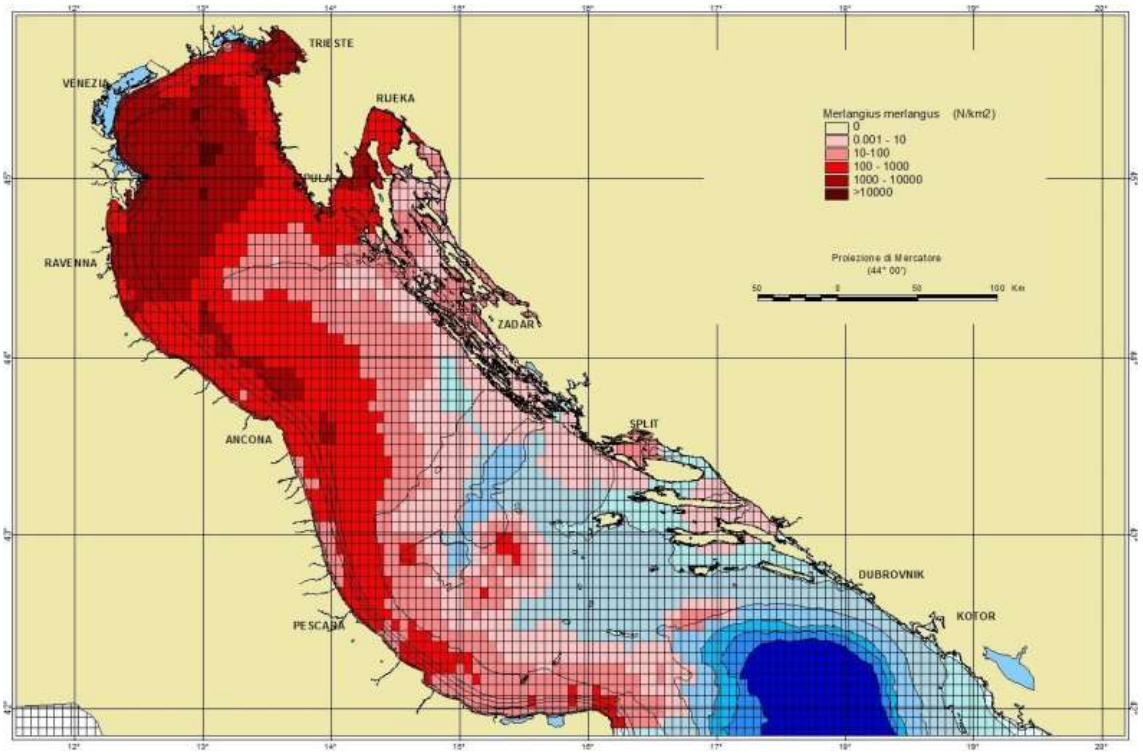

Figure 3.4.E – Spatial distribution of abundance of *M. merlangus* in the GSA17.

Trachurus mediterraneus - Mediterranean horse mackerel is widely distributed in the whole basin, despite highest abundances are found in the shallow water of the northern Adriatic and along the western coast (Figure 3.4.F).

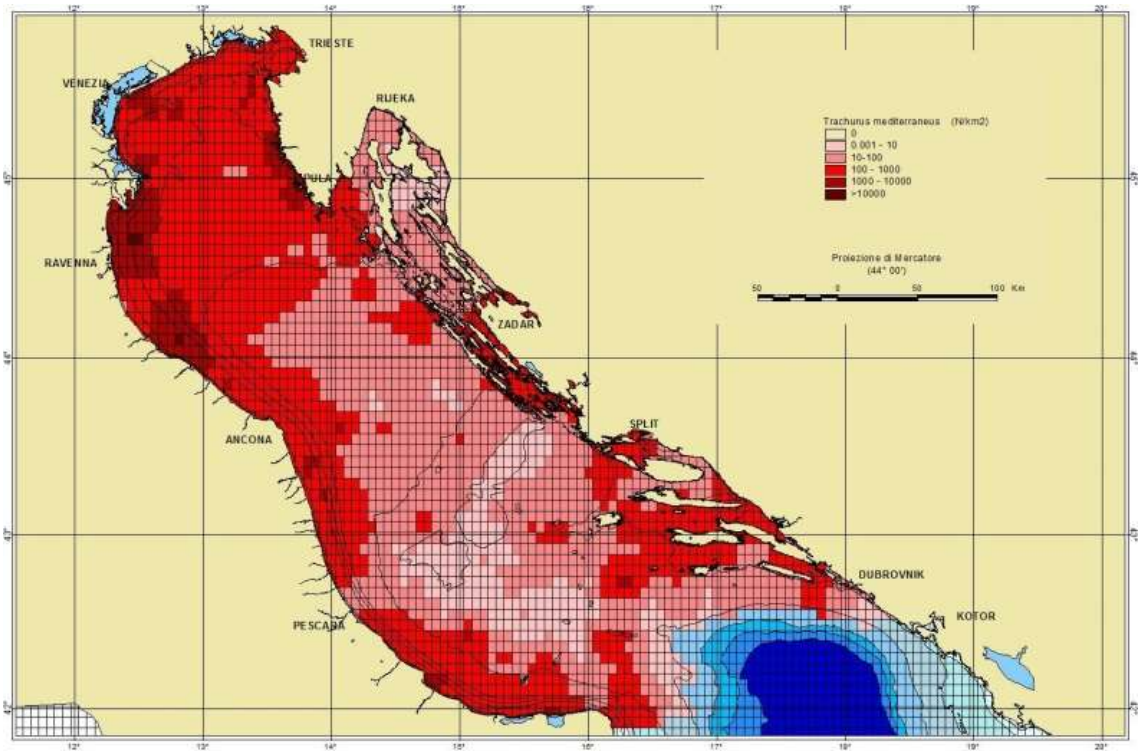

Figure 3.4.F – Spatial distribution of abundance of *M. mediterraneus* in the GSA17.

Trachurus trachurus - Horse mackerel is widely distributed in the whole basin although highest abundances are mainly located at depth lower than 200m (Figure 3.4.G).

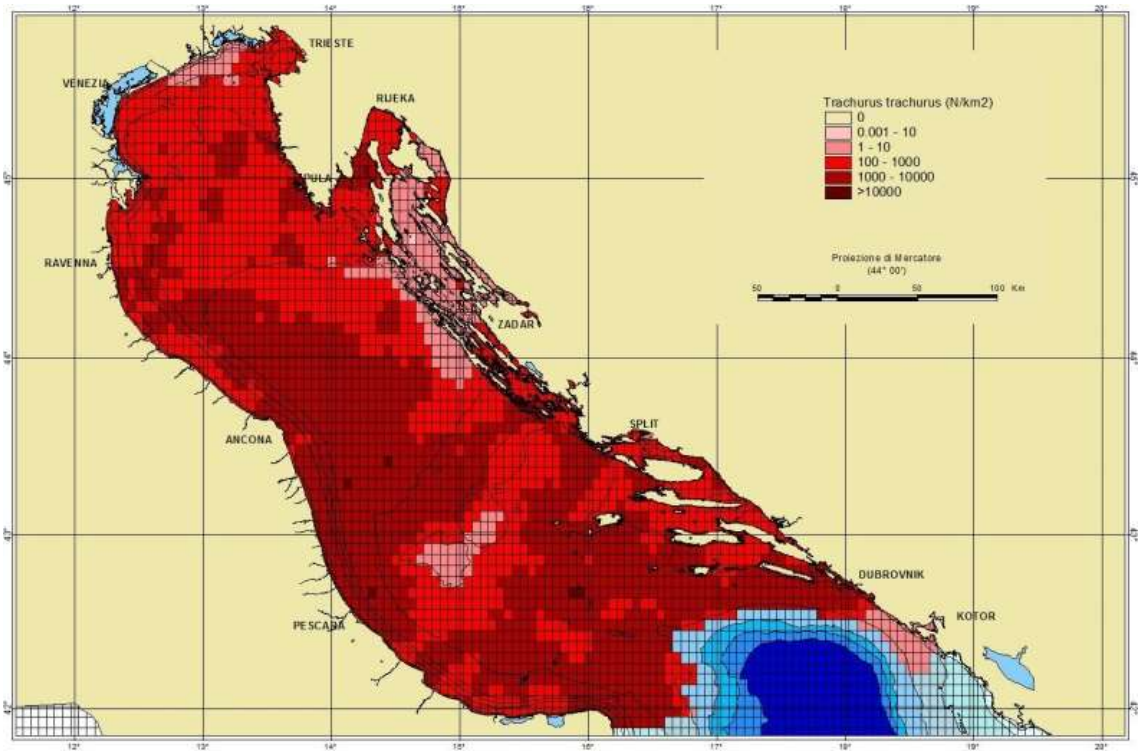

Figure 3.4.G – Spatial distribution of abundance of *T. trachurus* in the GSA17.

Eledone moschata - Musky octopus is widely distributed in the northern and central Adriatic up to 100 m of depth. Highest abundances are located in the northernmost part of the basin and in the southern channels area (Figure 3.4.H).

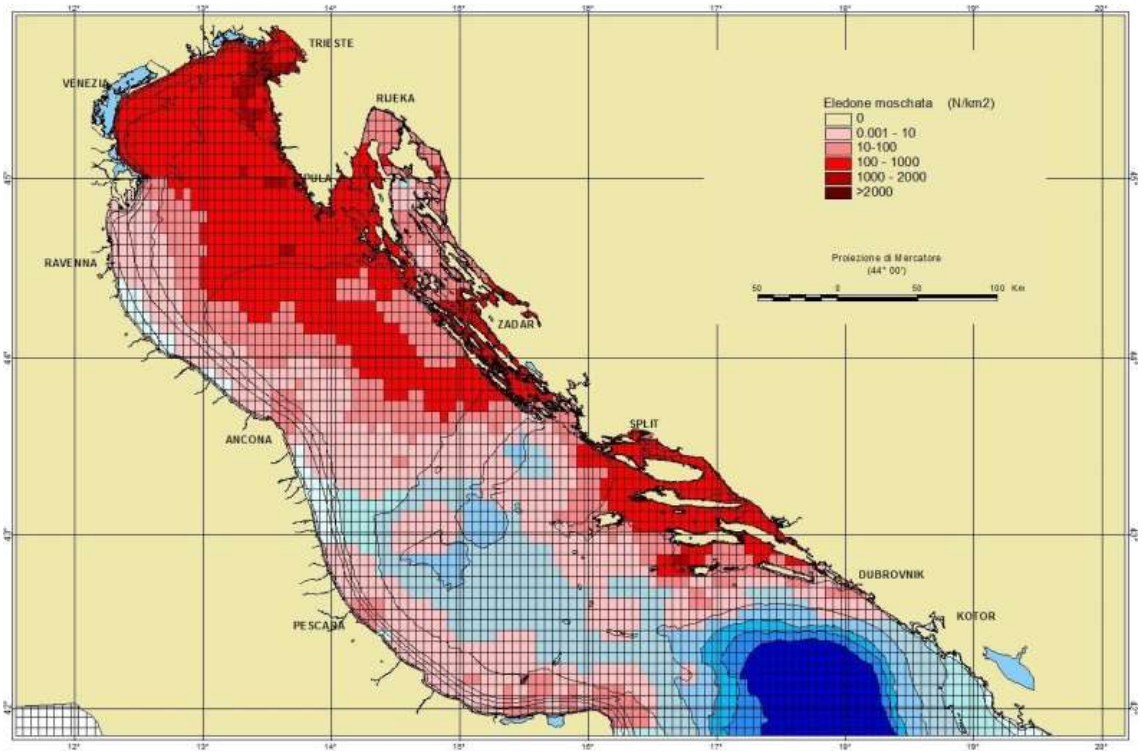

Figure 3.4.C – Spatial distribution of abundance of *E. moschata* in the GSA17.

Boops boops - Bogue is distributed in the whole basin; greatest abundances are located along both eastern and western shallow coastal water (Figure 3.4.I).

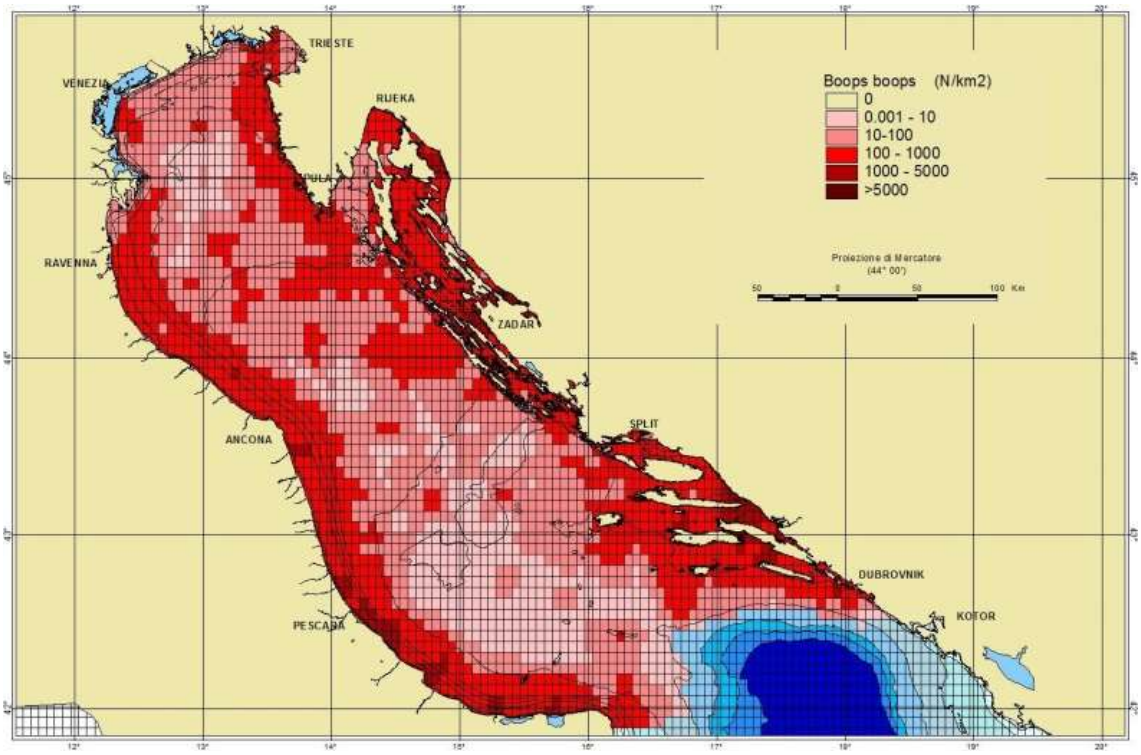

Figure 3.4.I – Spatial distribution of abundance of *B. boops* in the GSA17.

Serranus hepatus - Brown comber is distributed in the whole basin, with the exception of the deepest areas; greatest abundances are located inside the 100m isobath, mainly on the relict sand bottoms of the northern Adriatic and along the eastern coast (Figure 3.4.L).

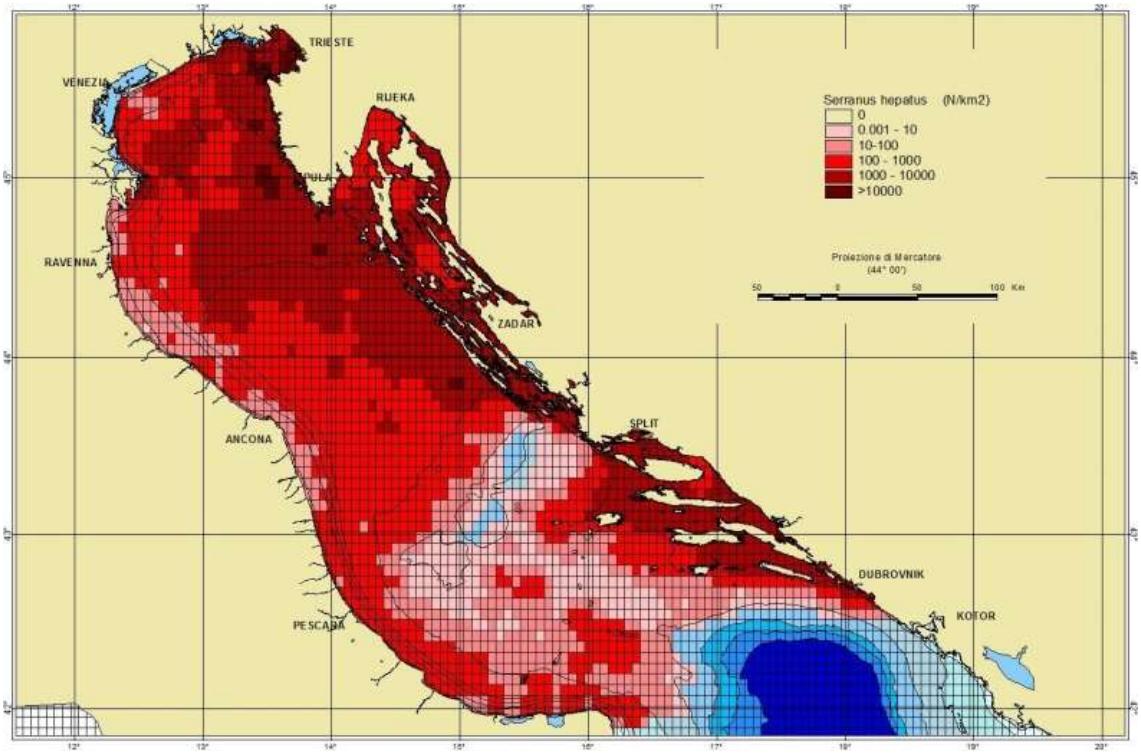

Figure 3.4.L – Spatial distribution of abundance of *S. hepatus* in the GSA17.

Loligo vulgaris - European squid is distributed throughout the whole basin mainly at depth lower than 150m. Greatest abundances are located in shallow coastal water and in the channels areas (Figure 3.4.M).

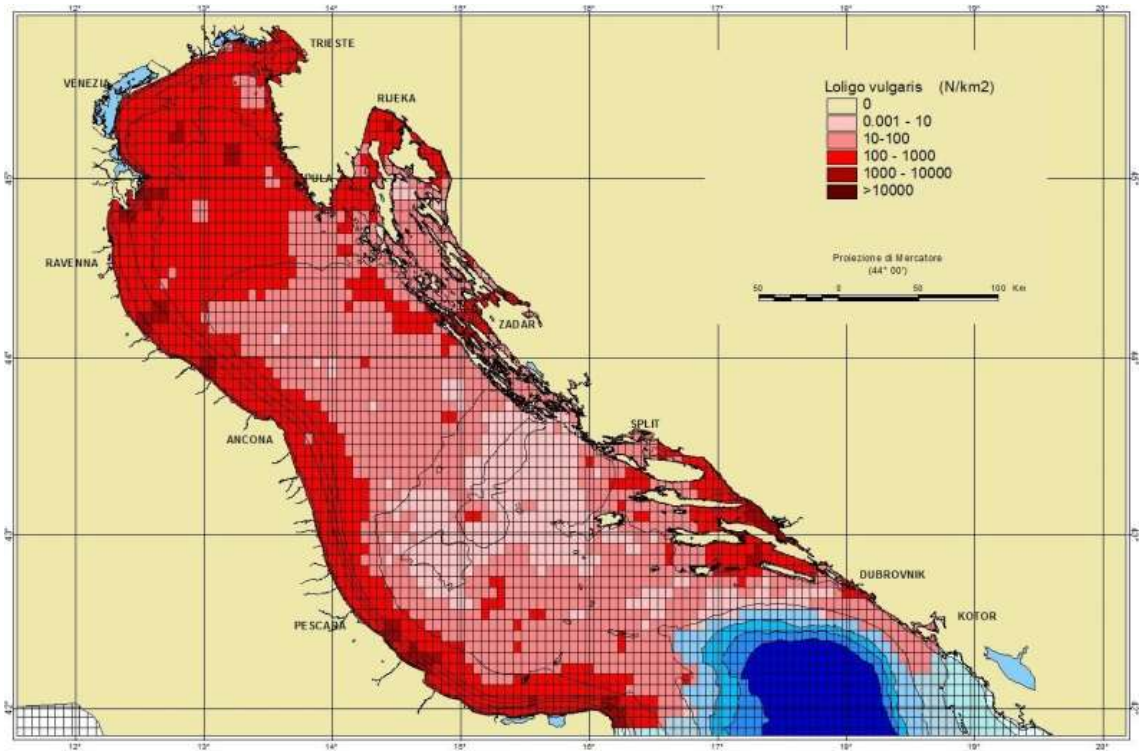

Figure 3.4.M – Spatial distribution of abundance of *L. vulgaris* in the GSA17.

Cepola macrophthalma - Red band fish is distributed in the whole basin except areas deeper than 200m. Greatest abundances are located between in the central part of the Adriatic and in the channels area of the eastern coast (Figure 3.4.N).

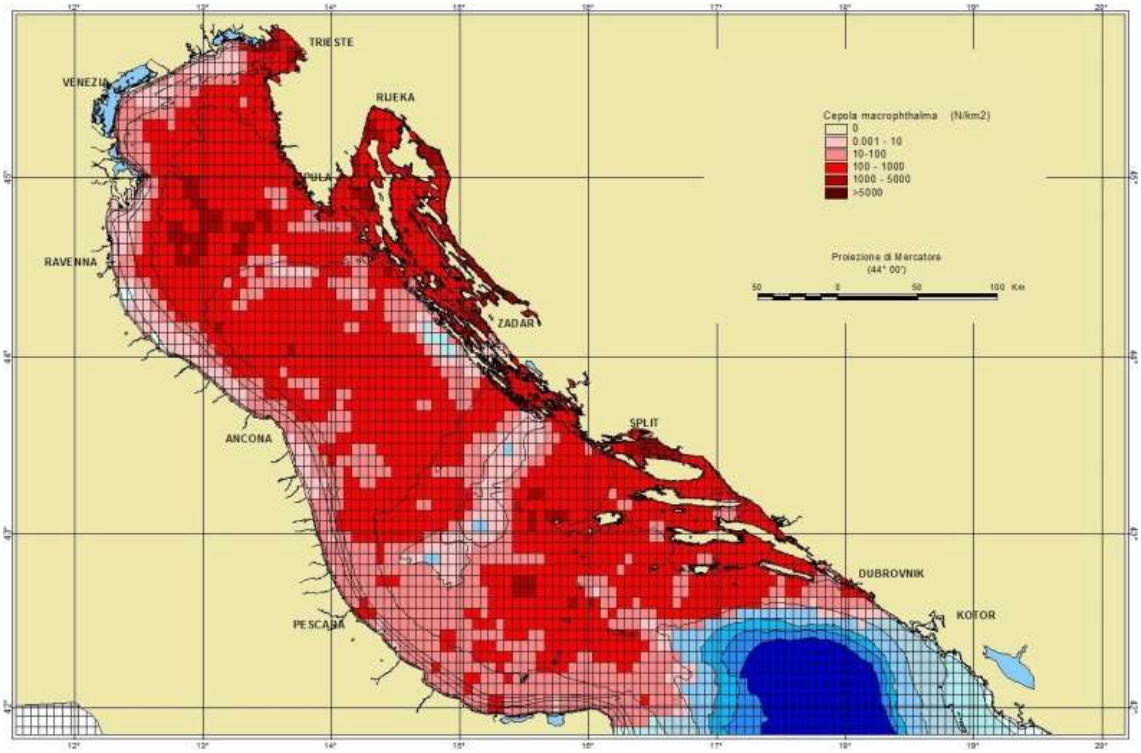

Figure 3.4.N – Spatial distribution of abundance of *C. macrophthalma* in the GSA17.

Pagellus erythrinus - Common pandora is widely distributed across the whole basin within 100m isobath. Greatest abundances are located in the southern channels area and on the relict sand bottoms of the northern Adriatic (Figure 3.4.O).

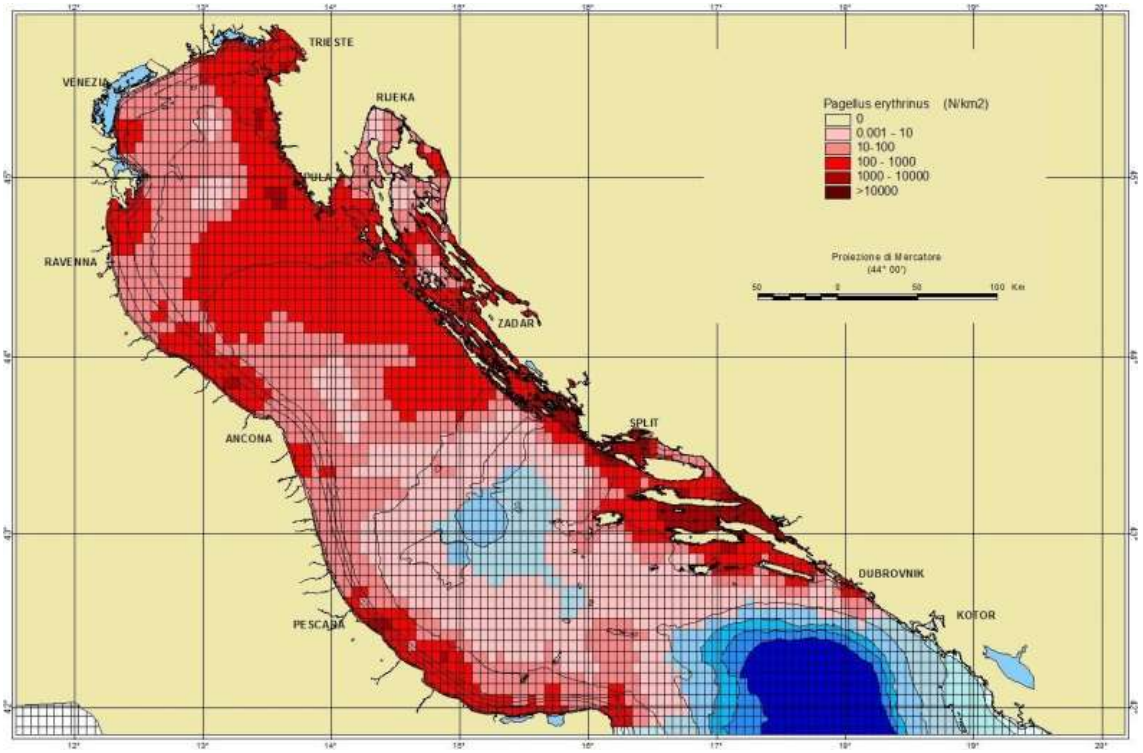

Figure 3.4.O – Spatial distribution of abundance of *P. erythrinus* in the GSA17.

Trisopterus minutus - Poor cod is widely distributed in the whole basin. Greatest catches were steadily found at deep lower than 200m (Figure 3.4.P).

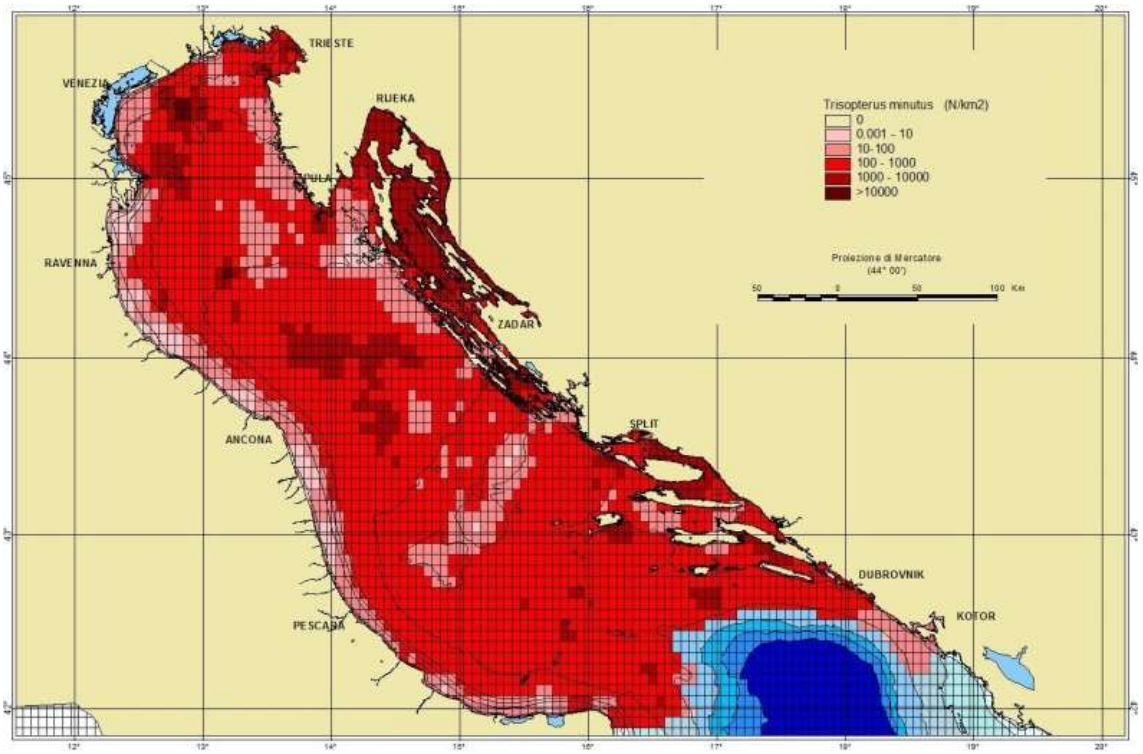

Figure 3.4.P – Spatial distribution of abundance of *T. minutus* in the GSA17.

Myliobatis aquila - Eagle ray is distributed on shallow water up to 50m, mainly in the northernmost basin and in the southern channels area (Figure 3.4.Q).

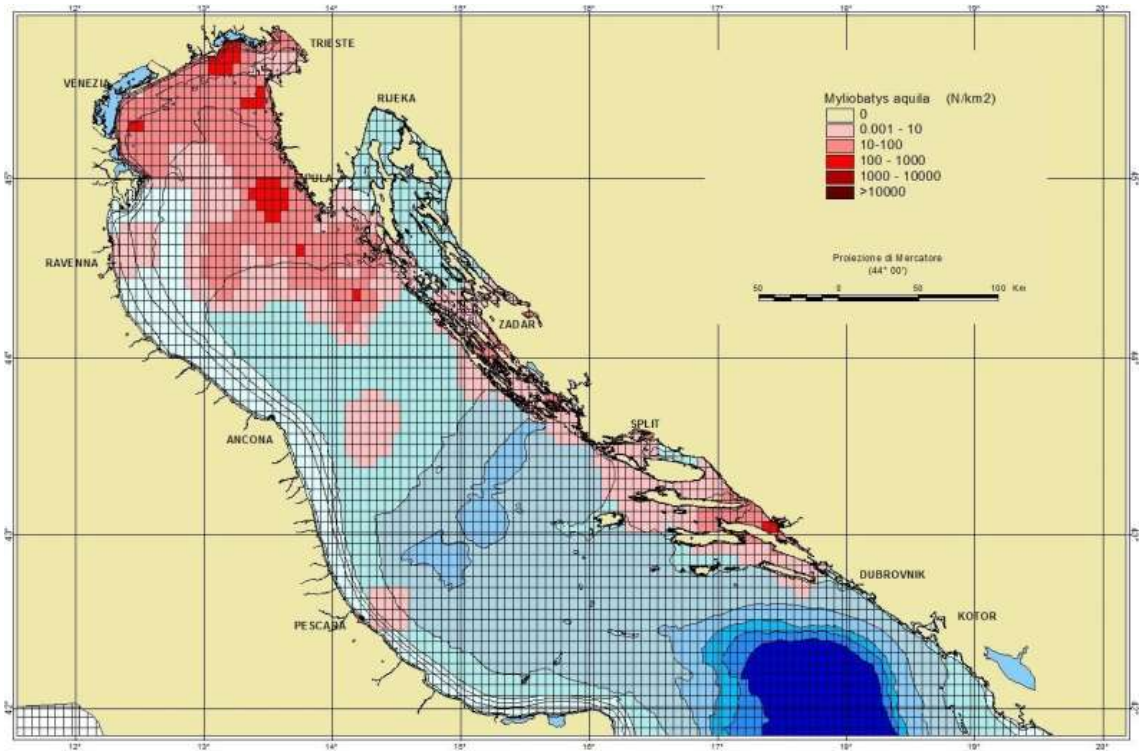

Figure 3.4.Q – Spatial distribution of abundance of *M. aquila* in the GSA17.

Parapenaeus longirostris - Deepwater rose shrimp is widely distributed in the basin from 70m pf depth. Greatest abundances are located in the south-eastern area of the central Adriatic (Figure 3.4.R).

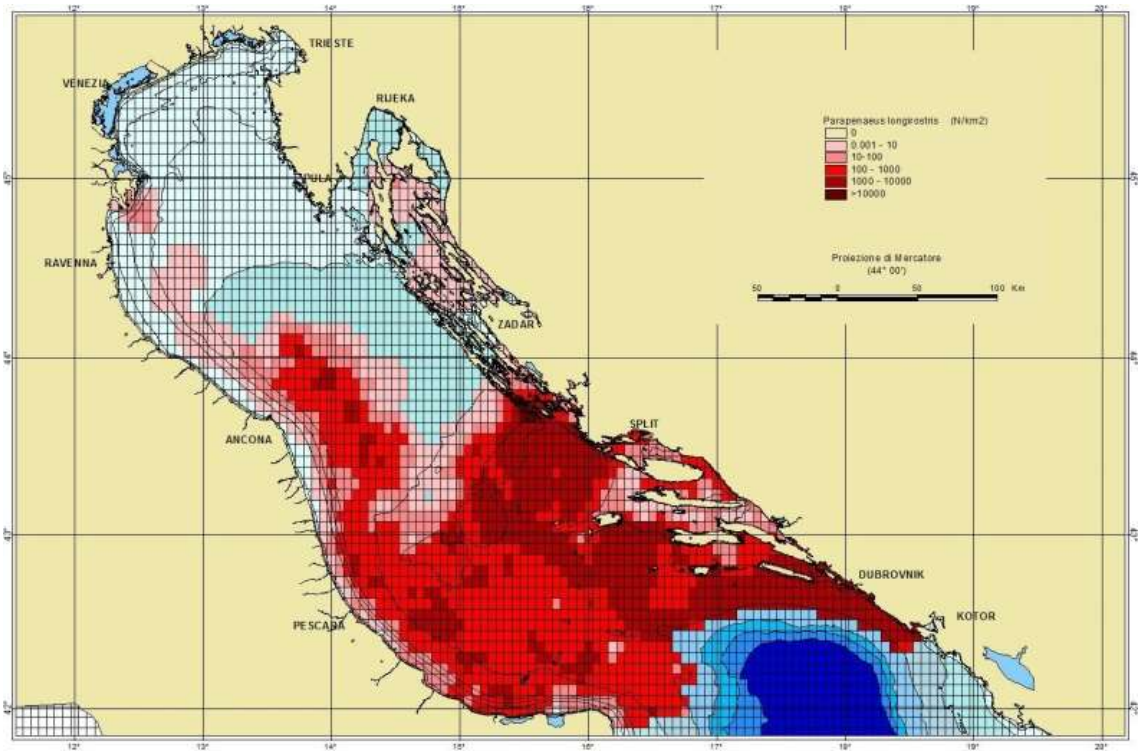

Figure 3.4.R – Spatial distribution of abundance of *P. longirostris* in the GSA17.

Squalus acanthias - Spiny dogfish is distributed throughout the basin, mainly in the northernmost part of the basin up to 50m of depth (Figure 3.4.S).

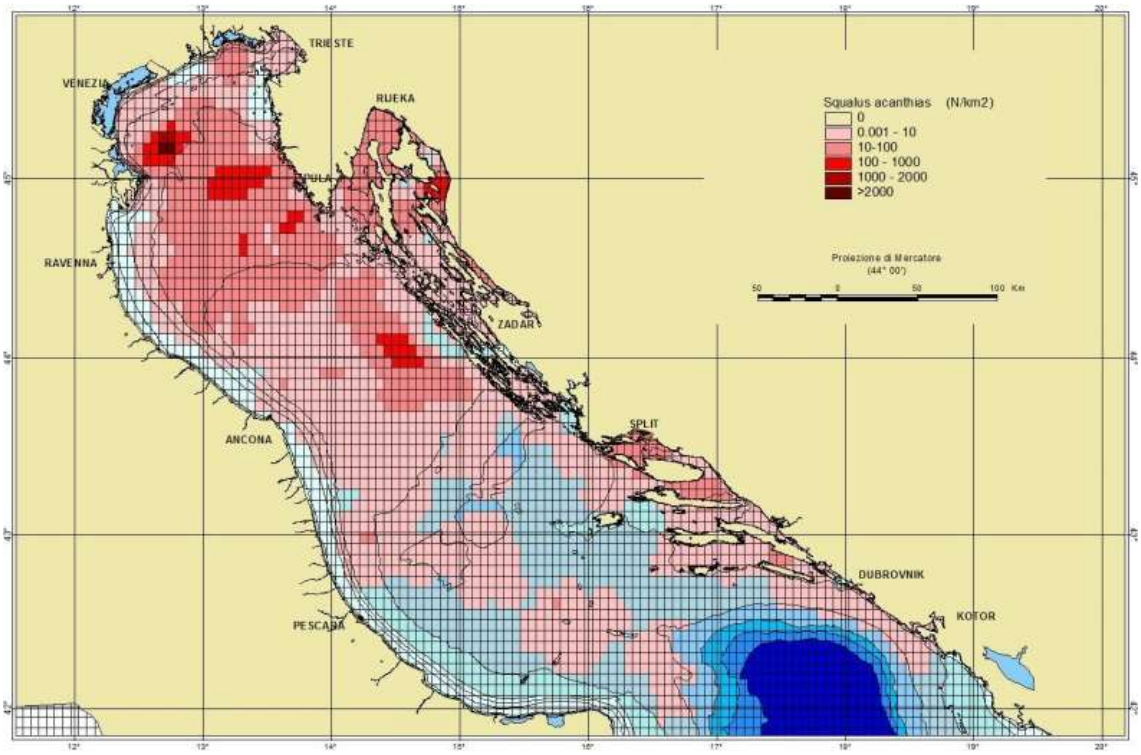

Figure 3.4.S – Spatial distribution of abundance of *S. acanthias* in the GSA17.

Scorpaena notate - Small red scorpionfish is mainly distributed up to 100m of depth. Greatest abundances are located on the relict sand bottoms of the northern Adriatic (Figure 3.4.T).

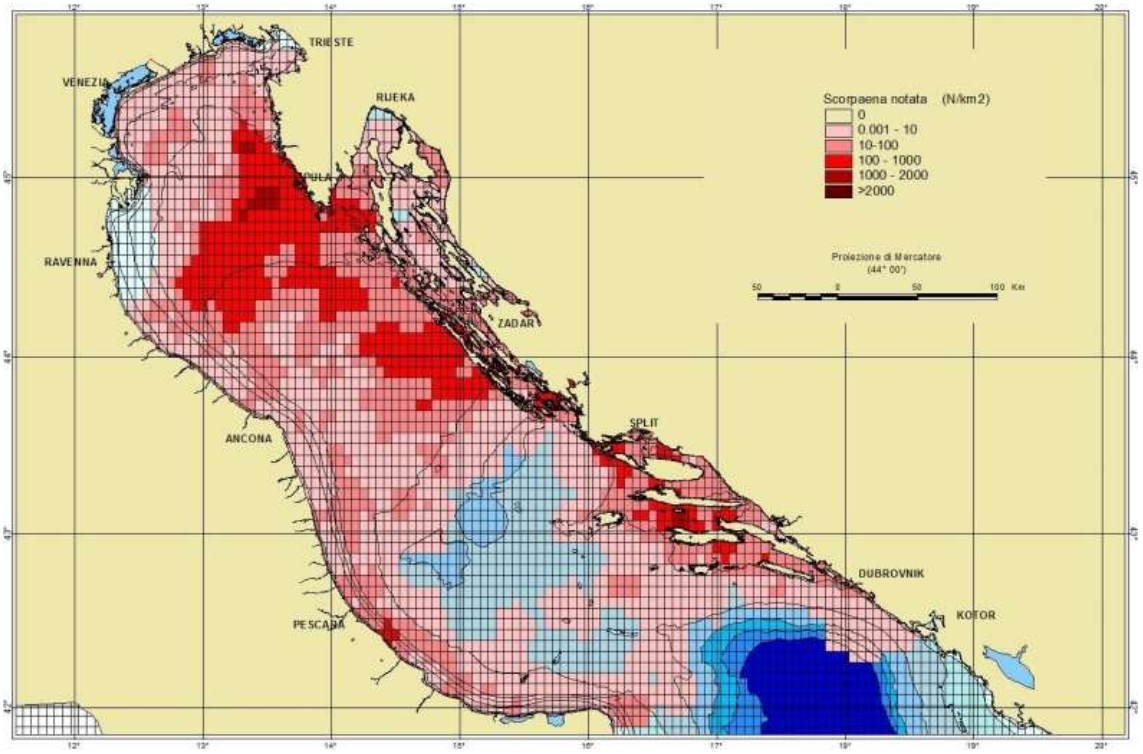

Figure 3.4.T – Spatial distribution of abundance of *S. notate* in the GSA17.

Raja clavata - Thornback ray is mainly distributed in the eastern channels area and in northern part of the basin around the 50m isobath (Figure 3.4.U).

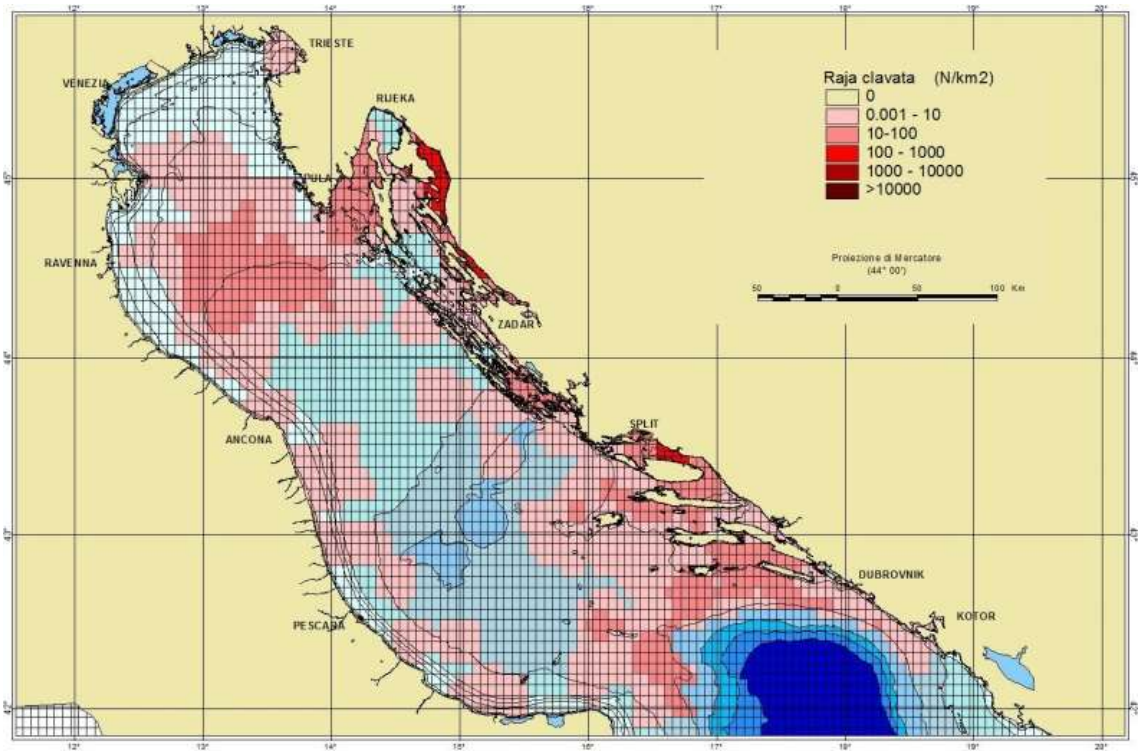

Figure 3.4.U – Spatial distribution of abundance of *R. clavata* in the GSA17.

Squilla mantis - Spottail mantis shrimp is distributed in shallow coastal water, mainly along the western coast and in the Gulf of Trieste (Figure 3.4.V).

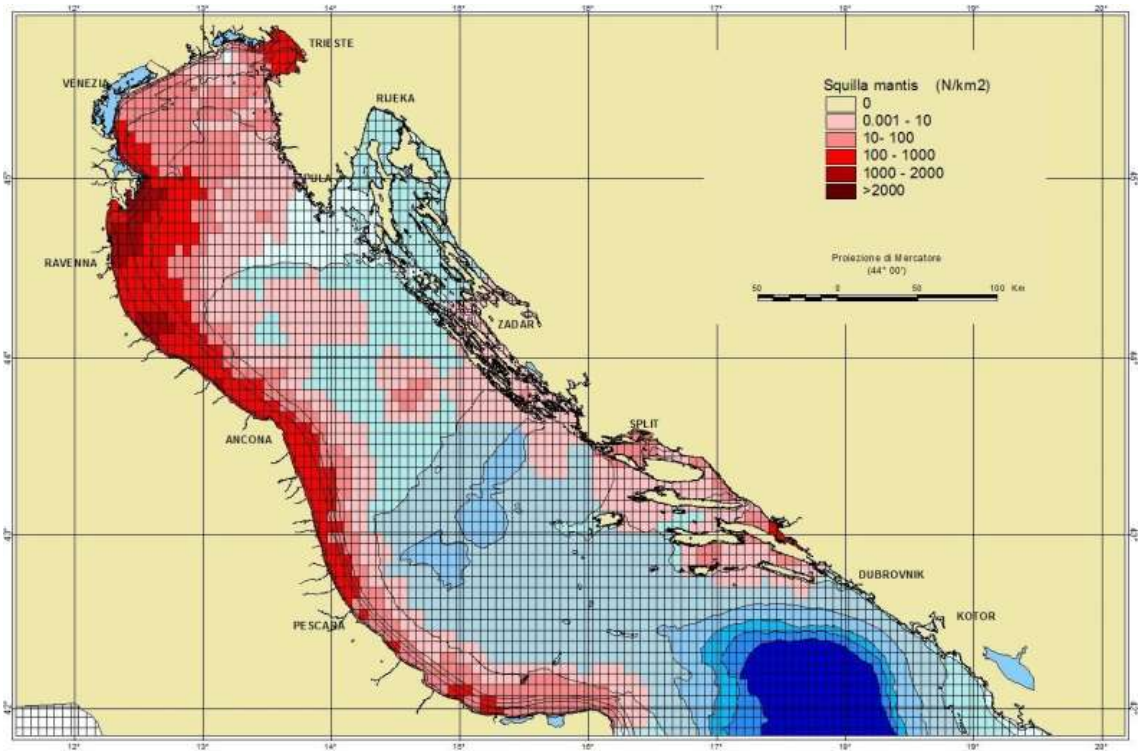

Figure 3.4.V – Spatial distribution of abundance of *S. mantis* in the GSA17.

4. CONCLUSION

This Deliverable 4.3.1-*Spatial distribution of marine resources* reports, accurately and synthetically, fishery independent information aimed at evaluating the status of demersal resources of commercial interest for fisheries occurring in the Adriatic and Western Ionian Sea (GSAs 17, 18, 19). The basic information concerning target species, such as estimates of population indices and of population structure indicators at different spatial and temporal scale were provided by the analysis of data from fishery-independent surveys, i.e., the MEDITS and SOLEMON trawl surveys. These data are available disaggregated by species, detailed by hauls, and for a long time series: thus they represent the most fine monitoring of demersal communities in the area. Target species for the analysis were selected according to different criteria that include i) representativeness in trawl survey data, ii) importance for commercial purposes. For the GSA17, 15 species were selected, of which 13 are target of MEDITS surveys and 2 are target of SOLEMON surveys. For GSA18 and GSA19, 26 and 18 species were selected, respectively, from species sampled during MEDITS surveys. Once the species have been selected for each GSA, key population indicators for an Ecosystem Approach to Fishery Management (EAFM), among them the biomass (kg/km^2) and abundance indices (number/km^2), recruits and spawners indices (number/km^2), were estimated at temporal and spatial scale by BioIndex routine developed by COISPA in R language. In particular, each species were analysed considering its own range of bathymetric distribution among macro-strata fixed: 10-200, 10-800 or 200-800 m. Exception is the GSA17 in which the bathymetric strata 10-800 m is substituted by the bathymetric range 10-500 m due to the morphological characteristics of area. A synthetic table of the principal indicators and trend provided by BioIndex analysis for the species analysed in each GSA as well as bubble plots of recruits and spawners are reported in this Deliverable.

The results of BioIndex showed an important increasing trend in the biomass and density indices of *M. barbatus* in all GSAs and for *P. longirostris* in the GSAs 17 ad 18. A significant positive trend was also observed for *I. coindetii* in all GSAs, accompanied only in GSA 18 by a positive trend for *L. vulgaris*. Finally, *S. vulgaris* in GSA 17 and red shrimps (*A. foliacea* and *A. antennatus*) in GSA 19 showed also significant trends in

abundance indices, while *N. norvegicus* in GSA 19 showed a significant decreasing trend. The analysis of the time series also reported in the BioStand results show that there are some common patterns in the temporal variations of the abundance indexes of some species in the three areas. Indeed, *M. merluccius* shows in all the GSAs higher abundance in correspondence of the first years of the time series (1994-1995), in a central period (2006-2009) and in the final part of the time series (2017). *P. longirostris*, on the other hand, shows a progressive increase of the abundance during all the time series until the last years (2017). Aproximately the same patter was showed by *M. barbatus* that shows, in particular in GSA 17 and 18, an increase of the index since 2011 up to the 2017. *I. coindetii* in GSA 17 and 18 shows a progressive increase of the index during all the time series, while in GSA 19, even if this trend was observed, a pick of abundance was shown during the year 2008.

All detailed outputs (trends of all indices estimated, maps and bubble plots) are upload in the FAIRSEA project sharepoint.

Following this preliminary analysis, the standardization of biomass indices of 5 selected species for each GSA was carried out by the application of BioStand routine developed by COISPA. This process of standardization, useful to provide unbiased results to be used also in stock assessment models, involved the use of Generalized Additive Models (GAM), in which the linear relationships between the response and predictor variables are replaced by non-linear 'smooths'. The advantage of these models is that they are nonparametric additive models in which also factorial predictors could be used producing step functions (Wood, 2017). The species considered in this step were identified among the ones previously selected and considered relevant for their commercial value. These specie for the GSA17 were the European hake *M. merluccius*, the red mullet *M. barbatus*, the deep-water rose shrimp *P. longirostris*, the broadtail shortfin squid *I. coindetii* and the common sole *Solea solea.* The same species were considered also in both GSA18 and GSA19 except for the common sole replaced by the giant red shrimp *A. foliacea* in both areas. The modelling process followed a forward stepwise procedure for the selection of predictive variables and explored different hypotheses of probability distributions and data transformations to test several GAM models for each species and in each GSA. The

model characterized by the lowest Generalized Cross-Validation value (GCV), by significant explanatory variables and the highest percentage of Deviance explained was selected in each step of the procedure, until the final phase, where the best model for the standardization of biomass index was selected.
This approach allowed to test the significance of relevant explanatory variables on the biomass indices. For all the 15 analyzed stocks the year was found significant, especially in the cases that highlighted a significant trend in the previous analysis (BioIndex).
Among the different family distributions tested the most effective ones during the standardization process for all the GSAs were the Tweedie and quasi-Poisson that used the log-link function, instead of the Gaussian distribution that was used applying the root square or the logarithmic transformation. These kind of distributions are particularly useful in case of zero-inflated data (Shono, 2008, Zuur et al., 2009), such as the case of the case of data collected during trawl survey (Arcuti et al., 2013).
The position (latitude, longitude, depth) was observed as an important element determining the annual index, across the spatial distribution of the species.
The month, defined in the modeling process as a factor and tested to determine possible effects of the survey time shift occurred along the years, was also tested and it was found significant for *M. merluccius* in GSA 18, but also in GSA 17 for *P. longirostris*, *M. barbatus* and *S. solea*.
The change in sampling intensity, expressed in number of hauls carried out by year, along the years, occurred with the implementation of the DCF in 2002, was also explored as a factor; it was found significantly influence the biomass index of *P. longirostris* and *A. foliacea* in GSA 18.
BioStand outputs were uploaded for each GSA in the FAIRSEA sharepoint.
An additional approach aimed at achieving the goal of the Activity 4.3 BSTAT was adopted on GSA17 data. The effort was focused to map the spatial distribution of abundance of selected species in GSA17 for the entire MEDITS time series 1994-2018. Abundance indices per hauls were computed using the software ATrIS, and then, a spatial interpolation method, the Inverse Distance Weighted (IDW) technique was applied in order to analyze all stations together and to obtain a global picture of the

distribution area of species. Finally, the grid with interpolated data was filtered by a mobile window (3 cells x 3 cells) and the mean value in the center of the window was calculated. This procedure was aimed to obtain the final map by species with a spatial resolution according to the COPERNICUS grid adopted by other PPs (horizontal resolution equals to 1/16°), considering the time-frame 1994-2018. The assumption was thus the stationarity of the species distribution along the whole time series analyzed.

5. REFERENCES

Adebiyi F.A., 2013. The sex ratio, gonadosomatic index, stages of gonadal development and fecundity of sompat grunt Pomadasys jubelini (Cuvier, 1830). Pakistan J. Zool. 45(1): 41-46.

Anonymous. 2017. MEDITS Handbook, Version n. 9. MEDITS Working Group, 106 pp. http://www.sibm.it/MEDITS%202011/principaledownload.htm

Arcuti S., Calculli C., Pollice A., D'Onghia G., Maiorano P., Tursi A. (2013). Spatio-temporal modelling of zero-inflated deep-sea shrimp data by Tweedie generalized additive. Statistica 73(1): 87-101.

Burrough P.A., McDonnell R.A., 1998. Principles of Geographical Information Systems. Oxford University Press, Oxford.

Cochran W.G., 1977. Sampling techniques. New York John Wiley Sons.

Cotter J., 2009. A selection of nonparametric statistical methods for assessing trends in trawl survey indicators as part of an ecosystem approach to fisheries management (EAFM). Aquat. Living Resour. 22, 173–185. DOI: 10.1051/alr/2009019

Cotter J., Petitgas P., Abella A., *et al.* 2009a. Towards an ecosystem approach to fisheries management (EAFM) when trawl surveys provide the main source of information. Aquat. Living Resour. 22: 243-254. https://doi.org/10.1051/alr/2009025

Cotter J., Mesnil B., Witthames P., *et al.* 2009b. Notes on nine biological indicators estimable from trawl surveys with an illustrative assessment for North Sea cod. Aquat. Living Resour. 22: 135-153. https://doi.org/10.1051/alr/2009016

Denis V., Lejeune J., Robin J.P., 2002. Spatio-temporal analysis of commercial trawler data using General Additive models: Patterns of Loliginid squid abundance in the north-east Atlantic. ICES J. Mar. Sci. https://doi.org/10.1006/jmsc.2001.1178

Mateo I., Hanselman D., 2014. A Comparison of Statistical Methods to Standardize Catch-Per-Unit-Effort of the Alaska Longline Sablefish Fishery. U.S.Dep.Commer.,NOAA Tech. Memo. NMFS-AFSC-269.

Piet G.J., Jennings S., 2005. Response of potential fish community indicators to fishing, ICES Journal of Marine Science, V.62-2, 214:225. Available on line at: http://icesjms.oxfordjournals.org/content/ 62/2/214.full.

Shono H., 2008. Application of the Tweedie distribution to zero-catch data in CPUE analysis. Fisheries Research 93(1-2): 154-162.

Souplet A., 1996. Calculation of abundance indices and length frequencies in the MEDITS survey, in: Bertrand, J.A. (Ed.), Campagne Internationale Du Chalutage Démersal En Méditerraneé. Campagne 1995. EU Final Report, Vol. III.

Spedicato M.T., Massutí E., Mérigot B., Tserpes G., Jadaud A., Relini G., 2019a. The MEDITS trawl survey specifications in an ecosystem approach to fishery management. Sci. Mar. 83S1: 9-20. https://doi. org/10.3989/scimar.04915.11X

Spedicato M.T., Tserpes G., Mérigot B., Massutí E. (eds). 2019b. Mediterranean demersal resources and ecosystems: 25 years of MEDITS trawl surveys. Sci. Mar. ISSN-L: 0214-8358

Trenkel V.M., Rochet M.J., 2009. Intersection–union tests for characterising recent changes in smoothed indicator time series. Ecological Indicators, Volume 9, Issue 4: 732-739

Trenkel V.M., Rochet M-J., Mesnil B., 2007. From model-based prescriptive advice to indicator-based interactive advice. – ICES Journal of Marine Science 64: 768–774.

Wood S.N., 2017. Generalized additive models: An introduction with R, second edition, Generalized Additive Models: An Introduction with R, Second Edition. https://doi.org/10.1201/9781315370279

Wood S.N., 2001. mgcv: GAMs and generalized ridge regression for R, R News. https://doi.org/10.1159/000323281

Zuur A.F., Ieno E. N., Walker,N.J., Saveliev A.A., Smith,G.M. (2009). Zero-truncated and zero-inflated models for count data. In Mixed effects models and extensions in ecology with R (pp. 261-293). Springer, New York, NY.